

**Beiträge  
zur  
Vibro- und Psychoakustik**

**Herausgeber: Helmut Fleischer und Hugo Fastl**

---

**Helmut Fleischer**

**DEAD SPOTS OF ELECTRIC BASSES**

**II. Diagnosis**

**2<sup>nd</sup> Edition**

# **DEAD SPOTS OF ELECTRIC BASSES**

## **II. Diagnosis**

2nd Edition

by

**Helmut Fleischer**

Institut für Mechanik  
Fakultät für Luft- und Raumfahrttechnik  
Universität der Bundeswehr München  
D-85577 Neubiberg

**Heft 1/00 der Reihe**

**Beiträge zur Vibro- und Psychoakustik**

**Herausgeber: Helmut Fleischer und Hugo Fastl**

ISSN 1430-936X

**Herausgeber:**

Prof. Dr.-Ing. habil. Helmut Fleischer  
Institut für Mechanik  
Fakultät für Luft- und Raumfahrttechnik  
Universität der Bundeswehr München

Prof. Dr.-Ing. habil. Hugo Fastl  
Lehrstuhl für Mensch-Maschine-Kommunikation  
Fakultät für Elektrotechnik und Informationstechnik  
Technische Universität München

**Postanschrift:**

LRT 4 UniBwM  
D-85577 Neubiberg

---

Fleischer, Helmut:  
Dead spots of electric basses. II. Diagnosis  
Beiträge zur Vibro- und Psychoakustik 1/00  
Neubiberg 2000  
**ISSN 1430-936X**

**Postanschrift des Verfassers:**

Prof. Dr.-Ing. Helmut Fleischer  
LRT 4 UniBwM  
85577 Neubiberg  
Deutschland  
Helmut.Fleischer@UniBw.de

Dieses Werk ist urheberrechtlich geschützt. Jede Verwertung außerhalb der Grenzen des Urheberrechtsgesetzes ist unzulässig und strafbar. Insbesondere gilt dies für die Übersetzung, den Nachdruck sowie die Speicherung auf Mikrofilm, mit vergleichbaren Verfahren oder in Datenverarbeitungsanlagen.

# CONTENT

## FOREWORD

1.	INTRODUCTION .....	1
2.	INSTRUMENTS UNDER CONSIDERATION .....	3
2.1.	Overview .....	3
2.2.	Action Bass .....	3
2.3.	Music Man Bass .....	4
2.4.	Dyna Bass .....	4
2.5.	Carvin Bass .....	5
2.6.	Riverhead Bass .....	5
2.7.	Concluding Remarks .....	7
3.	OPERATING DEFLECTION SHAPES .....	8
3.1.	Measuring Set-up and Procedure .....	8
3.2.	Results of <i>In-situ</i> Experiments .....	9
3.3.	Results of In-stand Experiments .....	12
3.4.	Comparison of <i>In-situ</i> to In-stand Results .....	18
3.5.	Concluding Remarks .....	20
4.	COMPARISON OF THE PRINCIPAL ODSs .....	21
4.1.	ODSs of the Action Bass .....	21
4.2.	ODSs of the Music Man Bass .....	24
4.3.	ODSs of the Dyna Bass .....	25
4.4.	ODSs of the Carvin Bass .....	27
4.5.	ODSs of the Riverhead Bass .....	27
4.6.	Modelling the Bass ODSs as Beam Eigenmodes .....	29
4.6.1.	Frequency Ratios .....	29
4.6.2.	Rigid Body Motion .....	30
4.6.3.	First Bending Vibration .....	30
4.6.4.	Second Bending Vibration .....	30
4.6.5.	Third Bending Vibration .....	31
4.6.6.	Fourth Bending Vibration .....	31
4.7.	Concluding remarks .....	31
5.	MECHANICAL CONDUCTANCE .....	33
5.1.	Measuring Set-up and Procedure .....	33
5.2.	Lateral Dependence of the Neck Conductance .....	37
5.3.	Neck and Bridge Conductance .....	42
5.4.	Concluding Remarks .....	45
6.	NECK CONDUCTANCE OF THE BASSES .....	46
6.1.	Evaluation .....	46
6.2.	Results of the Action Bass .....	47
6.3.	Results of the Music Man Bass .....	47
6.4.	Results of the Dyna Bass .....	48

6.5.	Results of the Carvin Bass .....	49
6.6.	Results of the Riverhead Bass.....	49
6.7.	Concluding Remarks.....	50
7.	DAMPING AND DECAY OF STRING VIBRATIONS.....	52
7.1.	Vibration of the String .....	52
7.2.	Air Damping .....	54
7.3.	Internal Damping .....	57
7.4.	Damping Due to Energy Loss via a Support.....	59
7.5.	"Addition" of Time Constants.....	62
7.6.	Comparison of the Time Constants for Bass Strings .....	63
7.6.1.	Normal Bass Strings.....	63
7.6.2.	Extreme Cases.....	66
7.7.	Concluding Remarks.....	68
8.	DECAYING OF BASS STRINGS .....	69
8.1.	Quantifying the Decay .....	69
8.1.1.	Measuring Procedure .....	69
8.1.2.	Decay of the Total Signal.....	70
8.1.3.	Decay of the Partial .....	71
8.2.	Comparing Experimental Data and Theoretical Decay of the Fundamental .....	73
8.2.1.	Internal Damping and Support Damping.....	73
8.2.2.	Decay of the E String .....	74
8.2.3.	Decay of the A String.....	75
8.2.4.	Decay of the D String.....	76
8.2.5.	Decay of the G String.....	77
8.2.6.	Evaluation .....	78
8.3.	Comparing Experimental Data and Theoretical Decay of Partial .....	80
8.3.1.	Internal Damping of the Partial .....	80
8.3.2.	Decay of the E String .....	81
8.3.3.	Decay of the A String.....	83
8.3.4.	Decay of the D String.....	85
8.3.5.	Decay of the G String.....	87
8.4.	Final Evaluation .....	89
8.5.	Concluding Remarks.....	93
9.	FINAL DISCUSSION .....	94
	LITERATURE.....	99

## SUMMARY

This study treats electric basses with solid body. Five structurally different instruments (with and without a head, made from wood and carbon fibre, neck screwed and glued to the body, four through six strings) serve as measuring objects; cf. Chapter 2. Players of such basses appreciate a long decay of the string signal as a quality attribute. However, there are particular locations on the fingerboard where, for distinct strings, the signal decays significantly faster than at adjacent frets. This effect is well known among bass players who call the corresponding location a "dead spot". It originates from the fact that the string may cause vibrations of the mechanical structure of the bass. Consequently, energy flows from the string to the instrument body. This results in additional damping, which leads to a faster decay of the string vibration.

At the beginning, the structural vibrations of the instruments are determined; cf. Chapters 3 and 4. For this purpose, by means of a laser scanning vibrometer operating deflection shapes (ODSs) are measured *in situ*, *i.e.* the bass is held by a player in normal playing position. The results compare to theoretical findings for the bending vibrations of the simply supported-free beam. As an object-oriented parameter, in Chapters 5 and 6 the mechanical point conductance at the end supports of the strings is ascertained. The conductance represents a measure for the (frequency-dependent) energy transfer via the end support under consideration, *i.e.* for an additional support damping. All experiments confirm that for a well-made solid-body bass the conductance may reach higher values on the fingerboard than at the bridge. This means that, as a rule, the more prominent support damping originates from the neck termination of a string.

In the following part, three different damping mechanisms acting on the string (air damping, internal damping and support damping) are treated theoretically and the corresponding time constants estimated; cf. Chapter 7. According to this estimation the (string-immanent) viscous damping by the surrounding air plays no role for bass strings. The (string-immanent) internal damping defines the normal case in which the time constants of the single partials decrease inversely proportional to their frequencies. Locations on the fingerboard, where only internal damping acts, may be called live spots. At distinct different locations and frequencies, the additional (instrument-immanent) support damping may decrease the time constants and thus cause dead spots. Support damping is a feature of the instrument and favourably represented by the conductance.

In Chapter 8 the results of experiments on two basses are presented, in which the decay of the total signals of the open and fingered strings is measured and compared to theoretical findings. The following functional model proves as promising: The decay of the total signal is ruled by the partial tone with the longest time constant. Live spots are characterised by a merely internally damped fundamental with a relatively long time constant. For explaining dead spots, the frequency-selectivity of the conductance has to be taken into account. As soon as the conductance exceeds a certain threshold for a partial frequency, the corresponding partial tone is "switched off" and the decay of the total signal governed by the subsequent partial. If for instance the fundamental is switched off, the decay of the total signal is determined by the (due to internal damping twice as fast decaying) second partial, *etc.*

The conductance at the string supports can be ascertained by a straightforward experimental procedure. It reflects the cues of vibrations of the instrument structure, which cause of the frequency- and location-dependent support damping of string vibrations. This contribution of the instrument, which adds to the damping mechanisms originating from the string itself, is the origin of dead spots. Thus, for the diagnosis of dead spots, the conductance measured at the neck of an electric bass (and guitar) is a key parameter.

# ZUSAMMENFASSUNG

## *Dead Spots elektrischer Bässe. II. Diagnose*

Die vorliegende Studie behandelt Elektrobässe mit Solid-Body. Fünf Instrumente unterschiedlicher Bauweise (mit oder ohne Wirbelbrett, aus Holz oder kohlefaserverstärktem Kunststoff gefertigt, Hals an den Korpus geschraubt oder geleimt, vier bis sechs Saiten) dienen als Messobjekte; vgl. Kapitel 2. Spieler solcher Bässe schätzen ein langes Nachklingen des Saitensignals als Qualitätsmerkmal. Es gibt jedoch Stellen auf dem Griffbrett, an denen für bestimmte Saiten das Signal deutlich rascher als an benachbarten Bündeln abklingt. Diese Erscheinung ist wohlbekannt unter Bassisten, welche die betreffende Stelle als "Dead Spot" bezeichnen. Sie hat ihre Ursache darin, dass die Saite Schwingungen der mechanischen Struktur des Basses hervorrufen kann. In der Folge fließt Energie von der Saite in den Instrumentenkörper. Daraus resultiert eine zusätzliche Dämpfung, die zum schnelleren Abklingen des Saitensignals führt.

Als erstes werden die Strukturschwingungen der Instrumente bestimmt; vgl. Kapitel 3 und 4. Zu diesem Zweck werden "Operating Deflection Shapes" (ODSs; aktuelle Schwingungsmuster) mittels eines Laser Scanning Vibrometers *in situ* gemessen, d.h. der Bass wird in normaler Spielhaltung von einem Spieler gehalten. Die Resultate gleichen den theoretischen Ergebnissen für Biegeschwingungen des Balkens der Lagerungsart gelenkig gelagert-frei. Als objektorientierte Messgröße wird in Kapitel 5 und 6 die mechanische Punkt-Konduktanz an den Auflagern der Saiten ermittelt. Die Konduktanz stellt ein Maß für die (frequenzabhängige) Übertragung von Energie über das betrachtete Auflager, d.h. für eine zusätzliche Auflagerdämpfung, dar. Alle Experimente stimmen darin überein, dass bei einem gut gefertigten Solid-Body Bass die Konduktanz auf dem Griffbrett höhere Werte erreichen kann als am Steg. Das bedeutet, dass die größere Auflagerdämpfung in aller Regel vom halsseitigen Abschluss der Saite herrührt.

Im nächsten Teil werden drei unterschiedliche Dämpfungsmechanismen, die auf die Saite wirken (Luftdämpfung, innere Dämpfung und Auflagerdämpfung), theoretisch behandelt und die zugehörigen Zeitkonstanten abgeschätzt; vgl. Kapitel 7. Dieser Abschätzung zufolge spielt für Basssaiten die (saitenimmanente) viskose Dämpfung durch die umgebende Luft keine Rolle. Die (saitenimmanente) innere Dämpfung bestimmt den Normalfall, in dem die Zeitkonstanten der einzelnen Teiltöne umgekehrt proportional zu deren Frequenz abnehmen. Stellen auf dem Griffbrett, an denen ausschließlich die innere Dämpfung der Saiten wirkt, können als Live Spots bezeichnet werden. Für bestimmte andere Stellen und Frequenzen kann die zusätzliche (instrumentimmanente) Auflagerdämpfung die Zeitkonstanten verkleinern und somit Dead Spots verursachen. Auflagerdämpfung ist eine Eigenheit des Instruments und lässt sich gut durch die Konduktanz beschreiben.

Im Kapitel 8 werden die Ergebnisse von Experimenten an zwei Bässen dargestellt, in denen das Abklingen der Gesamtsignale der leeren und gegriffenen Saiten gemessen und mit theoretischen Befunden verglichen wird. Die folgende Modellvorstellung erweist sich als tragfähig: Das Abklingen des Gesamtsignals wird durch den Teilton mit der längsten Zeitkonstante bestimmt. Live Spots zeichnen sich durch einen ausschließlich infolge innerer Reibung bedämpften Grundton mit relativ langer Zeitkonstante aus. Um Dead Spots erklären zu können, muss die Frequenzselektivität der Konduktanz in die Betrachtung einbezogen werden. Sobald die Konduktanz bei der Frequenz eines Teiltones eine bestimmte Schwelle übersteigt, wird der betreffende Teilton "abgeschaltet" und das Abklingen des Gesamtsignals vom nächsten Teilton geprägt. Wenn beispielsweise der Grundton abgeschaltet wird, bestimmt der zweite (infolge innerer Dämpfung doppelt so schnell abklingende) Teilton das Abklingen des Gesamtsignals, usw.

Die Konduktanz an den Auflagern der Saiten lässt sich mittels eines einfachen experimentellen Verfahrens bestimmen. Sie spiegelt diejenigen Merkmale der Schwingungen der Instrumentenstruktur wider, die ursächlich für die frequenz- und ortsabhängige Auflagerdämpfung der Saitenschwingungen sind. Dieser Beitrag des Instruments, der zusätzlich zu den Dämpfungsmechanismen wirkt, die ihren Ursprung in der Saite selbst haben, ist die Ursache von Dead Spots. Deshalb ist für die Diagnose dieser Dead Spots die Konduktanz, gemessen auf dem Hals eines Elektrobasses (oder einer Elektrogitarre), eine Messgröße von zentraler Bedeutung.

## FOREWORD

The first volume in the new millennium of our anthology on vibroacoustics and psychoacoustic is devoted to the second part of Helmut Fleischer's studies on dead spots of electric basses. While the first part (Vol. 2/99) described structural vibrations, in the second part, compiled in this volume, the diagnosis of dead spots is elaborated.

After a short introduction of the instruments considered in the studies, again the importance of *in-situ* measurements is stressed. In comparison to measurements, in which the instrument is held in normal playing position, the first bending mode is about ten (!) semitones higher when measured on a stand. Therefore, for meaningful measurements, natural boundary conditions are indispensable.

In extended studies of the principle operating deflection shapes Helmut Fleischer reveals that to a first approximation the electric bass can be modelled by a beam of constant bending stiffness that is simply supported at one end (the body) and free at the other end (the neck). Of great practical relevance is the finding that the node does *not* occur at the end of the corpus of the electric bass but rather more "inwards" close to the position of the bridge. Thus, the strings can "see" an immobile termination at the body, but more mobility at locations on the neck, leading to energy losses and hence dead spots.

The neck conductance is ascertained as a good predictor of a dead spot. Musicians will highly welcome Helmut Fleischer's overlay chart which gives clear indications, where in the "conductance landscape", *i.e.* at which fret for which string, dead spots are to be expected.

Since the quality of electric basses depends crucially on long, uniform sustain, the mechanisms of the decay of bass strings are studied in great detail. The internal damping of the strings yields a  $1/f$ -law for the time constant/decay time. Depending on the neck conductance, at a dead spot the first (or even the first two) harmonics can be "switched off". As a consequence of the  $1/f$ -law, the resulting time constant/decay time of the string signal amounts to only a half (or even a third) compared to a live spot. These large differences make clear why negative ratings of electric basses by musicians are centred on dead spots.

The two volumes on dead spots of electric basses by Helmut Fleischer combine theoretical elegance with solid advice for practical musicians. Scholars of mechanical engineering and acoustics will appreciate the theoretical considerations and hints for meaningful measurements. Musicians probably will profit most from the "conductance landscapes" helping them to find a fingering which avoids as much as possible dead spots on their respective instruments. For manufacturers of electric basses (and guitars) scientifically based knowledge is now at hand, to further improve the quality of their products.

Munich, in December 1999

Hugo Fastl

## 1. INTRODUCTION

This is the second part of a study that deals with a phenomenon well known among bass players: dead spots. In contrast to their acoustical sisters, electric basses (comparable to electric guitars) are no longer predominately mere rhythm instruments, but are played sometimes similar to wind instruments or bowed stringed instruments with long-sustaining notes. In principle, this has become possible since solid-body electric instruments are available on the market in which the function of radiating the sound is separate from the function of generating the musical signal. Because the signal is electrically picked up, amplified and electro-acoustically radiated, only the function of its generation is left to the musical instrument itself. There is no intrinsic need to transfer vibrational energy from the string to the body for the sake of radiating sound. Consequently, the energy contained in the string vibration after plucking decays not so fast on an electric bass as on an acoustic one. Or in the words of a bass player: The "sustain" is better on an electric bass than on a comparable acoustic instrument. "Good" sustain. *i.e.* the long decay of the string signal, is regarded as a quality attribute of an electric bass (and guitar, as well).

There are, however, exceptions to the rule of the uniformly "good" sustain. There are locations on the fingerboard where the signal decays much faster than at adjacent frets if a particular string is stopped at a particular fret. Players call this a "dead spot". Dead spots are related to the fact that an instrument body is not rigid but flexible and thus capable to vibrate. This is the reason why Heise (1993) performed modal analysis in order to ascertain the frequencies and shapes of vibration modes of electric basses. Since vibrations of continua, such as the bass structure, are known as very sensitive to the boundary conditions, care has to be taken to ensure "natural" and comparable conditions during the experiments. Laser vibrometry proved as a suitable tool to perform vibration measurements *in situ*, which means with the instrument in normal playing position, and thus to investigate the physical background of dead spots. Results on basses have been published in the first part of this study (Fleischer 1999b) and on electric guitars by Fleischer and Zwicker (1998), Fleischer (1998b) as well available on the World Wide Web; see Fleischer (1999c; in English) and (1999d; in German). There is no doubt that dead spots originate from mechanical vibrations of the instrument structure.

Not every structural vibration of the instrument is relevant for the string. There are two prerequisites for an excitation of a structural vibration and for an interaction with the string vibration:

- The frequency of a string vibration must be close enough to the frequency of a vibration of the instrument structure and
- the excitation must not be located in a node of the structural vibration.

The excitation takes place via the string supports. As a direct measure for the "vibration willingness" of the instrument structure, the mechanical admittance was measured at the points of contact between the strings and the instrument. Its real part, denoted conductance, characterises the energy that flows from the string to the instrument. Two paths are to be studied, the excitation firstly via the bridge and secondly via the neck termination of a string. This means that the bridge as well as the fingerboard including the nut have to be investigated. Fleischer and Zwicker (1996) have reported first steps in this direction on electric basses and guitars. They also used admittance measurements for an extensive analysis of electric guitars (Fleischer and Zwicker (1999)).

Loss of vibration energy means damping. In order to estimate the effect of energy loss via the supports, the different mechanisms of damping acting on a bass string have to be considered. Based on the work of Fletcher (1976, 1977), beside support damping, air friction as well as internal friction are to be studied. Their influence on the temporal decay of the string vibrations shall be subject to a

theoretical investigation. In the light of these considerations, results of experiments, in which the decay times of the string signals of two basses were ascertained, are to be discussed.

A first aim shall be to analyse the relationships between the results of various measurements including

- vibrational shapes and frequencies,
- bridge and neck conductances,
- string signals (vibration spectra versus time) and
- decay times of the string signals

and thus to give hints for better understanding the effect of dead spots. Once the physical background is clear, a tool for diagnosing dead spots is to be found. A functional model is to be formulated which gives an impression on the way, and some quantitative information on to which extent, the vibration of the instrument structure may deteriorate the sustain of an electric bass. The knowledge about the origin of dead spots, and an appropriate diagnostic tool, shall open the way to the final aim of minimising (or even preventing) dead spots.

## 2. INSTRUMENTS UNDER CONSIDERATION

### 2.1. Overview

In Tab. I the parameters of the basses considered in the following are compiled; cf. also Fleischer (1999b) where the same instruments have been investigated and the same numbers have been used. The instruments carry 20 to 24 frets and four to six strings with a vibrating length between 85 cm and 90 cm. They all have solid bodies and are equipped with electromagnetic pick-ups (which are not subject to investigation). The necks are reinforced by an adjustable steel rod. The prices cover the range of one order of magnitude between about 200 Euro and 2000 Euro.

No.	Name	Number of Strings	Number of Frets	String Length	Remarks
1	Action Bass	4	20	86 cm	Neck screwed to the body; copy of a Fender Precision Bass
2	Music Man	5	22	87 cm	Neck screwed to the body; Ernie Ball Sting Ray 5
3	Dyna Bass	4	21	90 cm	Neck glued to the body; Peavey
4	Carvin	6	24	87 cm	Neck glued to the body; LB 76
5	Riverhead	4	24	85 cm	Headless; body and neck from carbon fibre; Headway

*Tab. I. Numbers and main parameters of the basses under consideration.*

### 2.2. Action Bass

The four-string Action Bass (cf. Fig. 1 and No. 1 in Tab. I) is manufactured by an unidentified East German manufacturer and can be regarded as a lower-priced copy of a Fender Bass. The neck is attached to the body by four screws. Experimental results of this instrument have already been published by Fleischer and Zwicker (1996 and 1997).



*Fig. 1. Action Bass (Instrument No. 1).*

### **2.3. Music Man Bass**

The instrument No. 2 is Music Man Sting Ray 5 by Ernie Ball, a higher-priced bass equipped with five strings. The neck is screwed to the body. The wood under the transparent lacquer is visible. Fig. 2 shows a photograph.

### **2.4. Dyna Bass**

The Dyna Bass (cf. Fig. 3 and No. 3 in Tab. I) carries four strings and is manufactured by Peavey. The neck and body are covered by coloured paint and appear as one piece; presumably the neck is glued to the body. Fleischer and Zwicker (1996) have already published results of experiments on this instrument.



*Fig. 2. Ernie Ball Music Man Sting Ray 5 (Instrument No. 2).*

## **2.5. Carvin Bass**

The Carvin LB 76 Bass (cf. Fig. 4 and No. 4 in Tab. I) is six-stringed. The neck and body are painted with the appearance of one single piece. Most probably the body parts are glued from both sides to the extension of the neck. This instrument is high in reputation and price.

## **2.6. Riverhead Bass**

The Riverhead Bass (No. 5 in Tab. I), shown in Fig. 5, is conventionally equipped with four strings. The rest of the instrument, however, appears relatively unconventional. The instrument is headless, *i.e.* the mechanism for the adjustment of the string tension is located at the body-end. The neck and body consist of one common symmetric structure, which is manufactured from plastic-carbon fibre compound material. Of all five basses considered in this report, this one is the most adequate for an Aerospace Faculty because of its material and design.



*Fig. 3. Peavey Dyna Bass (Instrument No. 3).*



*Fig. 4. Carvin Bass (Instrument No. 4).*



*Fig. 5. Headway Riverhead Bass (Instrument No. 5).*

## **2.7. Concluding Remarks**

The ensemble of the basses under consideration comprises different types of instruments. They differ in

- material (wood: No. 1 through No. 4 and carbon fibre: No. 5, respectively),
- fixation of the neck to the body (screwed: No. 1 and No. 2, glued or integrated: No. 3 through No. 5, respectively),
- number of strings (four strings: No. 1, No. 3 and No. 5, five strings: No. 2 and six strings: No. 4, respectively).

Thus, a certain variety of test objects is provided in order to test the applicability of the methods suggested in the following and to yield a certain impression of the behaviour of commercially available instruments.

### 3. OPERATING DEFLECTION SHAPES

In order to measure the structural vibrations of the basses, a Polytec Scanning Vibrometer was used; cf. Fleischer (1999b). Its main part is a laser vibrometer, which determines the velocity of a vibrating surface by means of the Doppler effect. Controlled by a computer, the laser beam is deflected by galvo mirrors and scans the surface of the instrument. If no extreme accuracy is needed, a typical scan lasts only some minutes. This fast non-contact approach offers the possibility to measure *in situ*, that means with the instrument held by a person in normal playing position; cf. paragraph 3.2. Thus, the boundary conditions during the experiment are very close to the "natural" conditions. For comparison, the same instrument is investigated in a guitar stand (paragraph 3.3) and the different results compared in paragraph 3.4.

#### 3.1. Measuring Set-up and Procedure

The vibrometer measures the component of the surface velocity in the direction of the laser beam. The velocity is derived from the shift of the frequency of the reflected light relative to the frequency of the original laser light. As a rule, the reflection from the bass surfaces proved as strong enough to evaluate the Doppler effect, *i.e.* the shift of the light frequencies, and to yield a satisfactory signal-to-noise ratio.

In these experiments, the vibration was quantified by the velocity measured on the surface of the bass, normalised to the exciting force. An electrodynamic vibrator (shaker) was used to excite the instrument to vibrate. In order to simulate an excitation via the head-end string termination, the shaker was pressed against the rear of the neck close to the seventh fret. The force was measured by a B&K piezoelectric force gauge and a B&K charge amplifier. In the data processing system of the Scanning Vibrometer a dual-channel FFT was performed and the frequency response function (FRF) computed, which gave the ratio of the velocity and the excitation force. The result was a complex transfer admittance for each measuring point.

All transfer functions are stored and processed by the computer of the measuring system. They can be averaged to serve as a basis for selecting the evaluation bands, *i.e.* the frequencies for which the vibrational patterns are to be displayed. The direct results of the vibrometer measurements, which shall be presented in the following, are not modes in the closer sense, but operating deflection shapes (ODSs; cf. Richardson (1997)). They reflect the state in which the instrument vibrates at the selected frequency at the underlying boundary conditions and excitation. Neither the modal frequency (eigenfrequency) nor the modal damping, as calculated by Modal Analysis, are immediately available. The FRFs represent a superposition of the contributions of all modes and are not subject to a sophisticated decomposition. Nevertheless, the higher a maximum in the FRF is, the more dominates one mode and the less contribute the remaining modes. That means, if the frequency is thoroughly chosen from a peak in the FRF, it may serve as a good estimate for the eigenfrequency. Analogously, the displayed ODS may serve as a good estimate for the corresponding mode shape. In the following, the most essential ODSs are selected and displayed using the standard software of the Scanning Vibrometer. The original results are scaled in m/s per N or s/kg. Thus, the velocity refers to the excitation force 1 N acting at the neck close to the seventh fret perpendicular to the fingerboard plane.

### 3.2. Results of *In-situ* Experiments

The Action Bass No. 1 serves as an example to illustrate typical results. Further data for the other basses can be taken from Fleischer (1999b). As an excitation signal, white noise from a B&K 1405 generator was transduced by a B&K mini-shaker. Each measurement was four times averaged. By using 200 frequency lines in the range from 0 Hz to 500 Hz a frequency resolution of 2.5 Hz was achieved. The velocity was measured on a grid of 202 points. A sitting person held the bass during the whole experiment in playing position on his right thigh with the left hand grasping the neck at the lower frets. The shaker acted on the neck from the rear side in the vicinity of the seventh fret. The bass body was lying with its lower part on the thigh of the person. The right arm of the person was resting on the upper part of the bass body. The left hand was grasping the neck near the lower frets. The individual measuring situation can be taken from Fig. 6. This configuration was not changed during the measuring procedure.



*Fig. 6. Action Bass No. 1 including measuring grid during the in-situ determination of the operating deflection shapes by means of the Scanning Vibrometer.*

The whole of the results is characterised in Fig. 7 by the average of all measured frequency response functions. The maxima of the magnitude typically reach 5 ms/kg through 10 ms/kg. As an

example, at 295 Hz the average velocity is about 7 mm/s for 1N excitation force. The arrows in Fig. 7 mark the peaks, which served as indicators for the main resonances. Four frequencies were chosen for presentation. The corresponding vibrational patterns are compiled in Fig. 8.

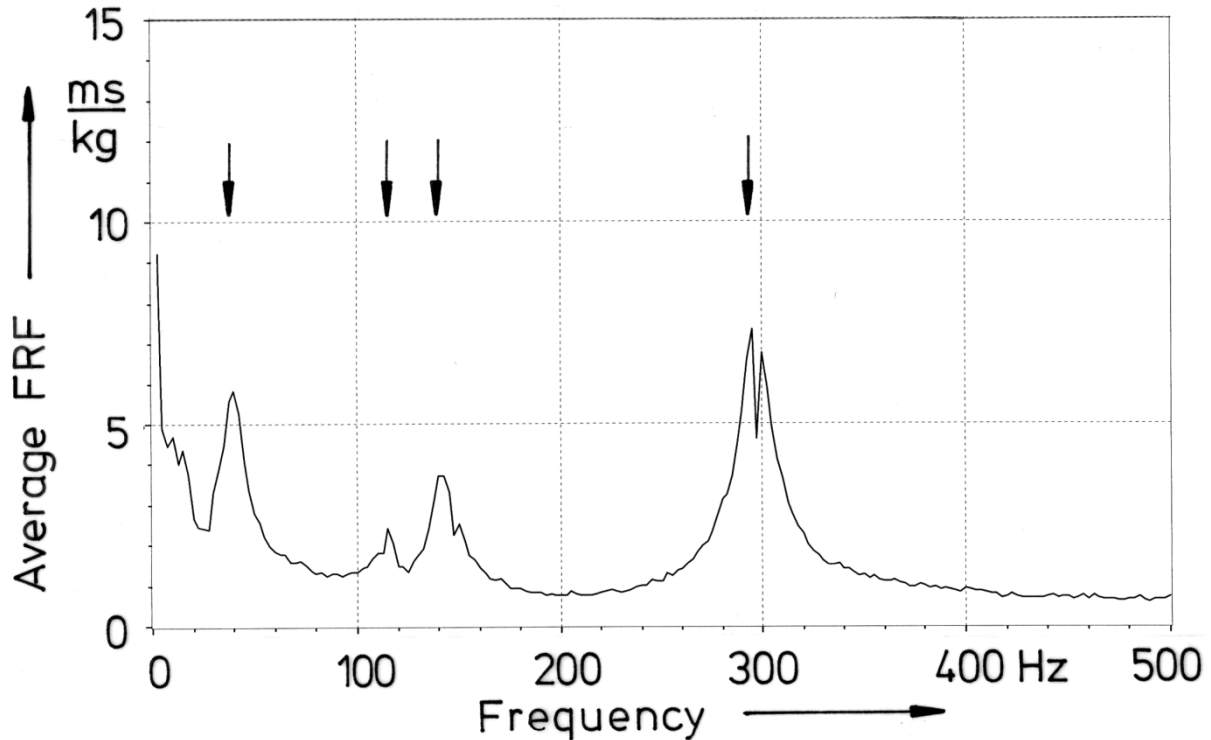


*Fig. 7. Average frequency response function (velocity at all points normalised to the excitation force as measured with the bass held by a person) of the Action Bass No. 1. The arrows mark the frequencies chosen for the visualisation of four main operating deflection shapes.*

The magnitude of the velocity, normalised to an excitation force of 1 N, is coded in black and white tones which creates pictures comparable to Chladni figures; cf. Chladni (1787). It is useful to imagine that a white bass is covered with black powder. The bass is vibrating with the given frequency and the powder grains move to locations where the instrument is not in motion. This way, the nodes become visible as black portions and the antinodes as white portions. For the sake of simplicity, the gauges that indicate the quantitative values are dropped in the following images.

In Figs. 8a - d four typical results are displayed. The frequency of the ODS in Fig. 8a is 40 Hz, *i.e.* close to the fundamental of the open E string (41 Hz). The frequencies of the remaining three ODSs range from 115 Hz (G string 3<sup>rd</sup> fret) to 295 Hz (G string 19<sup>th</sup> fret). Three fundamental vibrational patterns are observed with a node (Fig. 8a), an antinode (Figs. 8b and 8c) and a node again (Fig. 8d) in the vicinity of the grasping left hand. The differences between the ODSs, which belong to the same main type (Figs. 8b and 8c), are minor. For instance, they represent either an in-phase or an anti-phase motion of the body horns or an additional torsion of the neck, which superimposes the fundamental bending motion.

*Fig. 8a.*  
40 Hz

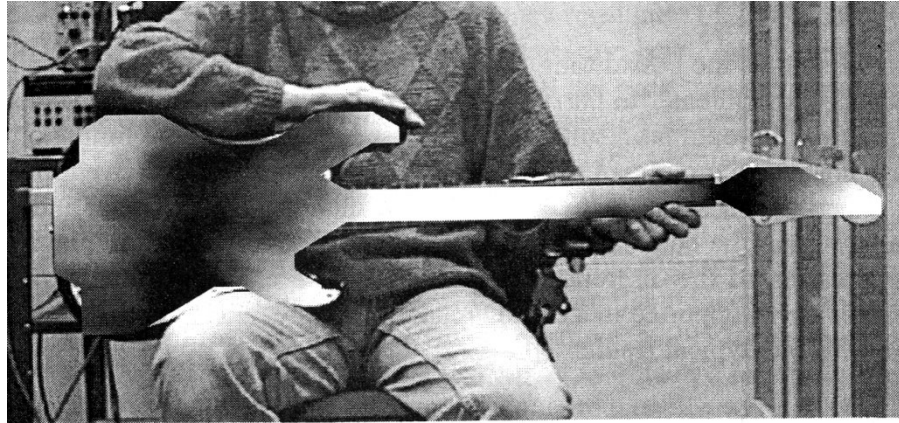


*Fig. 8b.*  
115 Hz

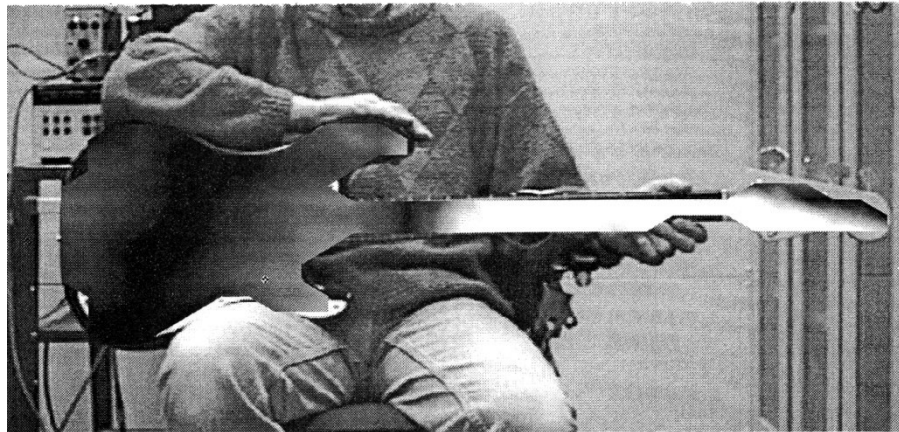


*Fig. 8c.*  
150 Hz



*Fig. 8d.*  
295 Hz



*Fig. 8. In-situ operating deflection shapes (vibration patterns for the announced frequencies) of the Action Bass No. 1 held by a person. Black areas indicate a low vibration magnitude, white areas a high magnitude.*

### 3.3. Results of In-stand Experiments

A person who holds the bass during the measuring procedure ensures realistic boundary conditions but forces the experimenter to hurry. For instance, the advantages of enhanced data acquisition and remeasuring of non-optimal results cannot be used because of time limitation. Since the measuring time plays not such a prominent role as in an *in-situ* experiment, a conventional measurement with a suitable experimental set-up would offer higher quality. The price for increased precision of the data would be that the boundary conditions could differ from those in playing practice. In order to get an impression of the discrepancies that have to be expected some experiments were made in which basses were supported in a commercially available guitar stand. Again, the Action Bass No. 1 is used to illustrate typical results.



*Fig. 9. Action Bass No. 1 including measuring points during the in-stand determination of the operating deflection shapes by means of the Scanning Vibrometer.*

The individual measuring situation can be taken from Fig. 9. The bass was positioned upright in a guitar stand made from metal tubes to which it had contact at the lower part only. A refined mesh of 567 measuring points was used. Pseudo-random noise from a hp 33120A arbitrary waveform generator served as an excitation signal. Each measurement was ten times averaged. 400 frequency

lines in the range from 10 Hz to 1000 Hz resulted in a frequency resolution of 2.5 Hz. The vibration was excited by a LDS V 406 shaker, which acted via a transmission beam on the rear side of the neck in the vicinity of the seventh fret. The force transmitted to the neck was measured by a force gauge between the end of the beam and the bass neck. The force gauge was pressed against the neck in such a way that the body was about 5 mm lifted off from the upper contact point of the guitar stand. Thus, the stand supported the bass at two points at the bottom edge of the body.

A survey on the results is given in Fig. 10 by the magnitude of the average frequency response function. A comparison to the *in-situ* results of Fig. 7 reveals a similar frequency dependence but more pronounced maxima which may reach 15 ms/kg. As an example, at 295 Hz the average velocity is about 16 mm/s for 1N excitation force compared to 7 mm/s as obtained for the *in-situ* experiment. The arrows in Fig. 10 indicate the main resonances. Four frequencies were chosen for presentation which correspond to the frequencies found in the *in-situ* measurement. The vibrational patterns are compiled in Fig. 11.

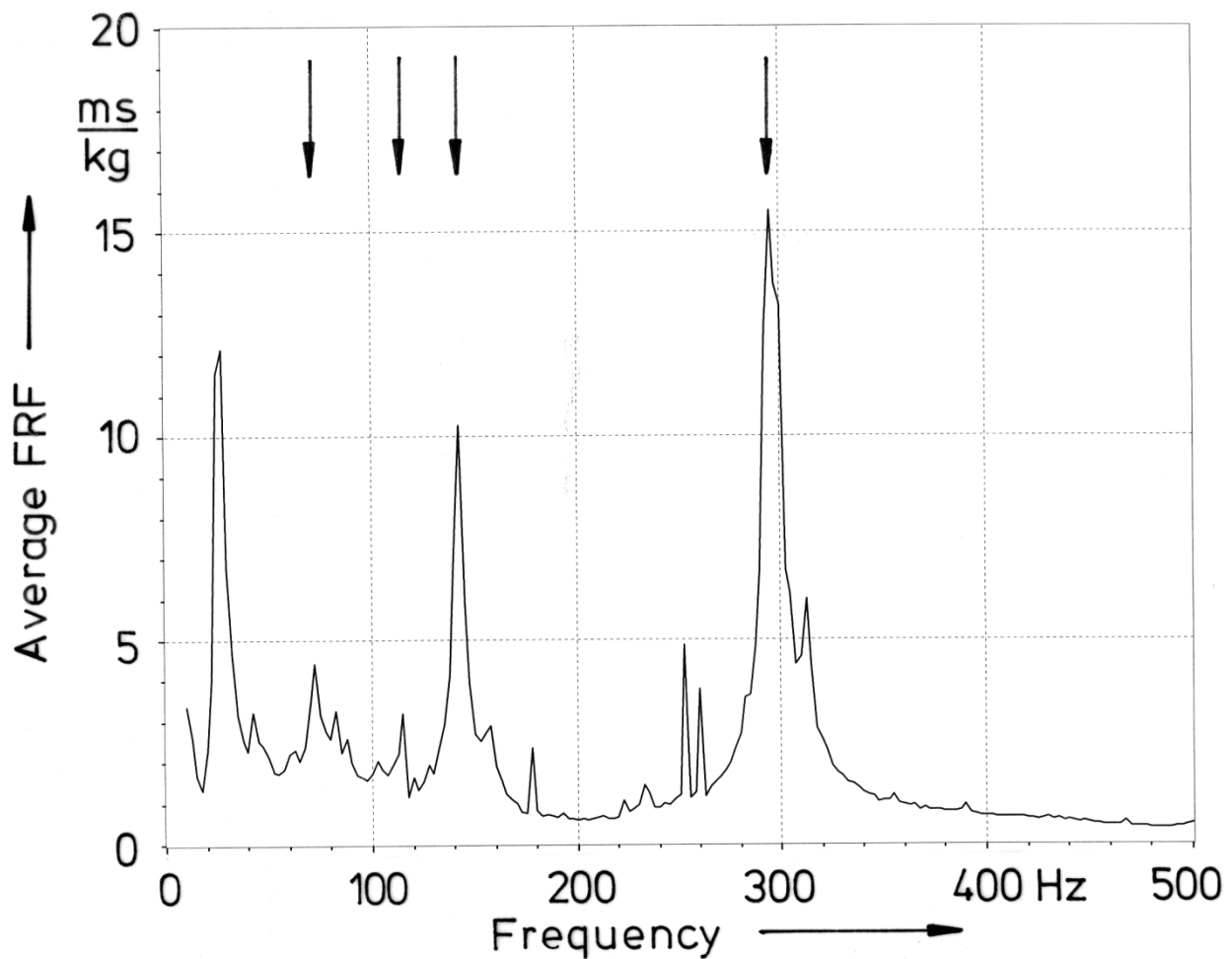
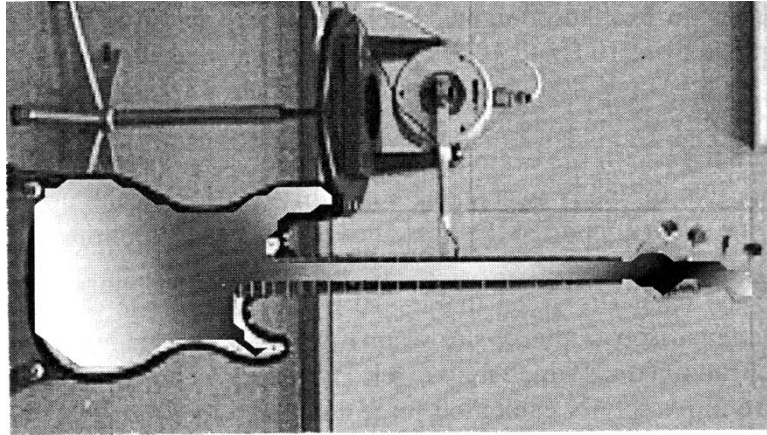


Fig. 10. Average frequency response function (velocity at all points normalised to the excitation force) of the Action Bass No. 1 as measured between 10 Hz and 500 Hz with the bass in a guitar stand. The arrows mark the frequencies chosen for the visualisation of four main operating deflection shapes.

For better comparison to Fig. 8 the diagrams in Fig. 11 are rotated by 90 degree. Again, the interpretation may be facilitated by the imagination that a white bass, covered with black powder, is vibrating with the announced frequency. The powder grains move to locations where the instrument is not in motion. Consequently, the nodes become visible as black portions and the antinodes as white portions.

*Fig. 11a.*  
72 Hz



*Fig. 11b.*  
115 Hz

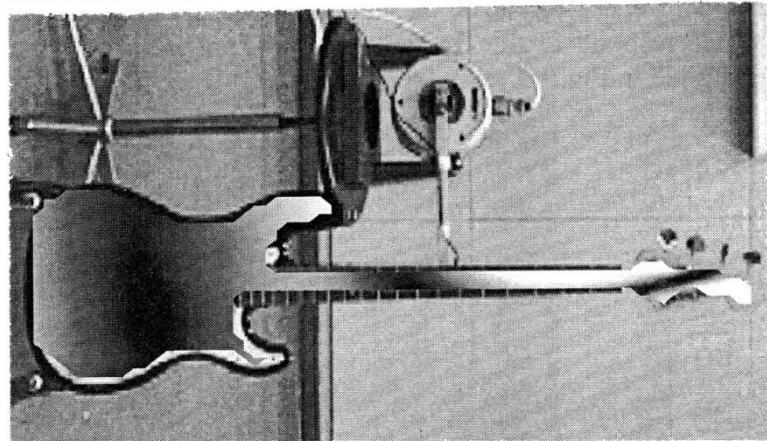


*Fig. 11c.*  
143 Hz

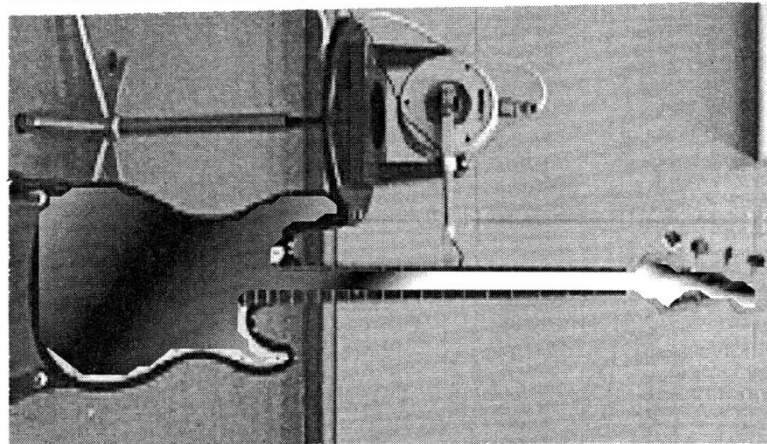


*Fig. 11d.*  
295 Hz

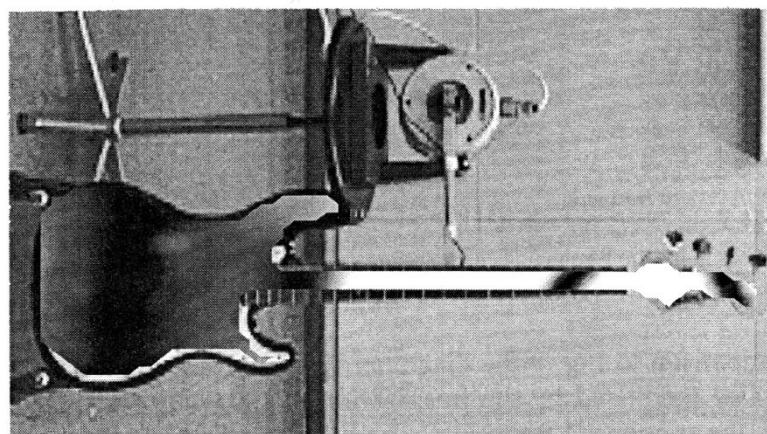


*Fig. 11. In-stand operating deflection shapes (vibration patterns for frequencies up to 500 Hz) of the Action Bass No. 1 in a guitar stand. Black areas indicate a low vibration magnitude, white areas a high magnitude.*

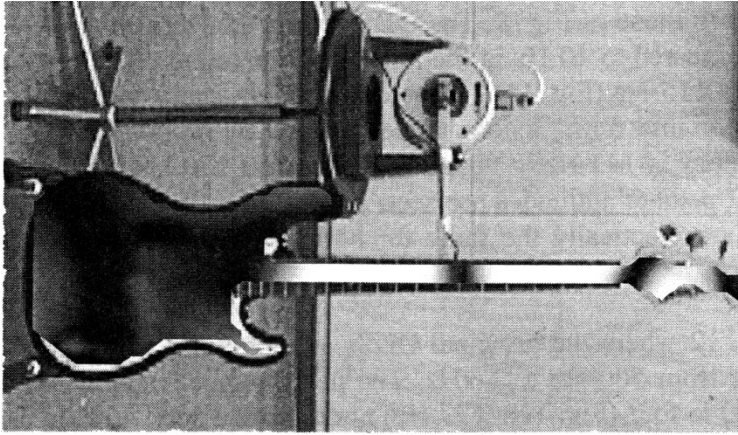


*Fig. 12a.*  
530 Hz

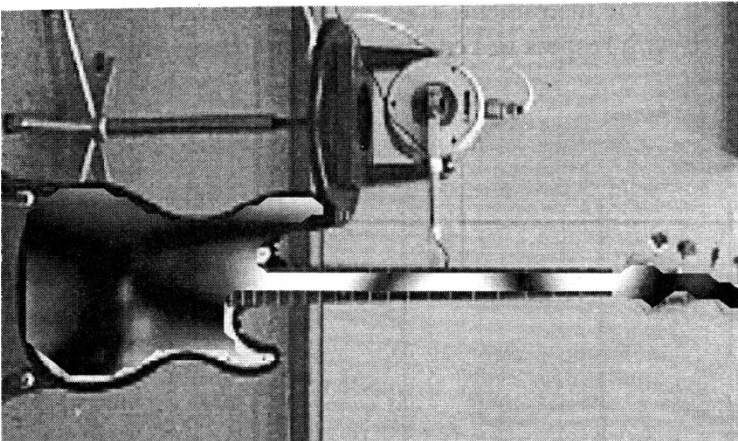


*Fig. 12b.*  
677 Hz.

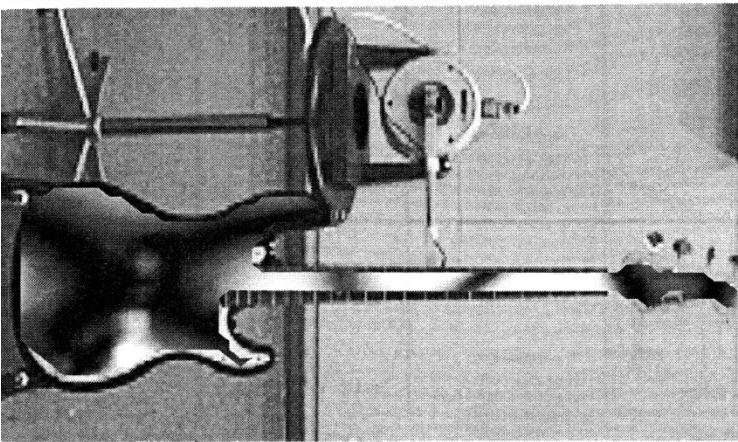


*Fig. 12c.*  
780 Hz.

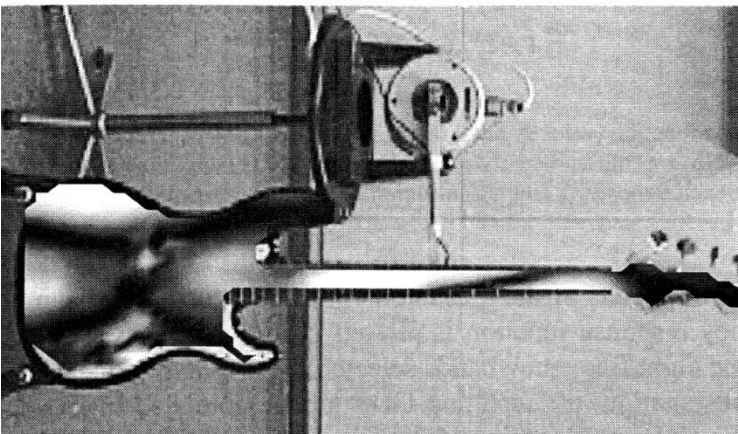


*Fig. 12d.*  
900 Hz.

*Fig. 12. In-stand operating deflection shapes (vibration patterns for frequencies between 500 Hz and 1000 Hz) of the Action Bass No. 1 in a guitar stand. Black areas indicate a low vibration magnitude, white areas a high magnitude.*

Apart from the absolute amplitude and - at least in some cases - frequency values, the patterns displayed in Fig. 11 are similar to those of Fig. 8. The ODS in Fig. 11a exhibits a node at the lower frets and occurs at 72 Hz (compared to 40 Hz in the *in-situ* measurement). The pattern and the frequency of the second ODS at 115 Hz (Fig. 11b) coincide for the in-stand and the *in-situ* measurement; a node is observed at the mid frets. Bending superimposed by pronounced torsion shows up in Fig. 11c, where the frequency is 143 Hz in the stand rather than 150 Hz for the *in situ* case. At 295 Hz two nodes with intermediate antinodes are seen on the neck. While the amplitudes differ, the shapes and frequencies are practically the same for both support types. A direct comparison shall be given in paragraph 3.4.

This series continues in Fig. 12 where the principal ODSs are compiled which were found in the consecutive frequency range from 500 Hz to 1 kHz. The node number increases by steps of one from three (Fig. 12a: 530 Hz) to four (Fig. 12b: 677 Hz) nodes on the neck. Finally, as much as six nodes occur over the total length of the instrument. The ODS at 780 Hz (Fig. 12c) and 900 Hz (Fig. 12d) prove as related to Fig. 12b with respect to bending. The differences result from superimposed torsion.

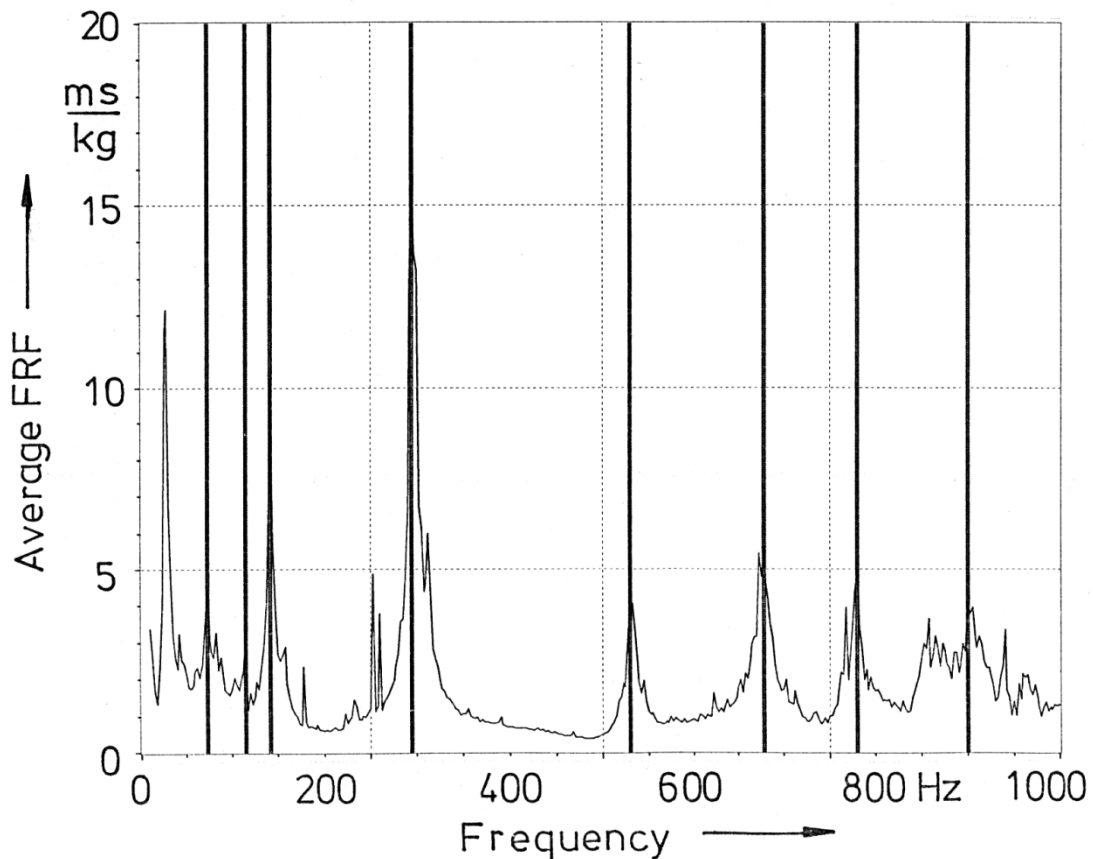
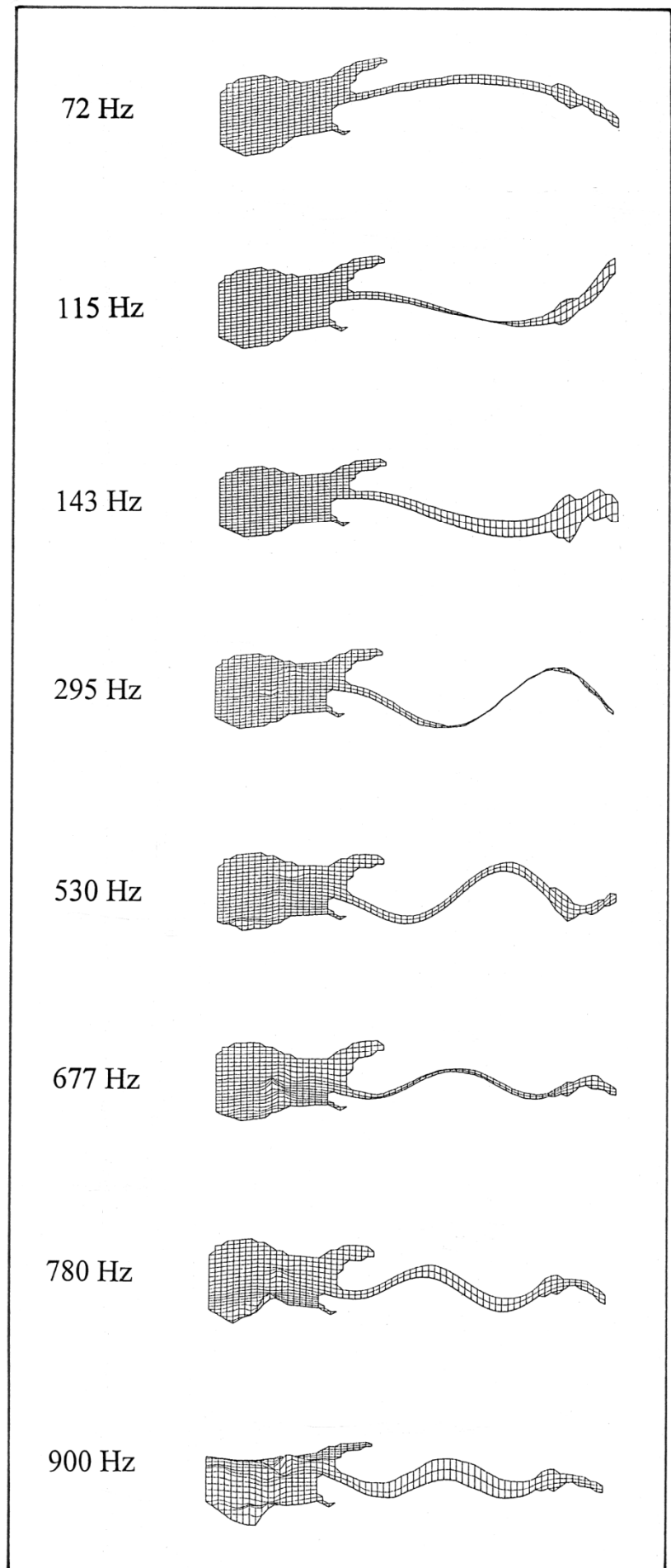


Fig. 13. Average frequency response function (velocity at all points normalised to the excitation force as a function of frequency) of the Action Bass No. 1 as measured between 10 Hz and 1000 Hz with the bass in a guitar stand. The stripes mark the frequencies chosen for the visualisation of the main operating deflection shapes.

An overview on the experimental results of the measurement in the guitar stand can be taken from Fig. 13. The average frequency response function is plotted versus frequency between 10 Hz and 1000 Hz. Dark stripes mark the eight frequency bands selected for displaying the vibration patterns. In order to complete the representation, the resulting ODS are accumulated in Fig. 14 as 3D-diagrams. In conjunction with the Chladni diagrams of the Figs. 11 and 12, the 3D-representation of Fig. 14 provides a comprehensive visualisation of the vibrations of the instrument.

*Fig. 14. In-stand operating deflection shapes (vibration patterns) for the given frequencies of the Action Bass No. 1 as measured between 10 Hz and 1000 Hz with the bass in a guitar stand.*



In particular, it becomes obvious which main components (bending and torsion) dominates the corresponding ODS. From Fig. 14 a series of fundamental bending modes can be taken. The number of nodes in the total length of the instrument increases in steps of one from two nodes (72 Hz) over three nodes (115 Hz and 143 Hz), four nodes (295 Hz), five nodes (530 Hz) up to finally six nodes (677 Hz, 780 Hz and 900 Hz). Similar ODSs, which occur at different adjacent frequencies, prove as variants of the same bending mode but superimposed by torsion. Examples are the two ODSs at 115 Hz and 143 Hz, respectively, as well as the three ODSs at 677 Hz through 900 Hz. The distinction between bending and torsion might be relevant for the motion of the end supports of the strings. If bending dominates, the motion at a distinct fret shall be the same for all strings. In the case of torsion, however, at one and the same fret the different strings might "see" different magnitudes and phases of motion at their neck-end supports. As can be taken from Fig. 14, although bending plays the major role, in some cases torsion has to be taken into account. This means that the mobility of the neck could exhibit a lateral dependence.

### 3.4. Comparison of *In-Situ* to In-stand Results

It has proved as possible to measure the structural vibrations of plucked string instruments *in situ*, that means held by a player. Examples of *in-situ* experiments on acoustic guitars have given by Fleischer (1997b, 1998a) and on electric guitars by Fleischer (1998a, 1999a) as well as Fleischer and Zwicker (1997, 1998). The vibrations of electric basses have already formerly been measured *in situ* for instance by Fleischer (1998a, 1999b). This method fulfils an essential prerequisite for relevant vibration measurements: The test object is acting under realistic boundary conditions. A certain shortcoming is that, because a person can hold the instrument without greater lateral displacement not for hours but only for several minutes, the measuring time is intrinsically limited. As a consequence, signal enhancing by extensive averaging as well as remeasuring non-optimal results is also limited. The experiences confirm that, nevertheless, the method yields reliable and reproducible results. However, further optimisation of the experimental data as well as an approach, which does not afford human resources, could be desired.

A lot of efforts have been undertaken to find an experimental set-up in which the bass can be supported such that the boundary conditions are close to those *in situ*. The best results obtained until now have been measured by means of the guitar stand as described in the previous paragraph. The bass is in upright position. The body is supported at two points by the guitar stand, and the neck rests on the force gauge at the rear side. Results acquired by this support are compiled in the right column of Fig. 15 and compared to the corresponding ODSs and frequencies gained *in situ* (left column of Fig. 15). As already mentioned in paragraph 3.3, the vibration amplitudes are regularly higher for the in-stand measurements than for the *in-situ* experiments. This means that, if quantitative data are needed, the experimental set-up shown in Fig. 9 yields unrealistically high values. Obviously, if the bass is held by and against a human body, the damping is considerably higher - and consequently the vibration amplitudes lower - than it is if the bass is resting in a guitar stand. In Fig. 15 the amplitudes are normalised in such a way that these discrepancies do not show up.

As a positive result of the comparison, a comprehensive coincidence between the ODSs measured with the bass held by a person and in a guitar stand, respectively, can be taken from Fig. 15. The differences in the vibration shapes are only minor. The more the frequency increases, the less important are the boundary conditions, and the higher becomes the global similarity of the corresponding ODSs. This means that, as long as the higher modes are in the focus of interest and if high spatial resolution and accuracy are needed, a measurement of the bass positioned in a guitar stand could be superior to an *in-situ* measurement.

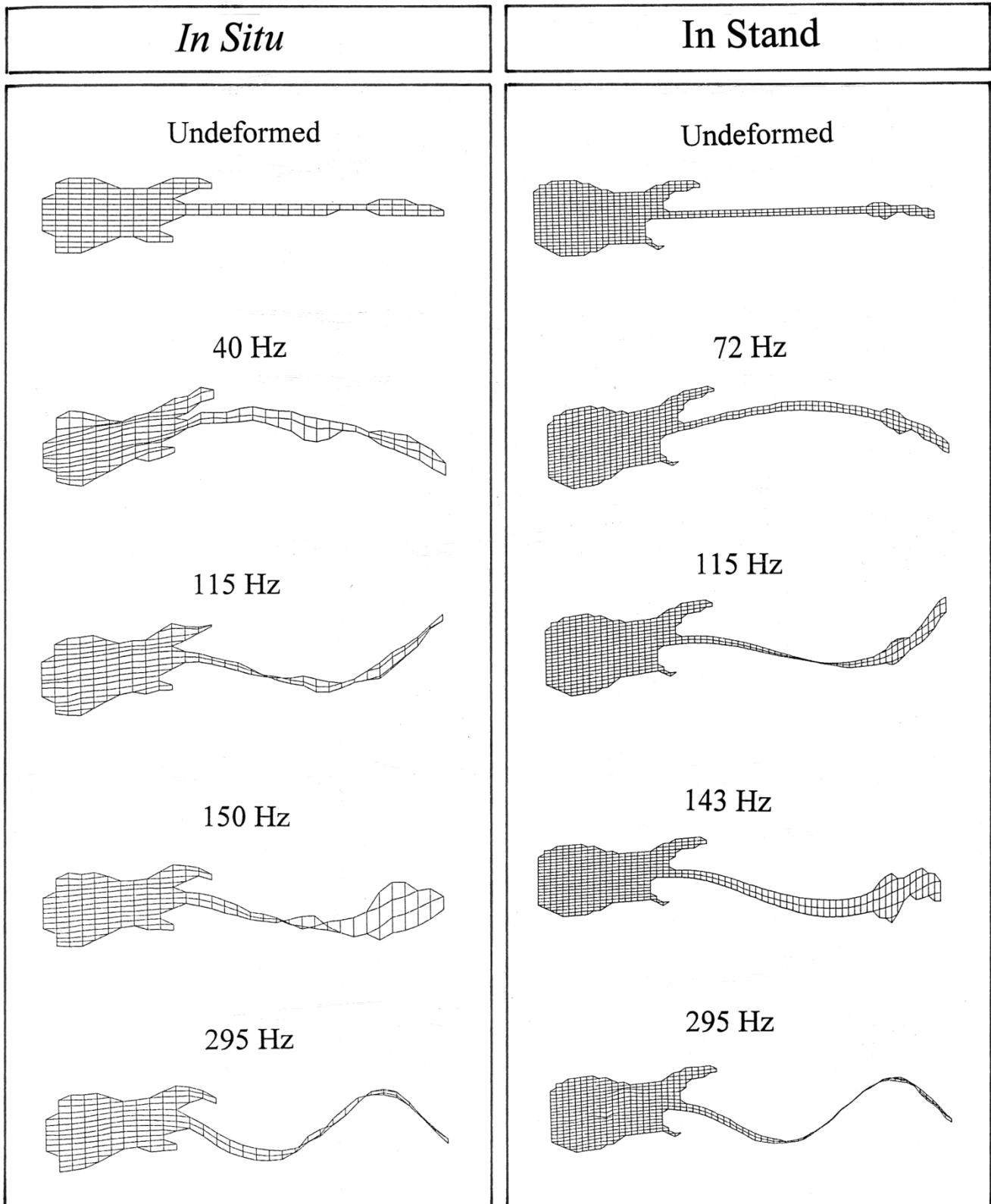


Fig. 15. Operating deflection shapes of the Action Bass No.1 including the undeformed structure.  
 Left column: measured with the bass held by a person (in situ);  
 right column: measured with the bass in a guitar stand.

It is common practice to extract the frequencies, for which the ODSs are displayed, by evaluating the maxima of the average frequency transfer function; cf. Figs. 7, 10 or 13. The frequencies of the

maxima are added to the corresponding vibration patterns in Fig. 15. With respect to these frequencies, only a partial coincidence is observed with the tendency to increase with growing frequency. The most prominent deviation is found for the first bending mode. When measuring *in situ*, its frequency is 40 Hz, while the in-stand measurement yields 72 Hz. This difference of 80% is not acceptable in most cases, particularly not when dealing with a bass for which almost an octave in the range of the lower notes is a too big uncertainty. The higher the number of nodes grows, the smaller becomes the discrepancy of the corresponding frequencies. It is a well-known matter of fact that the higher the number of a vibration mode is, the less it is influenced by the boundary conditions. The question remains, whether the higher or the lower modes are more important. In the present case of a bass, the lower modes are undoubtedly of higher interest. From this reason, the *in-situ* approach is preferred as long as no realistic experimental set-up is available which simulates the "human" boundary conditions to a satisfactory extent.

### 3.5. Concluding Remarks

Different experimental procedures have been tested with the aim to find a possibility to determine the resonance frequencies and vibration pattern which are relevant for the bass in musical practice. Although measurements with the bass resting on a guitar stand yield results of high resolution and precision, it was decided to prefer *in-situ* experiments. If during the measurement a person holds the bass, the boundary conditions are much closer to the conditions in normal playing practice than they are in a "non-human" experimental set-up. The shortcomings of the *in-situ* approach - such as crude spatial resolution and incomplete signal enhancement as a consequence of the limited measuring time - are obvious. However, they are not such severe that they could dominate the benefit of "natural" boundary conditions. That is why in all experiments described in the following the instruments shall be held by a person in playing position. Since in all experiments the boundary conditions (including the damping by the player's body) are comparable, the necessary prerequisite is provided for relating the different experimental results.

## 4. COMPARISON OF THE PRINCIPAL ODSs

In the present chapter the most prominent types of ODSs in the range up to 500 Hz are extracted, identified and structured. For this purpose, the experimental results of the *in-situ* measurements are visualised as 3D-meshes (as already practised in Figs. 14 and 15). The bass is viewed from the side such that a straight line represents the undeformed structure. In order to focus on the consequences of the vibrations of the instrument structure for the strings, the string supports are emphasised. The body-end of the strings, always defined by the bridge, is marked by a triangle. The neck-end of the strings is terminated by the nut or where the player fingers a string and presses it against a fret. Thus, the neck-end string support is situated somewhere along the fingerboard which is symbolised by the bold part of the line.

### 4.1. ODSs of the Action Bass

The six ODSs of the Action Bass No. 1 are compiled in Fig. 16. The measuring grid can be taken from Fig. 6 and, for comparison, the grey tone representation from Fig. 8. It becomes obvious that within the frequency range up to 500 Hz there are three main types of vibration:

- A first type (ODS I) at 40 Hz,
- a second type (ODS II) at 115 Hz, 142 Hz and 150 Hz and
- a third type (ODS III) at 295 Hz and 300 Hz.

The different main types are characterised by a fundamental bending motion with a growing number of nodes. The variants differ in a superimposed torsion or in bending of additional parts, *e.g.* the horns, which may vibrate out of phase or in phase with respect to the main body motion. In the following, the consideration is restricted to the principal bending motion. If a peak in the average FRF (cf. Fig. 7) has more than one local maximum, the ODS shall be discussed for the frequency for which the highest value is observed.

According to Fig. 7 the average FRF exhibits three main clusters of maxima. The values are highest for the frequencies  $f_1 = 39.7$  Hz,  $f_2 = 141.7$  Hz and  $f_3 = 294.7$  Hz. These frequencies are related by the ratios 1 : 3.57 : 7.42. As can be taken from the corresponding vibration patterns in Fig. 16, apart from the first mode (ODS I) the instrument does hardly move at the bridge (indicated by the triangle). On the fingerboard (bold line) there are no nodes (ODS I), one node (ODS II) and two nodes (ODS III), respectively.

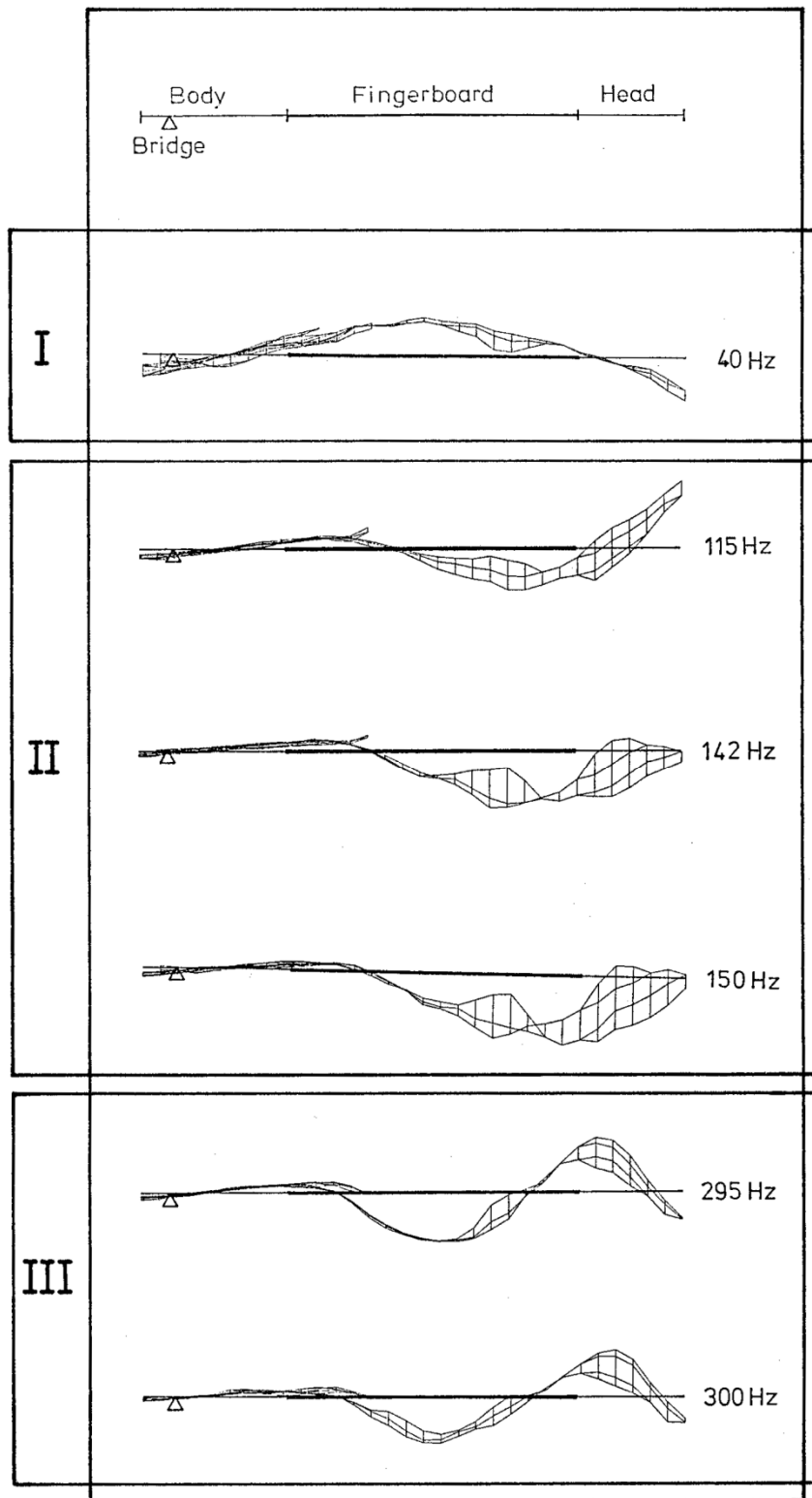


Fig. 16. ODSs of the Action Bass No. 1, measured in situ.

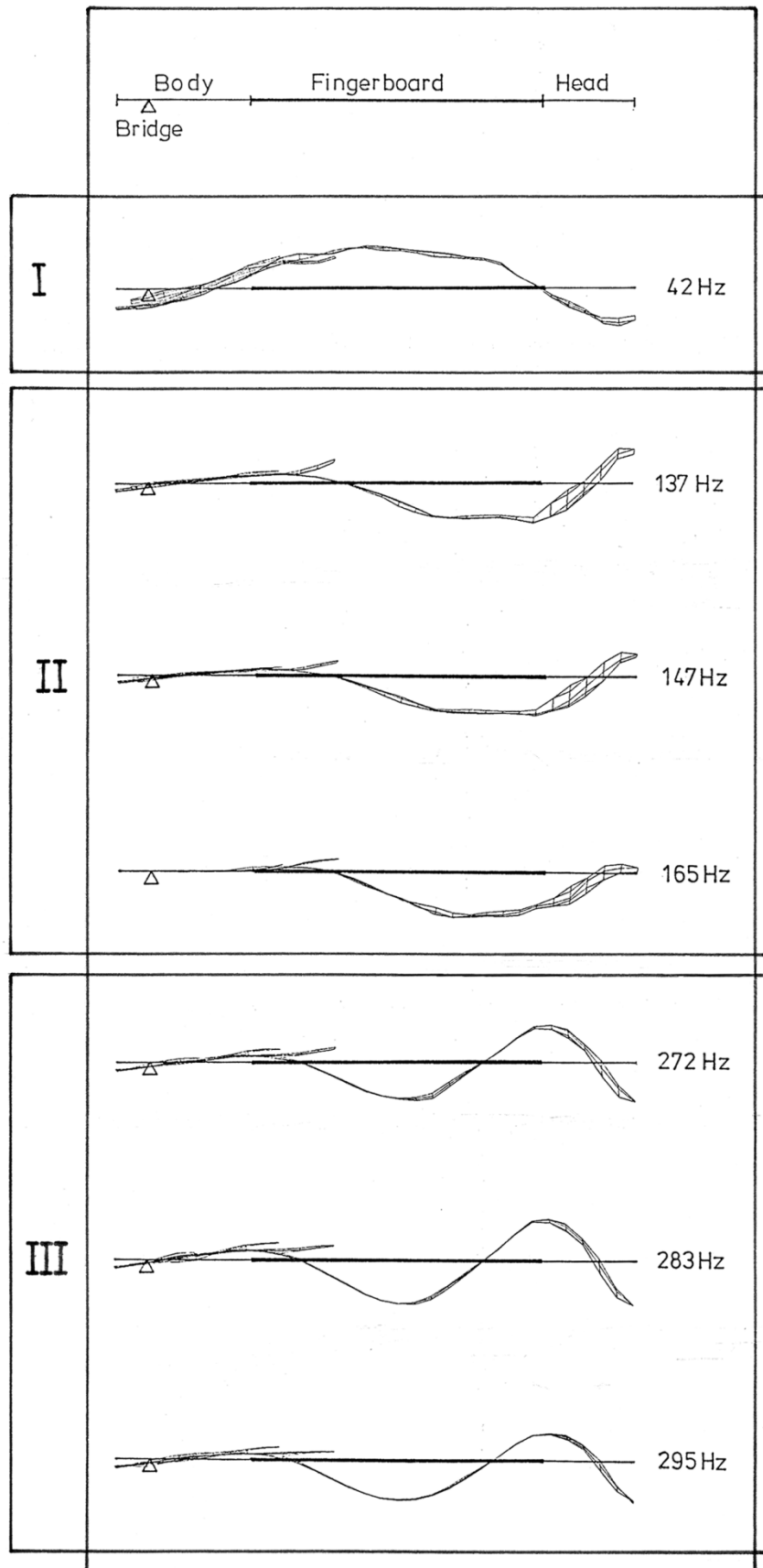


Fig. 17. ODSs of the Music Man Bass No. 2, measured in situ.

## 4.2. ODSs of the Music Man Bass

Fig. 17 refers to the instrument No. 2. The average FRF has three main maxima (cf. Fleischer 1999b) which are related to three main types of vibration:

- ODS I at 42 Hz,
- ODS II at 137 Hz, 147 Hz and 165 Hz and
- ODS III at 272 Hz, 283 Hz and 295 Hz.

The exact frequencies at which the highest peaks occur are  $f_1 = 42.3$  Hz (ODS I),  $f_2 = 137.5$  Hz (ODS II) and  $f_3 = 282.8$  Hz (ODS III). These frequencies are in the ratios 1 : 3.25 : 6.69. The respective three vibration patterns are among the seven ODS displayed in Fig. 17. The vibration shapes and frequencies are comparable to the ODSs of the Action Bass (Fig. 16), but differ in some details. Again, the bridge proves as relatively immobile with the exception of ODS I. On the fingerboard there are one node at the nut (ODS I), one node at the higher frets (ODS II) or two nodes (ODS III). Torsion is less pronounced for the Music Man Bass (Fig. 17) than for the Action Bass (Fig. 16).

## 4.3. ODSs of the Dyna Bass

Nine ODSs are compiled in Fig. 18 for the Dyna Bass No. 3. The vibrations are classified into four main types:

- ODS I at 42 Hz,
- ODS II at 120 Hz, 140 Hz, 150 Hz and 169 Hz,
- ODS III at 274 Hz and
- ODS IV at 468 Hz.

The ODS at 88 Hz seems to be a superposition of the types I and II, while the ODS at 417 Hz resembles type III and is characterised by a strong additional torsion.

The average FRF (cf. Fleischer 1999b) has shown three pronounced maxima and several additional peaks. Four main peaks are extracted with the frequencies  $f_1 = 42.5$  Hz,  $f_2 = 139.5$  Hz,  $f_3 = 273.6$  Hz and  $f_4 = 468.5$  Hz. This corresponds to the ratios 1 : 3.28 : 6.44 : 11.02. The respective four vibration patterns are included in Fig. 18. ODS I, II and III compare to what was found for the Action Bass (Fig. 16) and Music Man Bass (Fig. 17). In some cases the bridge proves to be relatively mobile, for instance at 88 Hz. On the fingerboard there are no (ODS I), one (ODS II) or two (ODS III) nodes. This series continues with a vibration pattern, which exhibits a further node. This ODS IV had not yet been observed during the investigation of the basses No. 1 and 2.

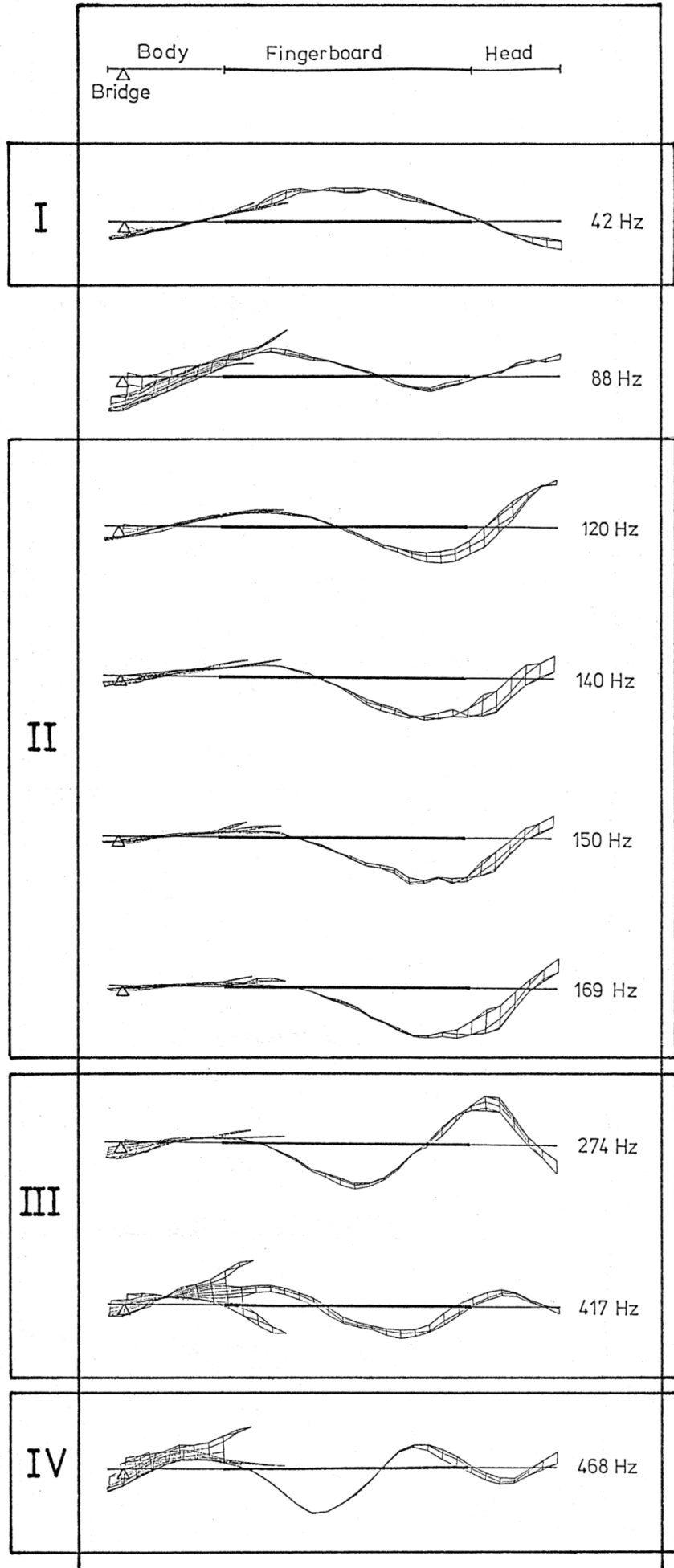


*Fig. 18. ODSs of the Dyna Bass No. 3, measured in situ.*

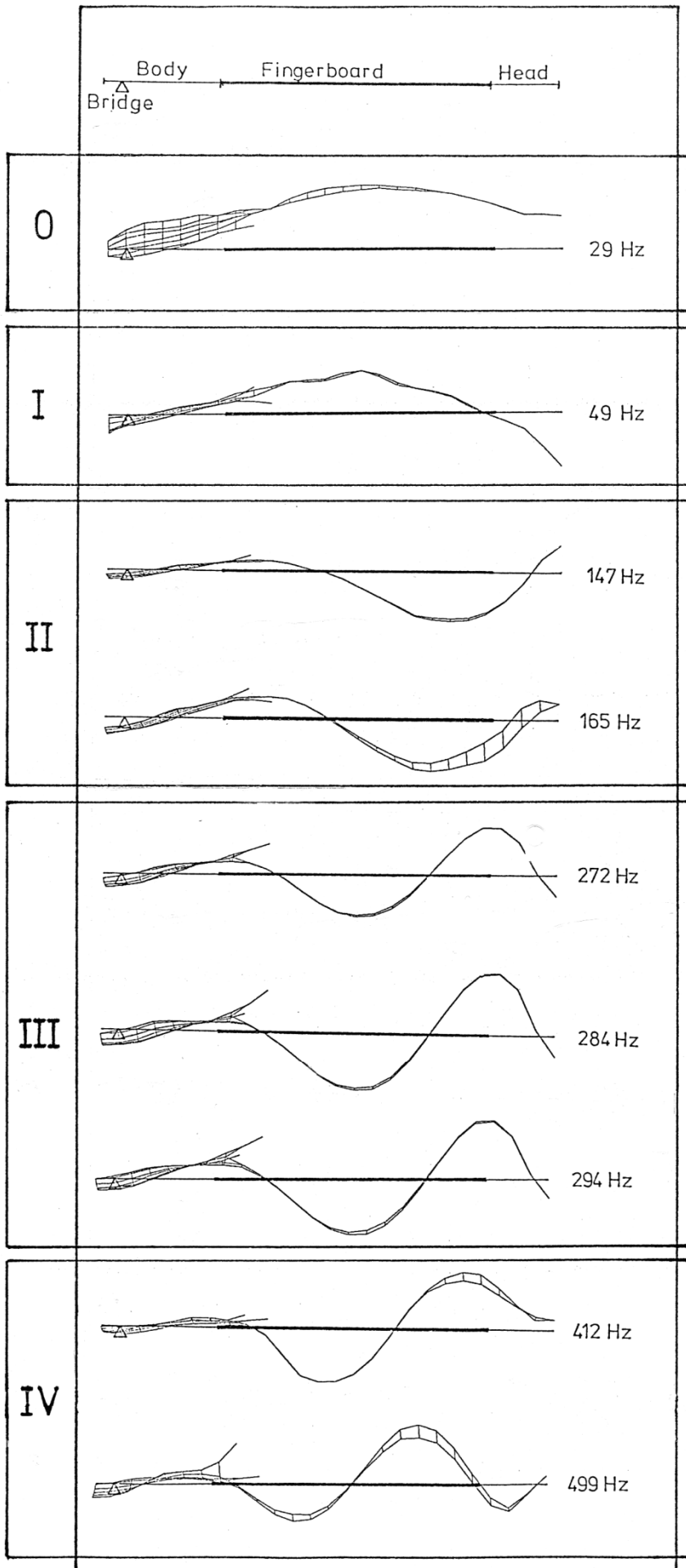


*Fig. 19. ODSs of the Carvin Bass No. 4, measured in situ.*

## 4.4. ODSs of the Carvin Bass

Nine ODSs of the Carvin Bass No. 4 are compiled in Fig. 19. Five main types of vibration can be extracted:

- ODS 0 at 29 Hz
- ODS I at 49 Hz,
- ODS II at 147 Hz and 165 Hz,
- ODS III at 272 Hz, 284 Hz and 294 Hz and
- ODS IV at 499 Hz.

The ODS at 412 Hz might be a combination of the main types III and IV.

From the average FRF (cf. Fleischer 1999b) a large number of maxima can be taken. Five peaks were selected with the frequencies  $f_1 = 49.1$  Hz,  $f_2 = 147.5$  Hz,  $f_3 = 284.5$  Hz and  $f_4 = 499.4$  Hz. An additional vibration pattern at  $f_0 = 29.2$  Hz is included because it is close to the fundamental frequency of the open B string of this particular six-string instrument. The respective ODS 0 in Fig. 19 resembles the first eigenmode of the clamped-free beam. More probably it represents a rigid body motion superimposed by the first mode (cf. ODS 1 in Fig. 19). If  $f_1$  is used as a normalising value, the frequencies are in the ratios 0.60 : 1 : 3.01 : 5.80 : 10.18. The mid three of the five main types in Fig. 19 were found for all basses. The additional ODS numbered 0 plays no role for the other basses under consideration. ODS IV, however, was also found for the Peavey Bass (Fig. 18). All patterns leave the bridge relatively immobile. On the fingerboard there are no node (ODS 0), one node at the nut (ODS I), one node at the higher frets (ODS II), two nodes (ODS III) or three nodes (ODS IV).

## 4.5. ODSs of the Riverhead Bass

Eight ODSs of the Riverhead Bass No. 5 are listed in Fig. 20 with four main types of vibration:

- ODS 0 at 40 Hz
- ODS I at 51 Hz and 67 Hz,
- ODS II at 202 Hz, 210 Hz and 215 Hz,
- ODS III at 470 Hz.

While these vibrations are dominated by bending, extreme torsion is observed at 421 Hz.

A cluster of maxima at about 200 Hz governs the average FRF (cf. Fleischer 1999b). Within the range up to 500 Hz four local peaks were chosen. The frequencies are  $f_1 = 67.5$  Hz,  $f_2 = 210.0$  Hz and  $f_3 = 470.0$  Hz. In addition, the maximum at  $f_0 = 40.0$  Hz was considered. The corresponding ODS 0 in Fig. 20 makes clear that it represents a rigid body motion in which the bass as a whole is in pendulum motion without flexible bending. With  $f_1$  as a normalising value the frequency ratios 0.59 : 1 : 3.11 : 6.96 are calculated. Three of the four main vibration patterns were found for all basses. The ODS numbered 0 plays no role for the other basses (except the six-string Carvin Bass; cf. ODS 0 in Fig. 19). This rigid body motion, which for the Riverhead Bass occurs at the frequency of the open E string, seems to be typical for this instrument and could be a consequence of the headless design or/and the carbon fibre construction. The further vibration patterns agree with those, which had been observed for the other instruments except the pronounced torsional motion at 412 Hz: A node appears always in the vicinity of the bridge. On the fingerboard there are no (ODS 0), one (ODS 1), two (ODS 2) or three (ODS 3) nodes. Since there is no head, the "head-end" node is placed on the fingerboard with the consequence that - compared to a normal construction - an additional node as well as an additional antinode is located on the fingerboard.

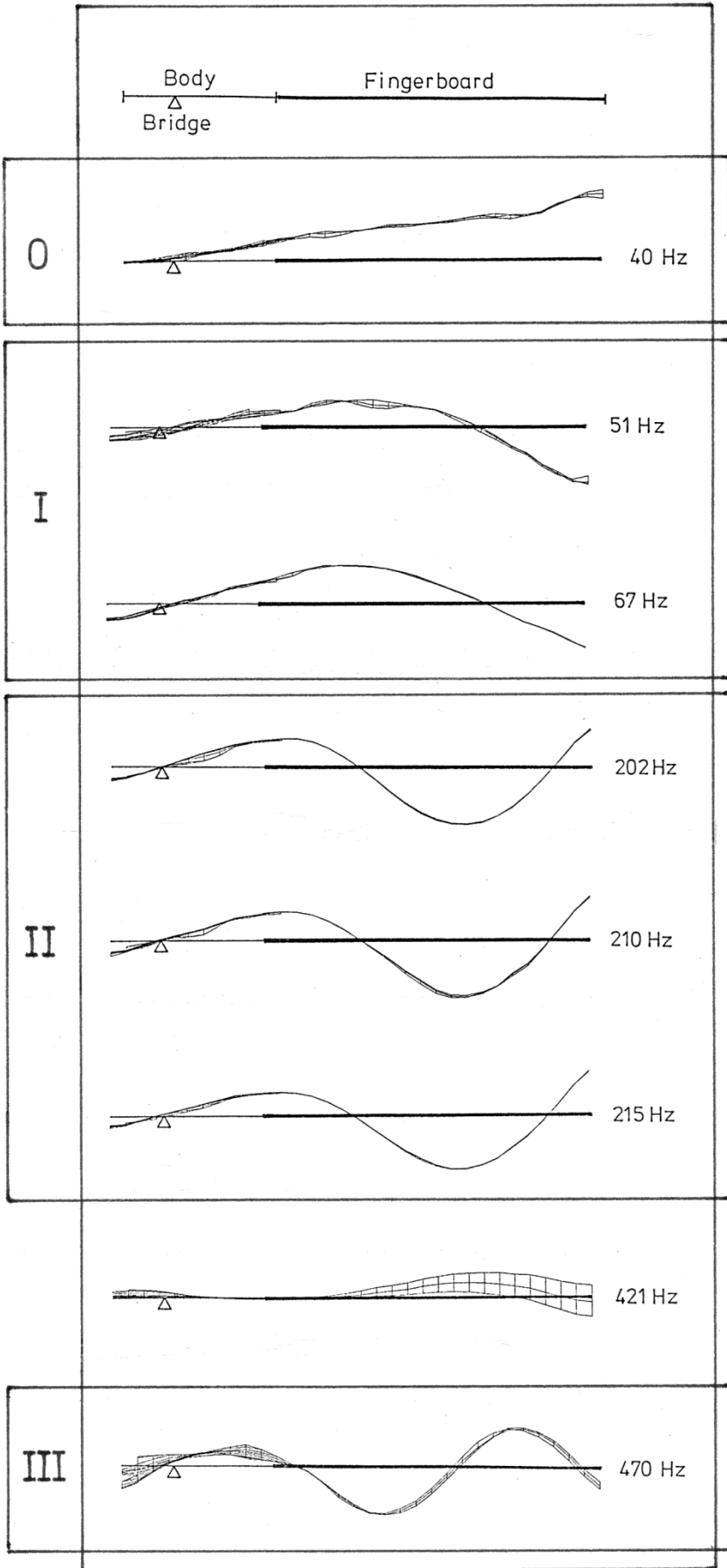


*Fig. 20. ODSs of the Riverhead Bass No. 5, measured in situ.*

## 4.6. Modelling the Bass ODSs as Beam Eigenmodes

### 4.6.1. Frequency Ratios

In the previous paragraph ODSs of the basses as measured *in situ* have been compiled. It became obvious that, to a high extent, the vibrations are governed by bending. The respective frequency ratios are listed in Tab. II. The bold numbers refer to the frequencies of the principal ODSs (as characterised by the main maxima of the FRF). Further ODSs, which are of the same bending type but differ in secondary features such as an additionally superimposed torsion, are characterised by standard format numbers. The values in the lowest row are obtained from theory for the first four bending eigenmodes of a beam of constant stiffness which is simply supported (hinged) at one end and free at the other end; cf. Fleischer (1999b).

	<b>ODS 0</b>	<b>ODS I</b>	<b>ODS II</b>	<b>ODS III</b>	<b>ODS IV</b>
Action Bass No. 1		<b>1</b>	2.89/ <b>3.57</b> /3.78	<b>7.42</b> /7.56	
Music Man Bass No. 2		<b>1</b>	<b>3.25</b> /3.49/3.90	6.44/ <b>6.69</b> /6.98	
Dyna Bass No. 3		<b>1</b>	2.82/ <b>3.28</b> / 3.53/3.98	<b>6.44</b>	<b>11.02</b>
Carvin Bass No. 4	<b>0.60</b>	<b>1</b>	<b>3.01</b> /3.36	5.55/ <b>5.80</b> /5.99	<b>10.18</b>
Riverhead Bass No. 5	<b>0.59</b>	0.76/1	3.00/ <b>3.11</b> /3.19	<b>6.96</b>	
Beam ss - f		<b>1</b>	<b>3.24</b>	<b>6.76</b>	<b>11.56</b>

Tab. II. Ratios of the frequencies of the ODSs; the frequency of the first bending vibration is used as a reference.

A comparison of the respective Figs. 16 through 20 to the eigenmodes of a simply supported-free (ss - f) beam reveals that the patterns of the beam vibration coincide with the principal ODSs of the basses to a certain extent. Moreover, the data in Tab. II show that the frequency ratios of the corresponding vibrations are relatively close together. This means that the simply supported beam can be taken as a first approximation and serve as a model in order to describe the bending vibrations of the basses. In the following paragraphs, this suggestion shall be discussed in more detail.

### 4.6.2. Rigid Body Motion

A rigid body motion (ODS 0) was observed for two of the instruments at about 0.6 times the frequency of the first bending vibration. It is most pronounced for the Riverhead Bass No. **5** and occurs at  $f_0 = 40$  Hz. The Carvin Bass No. **4** exhibits an ODS at  $f_0 = 29$  Hz that appears to be at least related to the rigid-body motion. Since this instrument is equipped with an additional B string, the frequency of the ODS 0 is close to the fundamental frequency ( $B_0 \cong 31$  Hz) of the lowest string. The other conventional basses (with a head and made from wood) do not exhibit this motion within the range of the string fundamentals. In contrast to the basses No. **1** through No. **4**, the Riverhead Bass No. **5** is of non-conventional shape and material. For this particular instrument, the frequency of the bending motion proves as close to the fundamental frequency of the lowest open string tuned to  $E_1 \cong 41$  Hz. This particularity in comparison to the wooden basses could be due to the carbon fibre, from which the instrument No. **5** is made, or to the particular design without a head which is expected to alter the balance of the whole instrument.

### 4.6.3. First Bending Vibration

The first principal operating deflection shape, denoted ODS I, is observed for all basses. It is closely related to the first eigenmode of the simply supported-free beam with a node in addition to the intrinsic node induced by the support; cf. Fleischer (1999b). The frequencies range from 40 Hz to 49 Hz for the conventional basses No. **1** through No. **4**. The highest value of 67 Hz is measured for the headless carbon fibre Riverhead Bass No. **5**. The frequencies appear slightly higher for the wooden one-piece basses (No. **3** and No. **4**) than for the wooden basses with a screwed-on neck (No. **1** and No. **2**). Because this is the first genuine continuum vibration and compares unambiguously to the first eigenmode of the simply supported-free beam, it seems justified to use its frequency as a reference. In general, the pattern is well pronounced and not superimposed by other vibrations. Therefore, it is characterised by one single frequency and simply extracted from a clear peak in the FRF.

### 4.6.4. Second Bending Vibration

In contrast to the first one, the second bending pattern (ODS II) is split and/or superimposed by torsion. That is why similar vibration patterns with three (support plus two additional) nodes occur at frequencies spread over a certain range. Typically three to six peaks are found in the FRF. The respective ODSs are dominated by a bending pattern, which obviously compares to the second mode of a simply supported-free beam. The corresponding frequencies are

- 115 Hz ... 150 Hz for the Action Bass No. **1**,
- 137 Hz ... 165 Hz for the Music Man Bass No. **2**,
- 120 Hz ... 169 Hz for the Dyna Bass No. **3**,
- 147 Hz ... 165 Hz for the Carvin Bass No. **4** and
- 202 Hz ... 215 Hz for the Riverhead Bass No. **5**.

The frequencies of the second bending pattern seem to be somewhat lower for the screwed basses No. **1** and No. **2** compared to the glued basses No. **3** and No. **4**. This coincides with the observation concerning the first bending pattern. The highest frequencies are found for the headless carbon bass No. **5**.

### 4.6.5. Third Bending Vibration

According to theory, the third mode of a simply supported-free beam exhibits one node at the support and additional three nodes. A similar shape is also found for ODS III of the basses. Again, in some cases not only one, but several patterns that have four nodes in common are observed for slightly differing frequencies. The ranges are

- 295 Hz ... 300 Hz for the Action Bass No. **1**,
- 272 Hz ... 295 Hz for the Music Man Bass No. **2**,
- 274 Hz for the Dyna Bass No. **3**,
- 272 Hz ... 294 Hz for the Carvin Bass No. **4** and
- 470 Hz for the Riverhead Bass No. **5**.

The observation that the frequency is highest for the headless carbon bass No. **5** is also confirmed for this ODS.

### 4.6.6. Fourth Bending Vibration

Within the investigated frequency range up to 500 Hz both one-piece basses No. **3** and No. **4** show a further vibration pattern (ODS IV) which corresponds to the fourth eigenmode of the simply supported-free beam. The instruments vibrate with five nodes at the frequencies 468 Hz (No. **3**) as well as 499 Hz (No. **4**).

## 4.7. Concluding Remarks

A comparison of the ODSs reveals that there are vibration patterns, which are common to all basses. They are denoted principal ODSs and identified as bending vibrations of the structure. These fundamental patterns compare to particular eigenmodes of a beam. This means that, to a first approximation, the bass can be modelled by a beam of constant bending stiffness which is simply supported at one (the body-)end and free at the other (the neck-)end. If once the frequency of the first bending vibration (ODS I) is known, the frequencies of the other principal ODSs can be estimated by means of this model to be about

- 3.2 times (ODS II),
- 6.8 times (ODS III) and
- 11.6 times (ODS IV)

as high as the frequency of the first bending ODS. In addition, the influence of material (Young's modulus  $E$ , density  $\rho$ ) and geometry parameters (length  $l$ , height  $h$ , width  $b$ ) can be at least roughly checked using the beam model (Fleischer (1999b)).

An obvious deviation of reality to model, however, is observed at the body-end. While the node of the beam occurs directly at the supported end, for the basses it is shifted away from the end. The body-end node of a bass is favourably located at the bridge in order to ensure that the strings "see" an immobile termination. The deviation in the location of the body-end node may be accounted for by an "effective" length of the beam, which differs from the geometrical length of the bass.

This simplified consideration is intrinsically restricted to pure bending. In practice, the principal modes may be modified. They happen to be superimposed by torsion and/or split by interaction with the in-phase or out-of-phase motion of accessory parts such as the horns of the body. Most probably the head - which is asymmetric as well as the body is for all instruments except the River-head Bass - plays an important role for the vibrations of the neck. Several of the related effects cannot be covered by the beam model. This means that experiments are not made superficial by the basic theory. Therefore, a dedicated measuring approach is suggested which, in addition, accounts for the fact that the excitation of the neck takes place at different locations on the fingerboard. The fundamentals shall be treated in the next chapter.

## 5. MECHANICAL CONDUCTANCE

An inevitable shortcoming of the ODS measurement is that there is one fixed excitation point, in our experiments at the seventh fret. In playing practice, the neck is excited by the strings, which are terminated depending on where they are fingered by the bass player. Until now, no quantitative information is available about the extent to which a vibration of the bass structure is evoked by such a "natural" excitation. In the extreme case, an ODS might be not detected in the measurement because it exhibits a node at the seventh fret and is consequently not evoked by an excitation at this particular shaker location. Nevertheless, it could be relevant for the playing function of the instrument. The aim of this chapter is to describe a more direct measuring approach apt for the given task.

### 5.1. Measuring Set-up and Procedure

The main topic of the present work is related to the undesired transfer of energy from the string to the neck or body of an electric instrument. The transfer may take place at two distinct points, namely at the end terminations of the string. The response of a particular point of a structure to an excitation can be expressed by the mechanical (driving) point impedance (cf. Fletcher and Rossing (1998)) or its reciprocal, the mechanical point admittance. The physical parameter admittance, which after Jansson (1983) is sometimes referred to as the "vibration willingness", is used in the following to characterise the mobility of the instrument and the deviation from the fiction of providing immobile terminations to the strings.

In contrast to the transfer admittance (cf. Figs. 7, 10 and 13), the point admittance is defined as the ratio of the complex amplitudes of the velocity and the force at the same point. The same direction for both parameters is presumed. A high admittance generally stands for a high mobility of the instrument at this particular location and frequency. According to the German standard DIN 1320 (1969) its real part is denoted conductance and its imaginary part susceptance. The susceptance (velocity and force shifted by  $\pm 90^\circ$ ) is a measure of the spring- or mass-type behaviour of the structure at the driving point. In the problem under consideration it can be relevant for an increase or decrease, respectively, of the frequency of the string compared to ideally rigid supports. The conductance (velocity in phase with the force) characterises the effect that active power generated by the driving system is transferred to the structure. In the case of a chordophone the string is the driving system. For an acoustic instrument the transfer of energy from the string to the body, preferably via the bridge, is a necessary prerequisite for the function of the instrument; cf. Fleischer (1997b). In the case of an electric instrument, however, the string vibration does not have to be converted to sound by the instrument body but is picked up, amplified and radiated by electric and electronic means. In general, the flow of vibration energy from the string to the body is undesired. It is parasitic in the sense that the vibration of the string decays more rapidly with than without the additional energy loss via the terminations. A non-zero conductance indicates that the instrument structure is able to accept vibrational energy from the string at this particular location and frequency. This is the cause for a dead spot.

The following set-up was used to ascertain the conductance. A noise generator (B&K 1405) fed pink noise via an amplifier (B&K 2706) to a mini-shaker (B&K 4810). On top of the driving system of the shaker an impedance head (B&K 8001) was mounted for simultaneous acquisition of force and acceleration. The shaker with the impedance head is shown in Fig. 21.

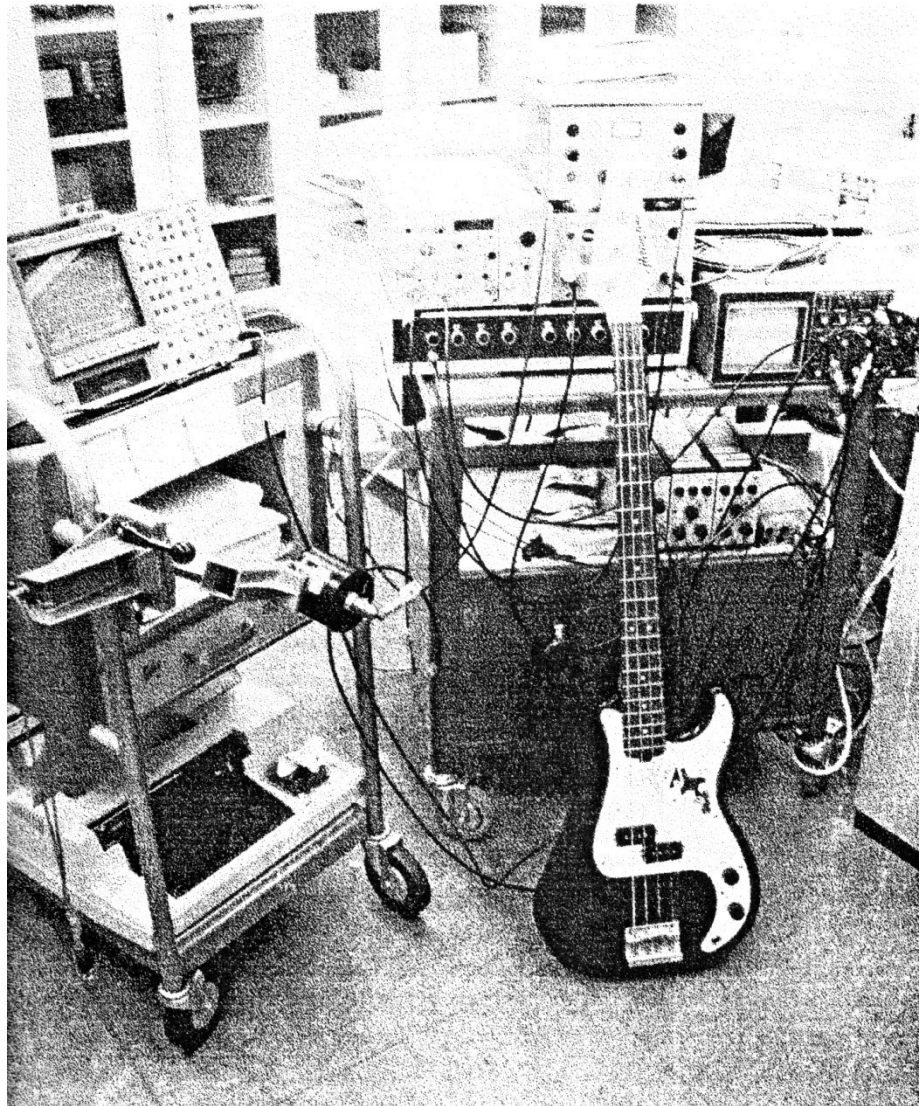


Fig. 21. Impedance head and mini-shaker as used for the conductance measurements.

The influence of the mass of the transducer "down-stream" the force flow, *i.e.* beyond (with respect to the shaker) the force gauge, was minimised by an electric mass compensation unit (B&K 5565). The force and acceleration signals were conditioned in two charge amplifiers (B&K 2626). After having reversed the polarity of the acceleration by a differential amplifier (Tektronix AM 502), FFT and additional calculations were performed in a dual channel analyser (Ono Sokki CF 350) which finally yielded the complex mechanical admittance and its real part, the conductance. A photograph of the experimental set-up is displayed in Fig. 22.

The fundamental frequency of the bottom open string on a five- or six-string bass is  $B_0 \cong 31$  Hz, on a normal four-string bass  $E_1 \cong 41$  Hz. For the conductance measurements 25 Hz was chosen as the lowest frequency. The top string on a four-string bass is  $G_2 \cong 98$  Hz and on a six-string bass  $C_3 \cong 131$  Hz. If these strings are fingered at the 12<sup>th</sup> fret, the corresponding fundamental frequencies are 196 Hz and 262 Hz. Since the range of fundamental frequencies up to at least the 12<sup>th</sup> fret of a six-string bass is covered, a highest frequency of 275 Hz was considered as sufficient.

The experience from the vibration measurements suggests to take great care that "natural" experimental conditions as close as possible to the normal playing situation are ensured. That is why the measurements were performed *in situ* in a similar condition as during the Scanning Vibrometer experiments described in Chapter 4. The shaker with the impedance head was positioned horizontally (cf. Fig. 22) in such a way that the bridge, nut or fingerboard of the bass could be slightly pressed against the tip of the impedance head. The pressure was such that the static force was always greater than the alternating force and the impedance head did never lift off during the measurement.



*Fig. 22. Complete experimental set-up used for the conductance measurements.*

In order to simulate normal fingering conditions, the experimenter's left hand grasped the neck close to the location where the conductance was actually measured. With respect to the "wandering" hand the conditions during the conductance experiments are even closer to playing practice than in the vibration experiments, where the hand remained in the same position during the whole measurement. The output plug of the bass pick-ups was left open-circuited. The strings were under normal tension and left undamped. The same person (the author) performed all experiments. A comparison of data obtained in repeated measurements revealed that the reproducibility was satisfactory.

In the first step, a decision had to be made concerning the direction in which the conductance was measured. In principle, the neck is flexible in both directions, but - as investigated by Fleischer (1999b) - to a different extent. It has proven as more mobile perpendicular to the fingerboard than in the fingerboard plane. An example for the Action Bass No. 1 is given in Fig. 23.

The neck conductance is shown as a function of frequency for the nut and the first nineteen frets. This 3D-representation creates a mountainous "landscape". The "mountains" indicate increased ability of the neck to accept energy, *i.e.* higher damping at particular measuring positions in the corresponding frequency band. In each diagram of Fig. 23 two principal types of mountain chains are observed. The second one may be split into two or more summits; cf. the bottom (out-of-plane) diagram. With respect to the mountains, the results given in Fig. 23 differ in two main aspects.

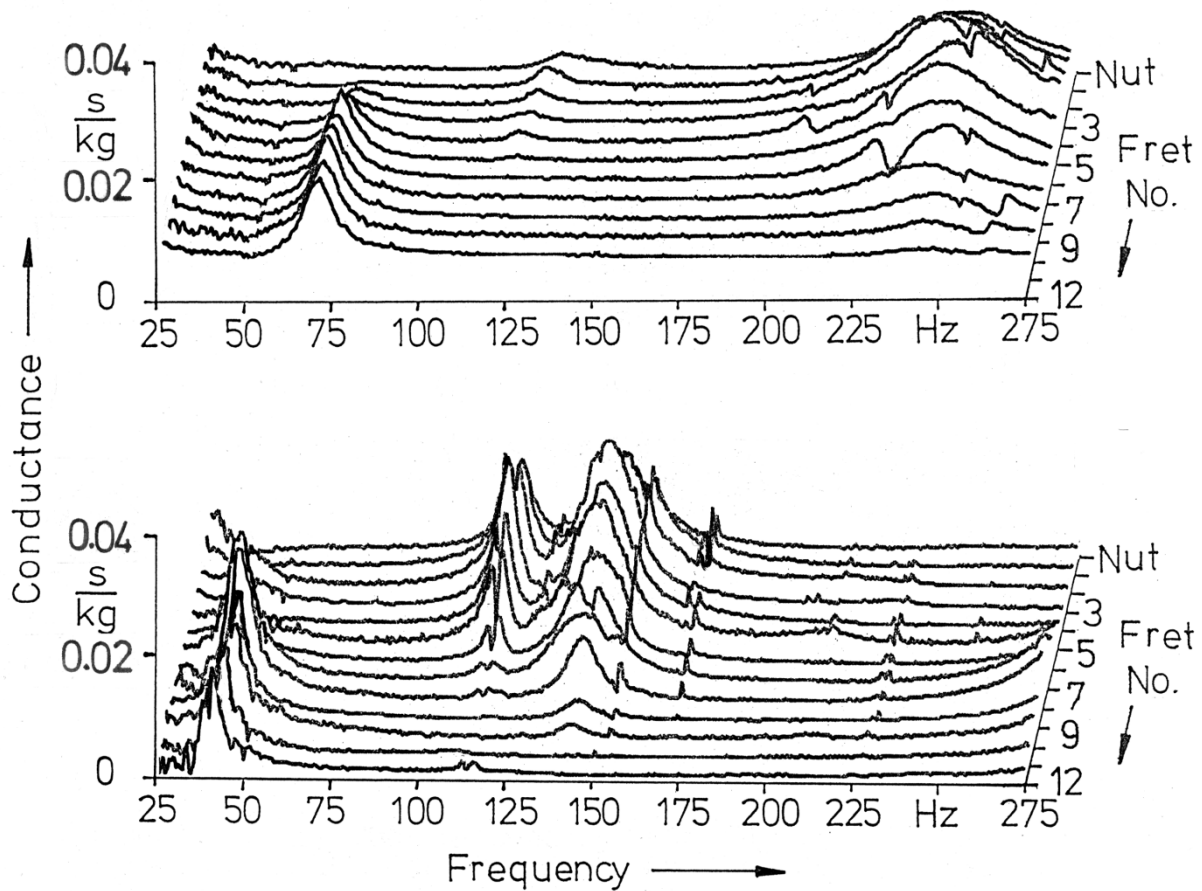


Fig. 23. Conductance on the neck of the Action Bass No. 1 as a function of frequency measured at different locations from the nut to the 10<sup>th</sup> and 12<sup>th</sup> fret, respectively. Measuring directions are in the fingerboard plane (top) and perpendicular to the fingerboard at the centre line between the A<sub>1</sub> and D<sub>2</sub> strings (bottom).

The frequencies, at which mountains of the same type occur, are higher when measuring in the fingerboard plane (Fig. 23 top) than out of the plane along the centre of the fingerboard (Fig. 23 bottom). This is a consequence of the direction-dependent bending stiffnesses. As predicted by beam theory, the eigenfrequencies are proportional to the height  $h$  of the beam; cf. Eq. (5) in Fleischer (1999b). Since the neck of a bass is roughly twice as broad as high, the in-plane eigenfrequencies can be estimated to be twice as high as the out-of-plane frequencies of the corresponding bending modes.

The heights of corresponding mountains are different for the two measuring directions. When measuring in the fingerboard plane (Fig. 23 top), both mountains are relatively flat and not very high. In contrast to this result, when measuring out-of-plane (Fig. 23 bottom), sharply pronounced mountain chains appear which reflect the body-neck modes ODS I at about 40 Hz and ODS II with its variants between 115 Hz and 150 Hz (cf. Fig. 16).

The global comparison of the results for this example reveals that the conductance reaches higher values at lower frequencies out-of-plane than in-plane. Consequently, comparable to the case of an acoustic instrument such as the classic guitars (cf. Jansson (1983), Fletcher and Rossing (1998)), the out-of-plane conductance dominates the damping effects. Because the out-of-plane direction is judged as more important than the direction in the fingerboard plane, all measurements which follow shall be taken perpendicular to the fingerboard-body plane.

## 5.2. Lateral Dependence of the Neck Conductance

The ODSs presented in Chapter 4 indicate that torsion may superimpose the bending of the neck. The influence of the torsional motion was checked by measuring the point conductance at different lateral positions on the fingerboard. Three examples (referring to one five-string bass and two four-string basses), each representative for a basic type of the instrument, are given in this paragraph. The measurements were taken along four and three lines, respectively, between the five or four strings.

The 3D-representation as introduced by Fig. 23 is used for compiling the results. Fig. 24 refers to the Music Man Bass No. 2 that is made from wood, the neck screwed to the body, and with an asymmetric head. The four diagrams represent the measurements between the single strings as indicated in the legend. The conductance landscapes show overall-similarities, but differences in detail. The discrepancies are most pronounced for the vibrations between about 100 Hz and 150 Hz. For their interpretation a comparison to the ODSs displayed in Fig. 17 is helpful. The frequencies of the maxima yielded by the vibration (Chapter 4) and the conductance measurements, respectively, are not exactly the same. This might be a consequence of the differing support by the left hand: While during the vibration measurements (cf. Fig. 6) the hand grasped the neck at a constant position in the low-fret region, during the conductance measurements the hand wandered along with the measuring point in order to simulate the player fingering the string at the corresponding fret.

The basic differences concentrate on the multiple chain between about 100 Hz and 150 Hz. The single mountain chains are similar in shape; maxima always occur at the lower frets while minima are observed at about the 12<sup>th</sup> fret. The two bottom diagrams of Fig. 24 (obtained between the D<sub>2</sub> and G<sub>2</sub> strings and between the A<sub>1</sub> and D<sub>2</sub> strings, respectively) coincide to a high degree. The maximum values of the conductance exceed the chosen measuring range and are therefore clipped. In the diagram measured between the E<sub>1</sub> and A<sub>2</sub> strings the mountain chain is lower, but broader. As a pronounced difference, the measurement between the B<sub>0</sub> and E<sub>1</sub> strings (Fig. 24 top) yields an additional mountain chain close to 100 Hz. These multiple chains are related to the variants of the ODSs at 137 Hz, 147 Hz and 165 Hz. According to the nomenclature introduced in Chapter 4 they are of the ODS II type. Their variants originate from superimposed torsion that is most pronounced in region of the nut and lower frets. Depending on the lateral position of the excitation, it is more or less pronounced and adds in phase and out of phase, respectively, to the basic bending motion. As a consequence, for this instrument the conductance may depend on the lateral position on the fingerboard.

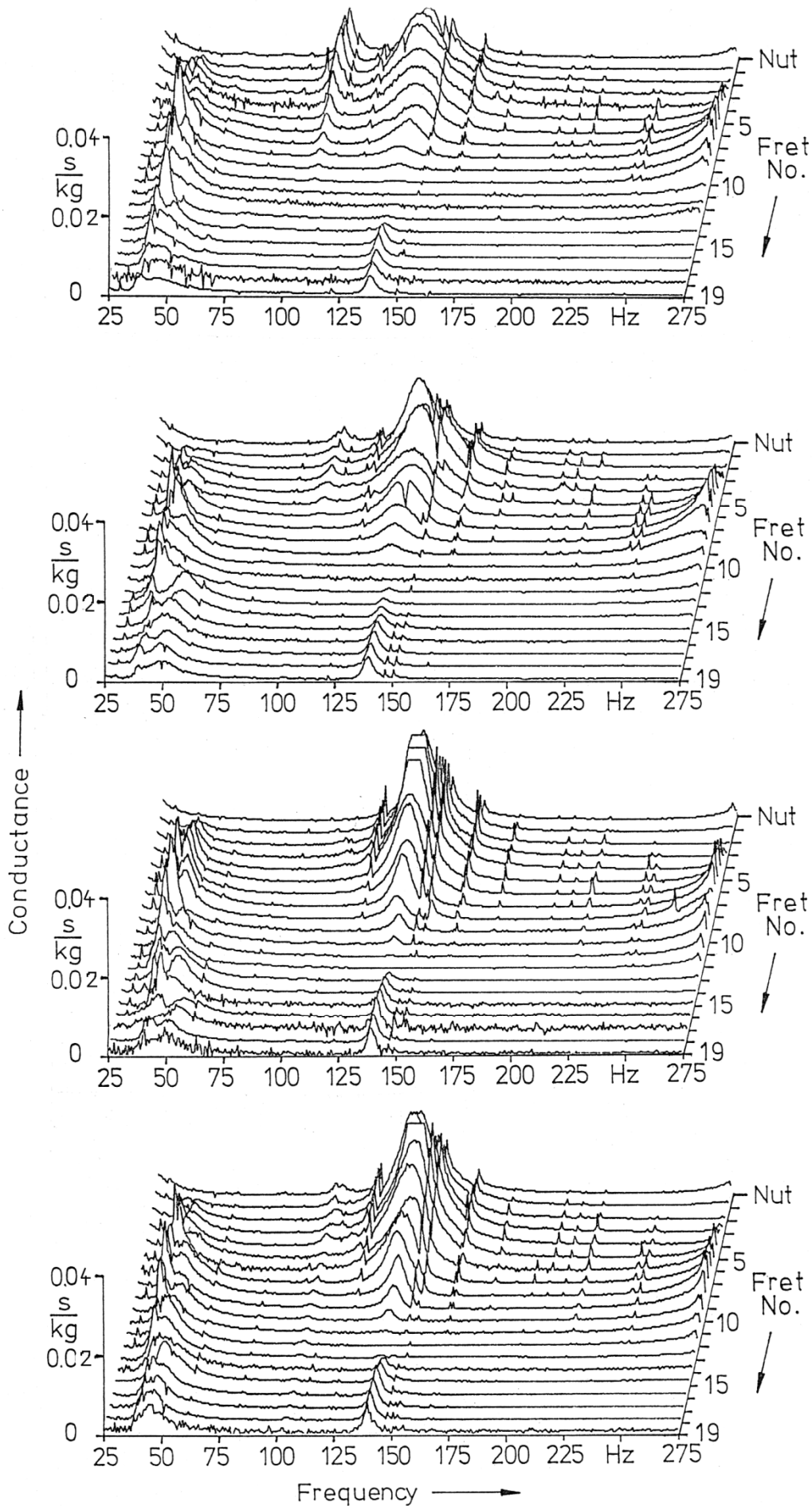
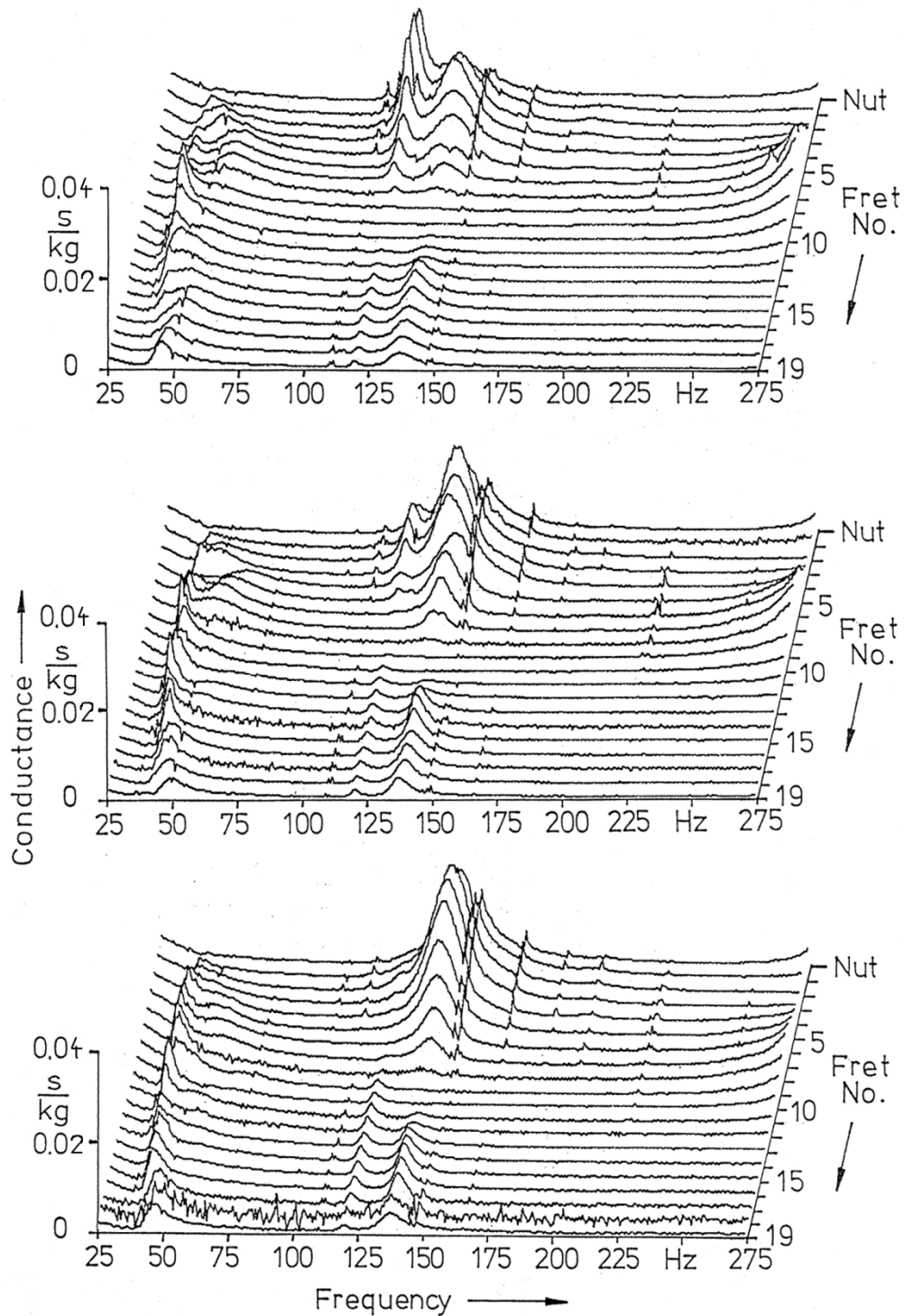


Fig. 24. Out-of-plane conductance on the neck of the MusicMan Bass No. 2 as a function of frequency measured at twenty locations from the nut to the 19<sup>th</sup> fret. Measuring positions (from top to bottom) are between the  $B_0$  and  $E_1$  strings, between the  $E_1$  and  $A_1$  strings, between the  $A_1$  and  $D_2$  strings, between the  $D_2$  and  $G_2$  strings.



*Fig. 25. Out-of-plane conductance on the neck of the Dyna Bass No. 3 as a function of frequency measured at twenty locations from the nut to the 19<sup>th</sup> fret. Measuring positions are between the low  $E_1$  and the  $A_1$  strings (top), between the mid  $A_1$  and  $D_2$  strings (middle) and between the  $D_2$  and the high  $G_2$  strings (bottom).*

A further example, concerning the Dyna Bass No. 3, is given in Fig. 25. It may be regarded as representative for an instrument made from wood, with the neck glued to the body, and with an asymmetric head. The conductance was measured between the bottom strings, along the centre line of the

fingerboard and between the top strings, respectively. The conductance mountains at about 40 Hz and 275 Hz are not dependent on the lateral measuring position. Discrepancies are observed in the frequency region between 120 Hz and 150 Hz. A multiple-peak structure with varying heights is

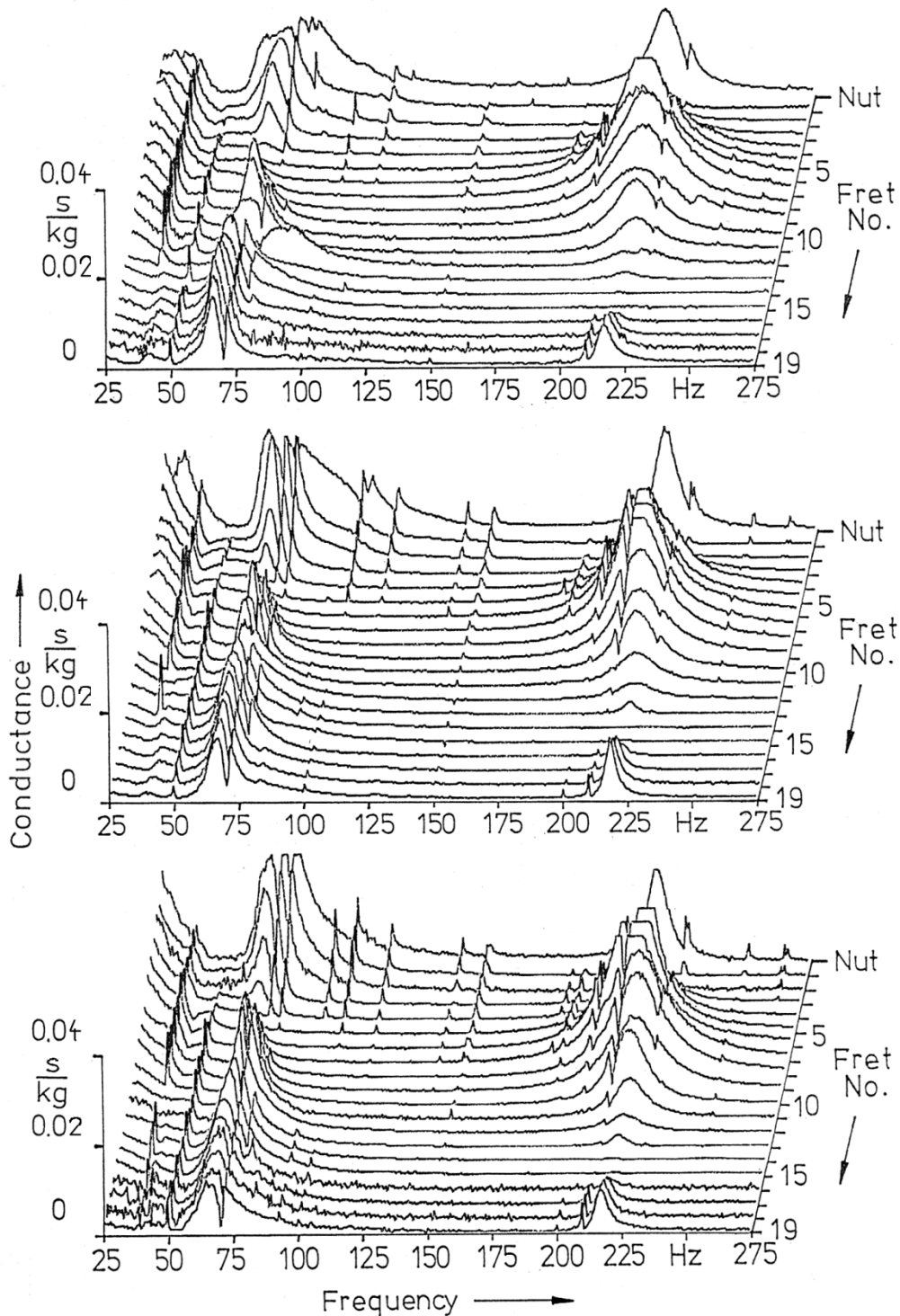


*Fig. 26. Out-of-plane conductance on the neck of the Riverhead Bass No. 5 as a function of frequency measured at twenty locations from the nut to the 19<sup>th</sup> fret. Measuring positions are between the low  $E_1$  and the  $A_1$  strings (top), between the mid  $A_1$  and  $D_2$  strings (middle) and between the  $D_2$  and the high  $G_2$  strings (bottom).*

observed. The respective conductance mountains are related to the variants of ODS II at 120 Hz, 140 Hz, 150 Hz and 169 Hz (cf. Fig. 18). These variants differ in a torsional motion superimposed on the basic bending. The resulting patterns are similar, but - as can be taken from Fig. 18 - differ in frequency. They all exhibit maxima at the lower frets and minima at about the 10<sup>th</sup> fret. The frequencies, at which these closely related vibration patterns are maximally evoked, depend on the lateral position of the excitation. While an excitation at the bottom strings (Fig. 25 top) results in a pronounced response of the low-fret region of the neck at about 120 Hz, a lateral shift towards the top strings yields maximum conductance at about 140 Hz. For an excitation along the centre line of the fingerboard (Fig. 25 middle) as well as close to the top strings (Fig. 25 bottom) the maximum conductance is observed at the same frequency with only minor differences in height. Comparable to the Music Man Bass (Fig. 24) there may be a lateral dependence of the conductance within distinct frequency regions.

Fig. 26 refers to the Riverhead Bass No. 5. As already mentioned, this instrument is made from carbon fibre, with the neck as well as the body in one piece, and without a head. Its shape is symmetric. The typical conductance landscape differs from the results for the other two basses. It is fairly rugged. There are more mountain chains with high summits, several of which are clipped indicating overload of the measuring range. Along the fingerboard there are one more valley and one more summit compared to Figs. 24 and 25. The measurements (cf. Fig. 20) by means of the vibrometer have already shown that this instrument exhibits a wide variety of bending vibrations. Since no head terminates the neck, an additional node and antinode, respectively, are situated on the fingerboard. This is in clear contrast to headed basses, where this antinode is shifted off of the fingerboard toward the nut and head, respectively. In divergence to the other two examples, the height of the mountain chains differs hardly for the three measuring positions. In the range below 275 Hz, a headless symmetric bass proves as less prone to torsion than a headed asymmetric instrument. As a consequence, the lateral dependence of the conductance is less marked for this instrument than it is for basses with a head that, in addition, is asymmetric.

These results indicate that, in principle, the conductance at one and the same fret may depend on the lateral position and, as a consequence, differ between strings. During experiments on electric guitars (Fleischer and Zwicker (1998)) an interaction between bending of the neck (ODS II) and torsion of the neck-head system was observed. It was most pronounced for instruments with asymmetric headstocks. In consequence, the conductance proved as highly dependent on the lateral measuring position for asymmetric instruments. Since most basses are conventionally constructed with asymmetric heads, in the normal case the conductance shall be different at the low-string edge, the centre and the high-string edge of the fingerboard. For the headless Riverhead Bass No. 5, however, no prominent superposition of torsion and bending was observed in the region of lower frequencies (see Fig. 20 where extreme torsion showed up at a frequency as high as 421 Hz). At least in the low-frequency range the conductance of an instrument of this type can be expected to depend only weakly on the lateral position and, consequently, the mid-string conductance can be regarded as representative for all strings. In the normal case, however, it has to be kept in mind that the measurements at the centre position barely represent some kind of a mean value of the conductances at the outer positions and are directly relevant only for the mid strings.

### 5.3. Neck and Bridge Conductance

In contrast to the complete landscapes displayed in the previous figures, in Figs. 27 and 28 pairs of single conductance curves, plotted versus frequency, are compiled. Each upper diagram refers to the nut, each lower one to the bridge. The circled letters in the diagrams indicates the string at which the conductance was measured. As usual in the following, the measuring direction is perpendicular to the fingerboard-body plane.

Measurement results for the Action Bass No. 1 are given in Fig. 27. At the bridge terminations of the strings (as shown by the lower curves in each pair) the conductance proves as relatively small and hardly dependent on frequency. The corresponding curves are flat with only minor deviations, which above all concentrate on very low frequencies. At the nut, however, the conductance (upper curves in each pair) exhibits the pronounced maxima, which are well known from the neck conductance landscapes and may reach the order of 20 ms/kg. As a rule, even for this lower-priced instrument, the conductance turns out to be considerably smaller at the bridge of a solid-body bass than it may be on the neck.

This principal result holds also if the measuring position is laterally shifted, but to a different extent. The frequency, at which the nut conductance becomes maximal, is different for the four strings. For the  $E_1$  and  $A_1$  strings the conductance maximum occurs at about 115 Hz, for the  $D_2$  string at 115 Hz as well as 140 Hz and for the  $G_2$  string at about 140 Hz. The reason is that, depending on the lateral position, different variants of the ODS II (cf. Fig. 16) dominate. Although the lateral dependence of the conductance becomes obvious, all results imply that, as a rule, each string "sees" a relatively immobile support at the bridge end, whereas at the neck the conductance may be much higher. This means that, in general, minor losses of vibration energy via the bridge termination of a string are expected. With respect to energy losses, the opposite termination (nut or fret) proves as the "weaker" end. That is why the neck conductance is a strong indicator for dead spots.

This observation is confirmed by Fig. 28. The five diagram pairs (nut and bridge conductance) refer to the Music Man Bass No. 2. This instrument is similar in design to the Action Bass No. 1, which means that a pronounced dependence of the nut conductance on the string position is expected. As can be taken from comparison of the respective diagrams in Fig. 28, the maximum shifts from about 106 Hz ( $B_0$  string; top of Fig. 28) to about 140 Hz ( $G_2$  string; bottom of Fig. 28) which reflects different variants of the ODS II.

As a first step towards an application of the conductance measurements to the musical function of the bass, the fundamental frequencies of the open strings, ranging from 31 Hz to 98 Hz, are marked by black dots. This way, the frequencies relevant for the different strings become visible. In the case of the open  $B_0$  string (top of Fig. 28) the conductance both at the nut and the bridge amounts to about 3 ms/kg. Compared to the other strings, these values are uncommonly high. For the open  $E_1$  string the nut conductance is less than 2 ms/kg and somewhat smaller, but similar in magnitude to the bridge conductance. These two strings must not be considered as representative. The normal case is better represented by the remaining three open strings that exhibit a much smaller conductance, especially at their bridge terminations. The measured values are about 0.3 ms/kg or less.

From both Figs. 27 and 28 can be taken that for higher frequencies the conductance may reach much higher values at the neck than at the bridge. This tendency is relevant as well for the fundamental frequencies as for the single partials of the string signals. The bridge conductance tends to decrease with frequency, while the neck conductance proves as extremely dependent on frequency and may reach values as high as about 20 ms/kg at particular frequencies.

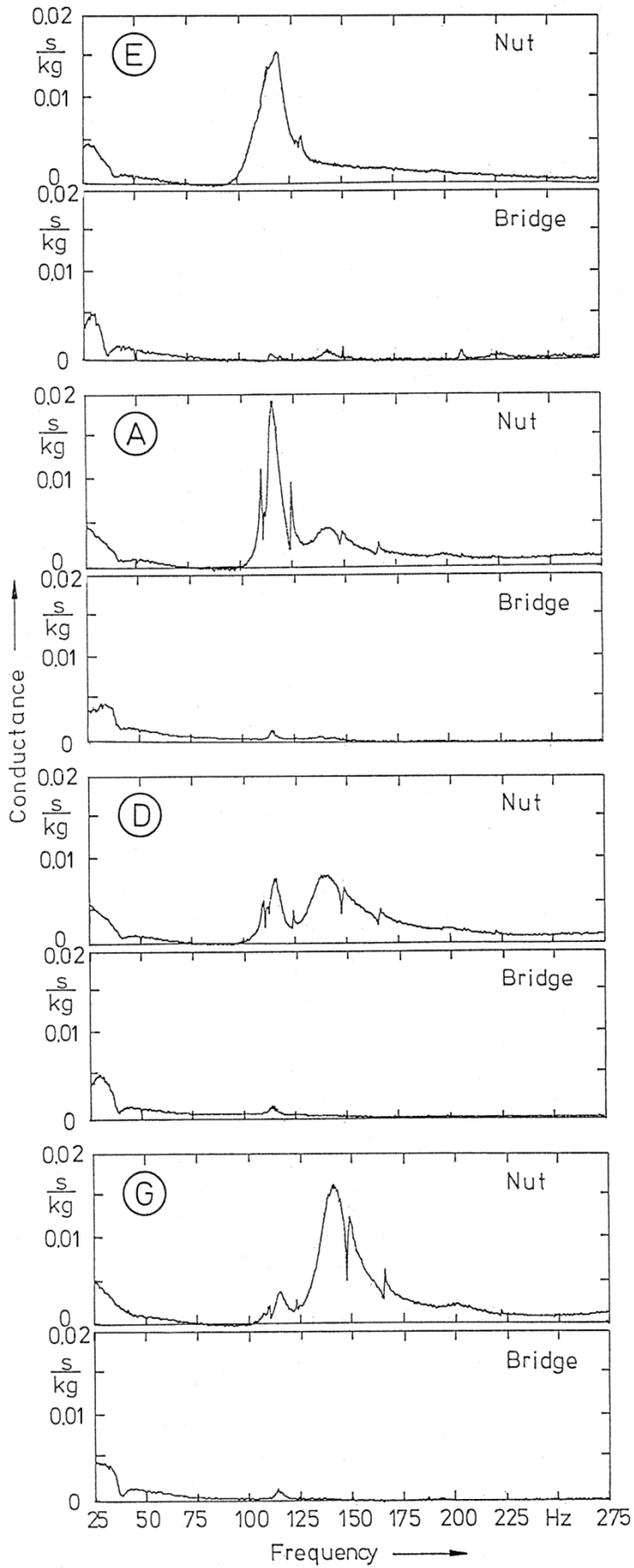


Fig. 27. Out-of-plane conductance at the nut and bridge of the Action Bass No. 1 as a function of frequency, measured at the terminations of the low  $E_1$  string,  $A_1$  string,  $D_2$  string and high  $G_2$  string (from top to bottom).

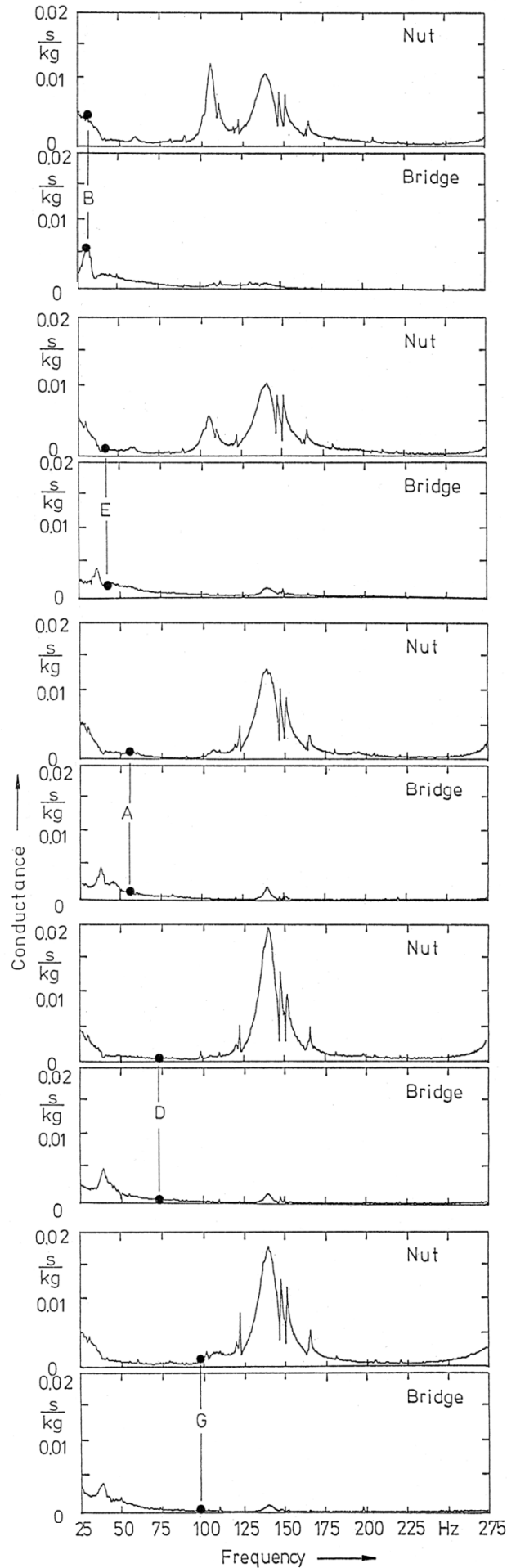


Fig. 28. Conductance at the nut and bridge of the Music Man function of frequency, measured at the terminations of the low  $B_0$  string,  $E_1$  string,  $A_1$  string,  $D_2$  string and high  $G_2$  string (from top to bottom). The dots indicate the fundamentals of the open strings.

## 5.4. Concluding Remarks

The measurements described in this chapter deal with the energy-consuming mobility of the instrument structure. They reveal that, as a rule, the bridge of a well-balanced solid-body bass is much less mobile than the neck at the position of the nut (open strings) and frets (considering the fingered situation). The conductance, measured perpendicular to the fingerboard, is regarded as the most relevant parameter to describe energy losses at the neck-end terminations of the strings. To a certain extent, the conductance may depend on the lateral measuring position indicating that at the same fret the different strings may "see" different conductances. Within the low-frequency range under consideration, this dependence proves as more pronounced for basses of asymmetric shape. For the symmetric bass no strong lateral dependence is observed. In conclusion, the conductance determined along the centre line of the fingerboard is at least some kind of a mean value for a given fret. Therefore, it serves as a good measure of the energy flow via the neck support of the string. The damping of the vibration, which may originate from the support of the string, shall be considered in Chapter 7 in detail. Examples of measured neck conductance landscapes and hints for the evaluation shall be given in the following chapter.

## 6. NECK CONDUCTANCE OF THE BASSES

In this chapter the out-of-plane conductances of the five basses as measured along the centre lines of the necks are compiled. The 3D-landscape representation, which was introduced in the previous chapter, is used in order to compress the results of twenty measurements on the fingerboard of each bass. The conductance is plotted as a function of fret position and of frequency within the range from 25 Hz to 275 Hz.

### 6.1. Evaluation

The bass player controls the frequency of the string vibration by leaving the string open or to finger it, *i.e.* to shorten the string by pressing it against a fret. If the consideration is restricted to the fundamentals of the complex string signals, each string-fret combination is characterised by one (fundamental) frequency. Plotting the corresponding points into a 3D-scheme as used for the presentation of the neck conductance creates a chart, which is given in Fig. 29. Standard tuning is presumed.

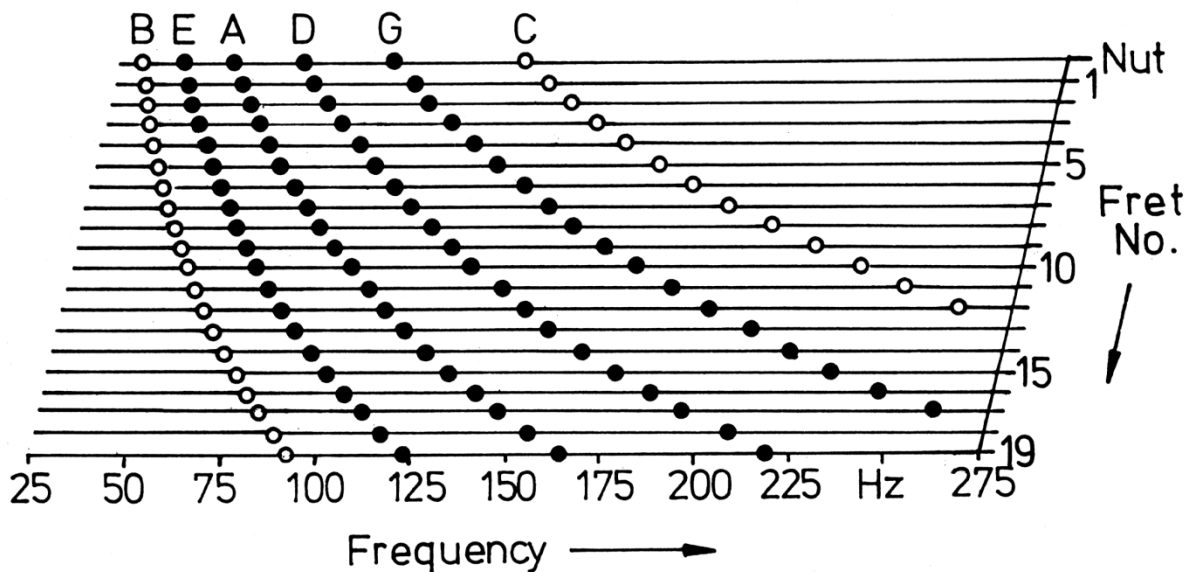


Fig. 29. "Overlay chart" for the evaluation of the neck conductance diagrams.  
The dots indicate the fundamental frequencies of all string-fret combinations.

This chart can be used as an overlay to evaluate and interpret the conductance landscapes given in the following paragraphs. It shows the fundamental frequencies versus fret position for all six strings including the standard strings (black dots) of a normal four-string bass, open and fingered. The conductance magnitude has to be checked for each string-fret combination. Coincidence with a high value suggests a dead spot at the particular string-fret location. Correspondingly, a very small conductance indicates the contrary of a dead spot denoted a "live spot".

## 6.2. Results of the Action Bass

For better comparability, the same scaling with a maximum conductance of 20 ms/kg is used in all diagrams. The 3D-representation gives a holistic impression of at which fret and at which frequency the neck tends to draw vibration energy from the string. This way, the frets and frequencies are emphasised at which prerequisites for dead spots are given.

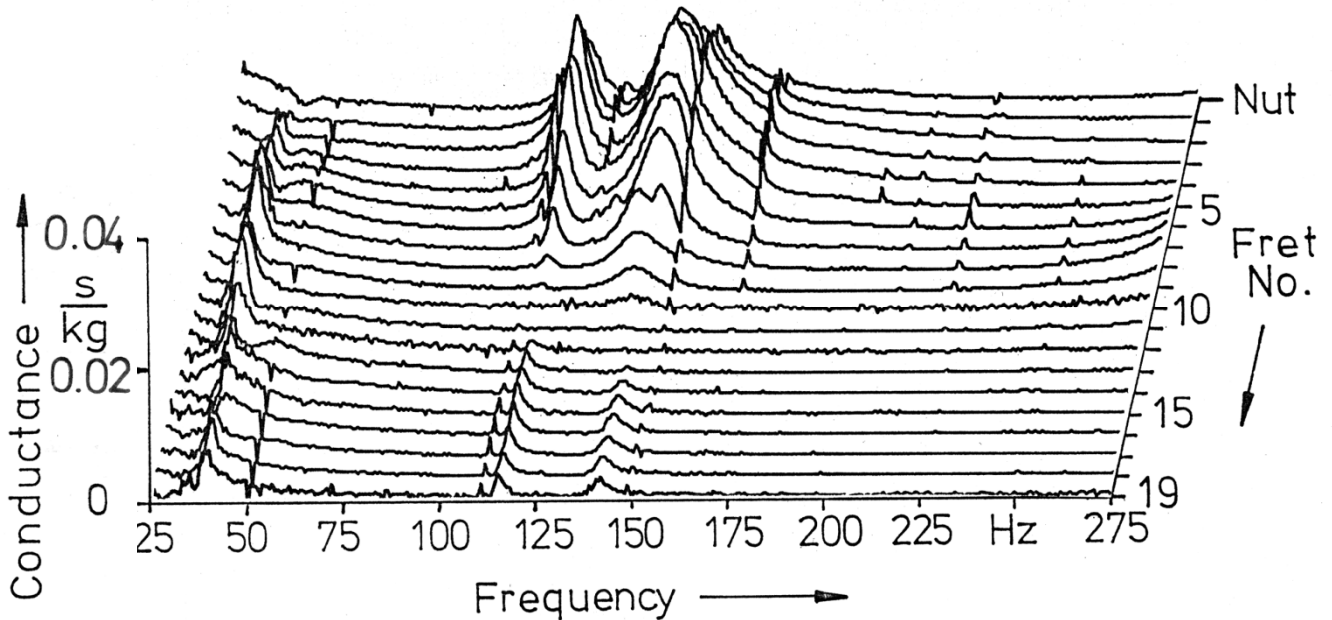


Fig. 30. Conductance at the nut and the first nineteen frets of the Action Bass No. 1 as a function of frequency measured along the centre line of the fingerboard between the  $A_1$  and  $D_2$  strings.

Fig. 30 shows three sharply pronounced mountain chains in the conductance landscape of the Action Bass No. 1 at about 40 Hz as well as between 110 Hz and about 150 Hz. The mountains correspond to ODSs I and II, respectively; cf. Fig. 16. They can be distinguished by the number and location of the nodes in which the conductance equals zero. No clipping occurs which means that the maximum conductance is always smaller than 20 ms/kg.

## 6.3. Results of the Music Man Bass

Fig. 31 refers to the Music Man Bass No. 2. Comparable to the previous figure, the ODS I (cf. Fig. 17) with a node close to the nut is reflected by the mountain chain at about 40 Hz. In contrast to the Action Bass No. 1 (cf. Fig. 30), the Music Man Bass exhibits not such an extreme splitting of the ODS II. In the region around 140 Hz essentially one mountain chain is found on the centre line of the fingerboard. The highest maxima do not reach 20 ms/kg.

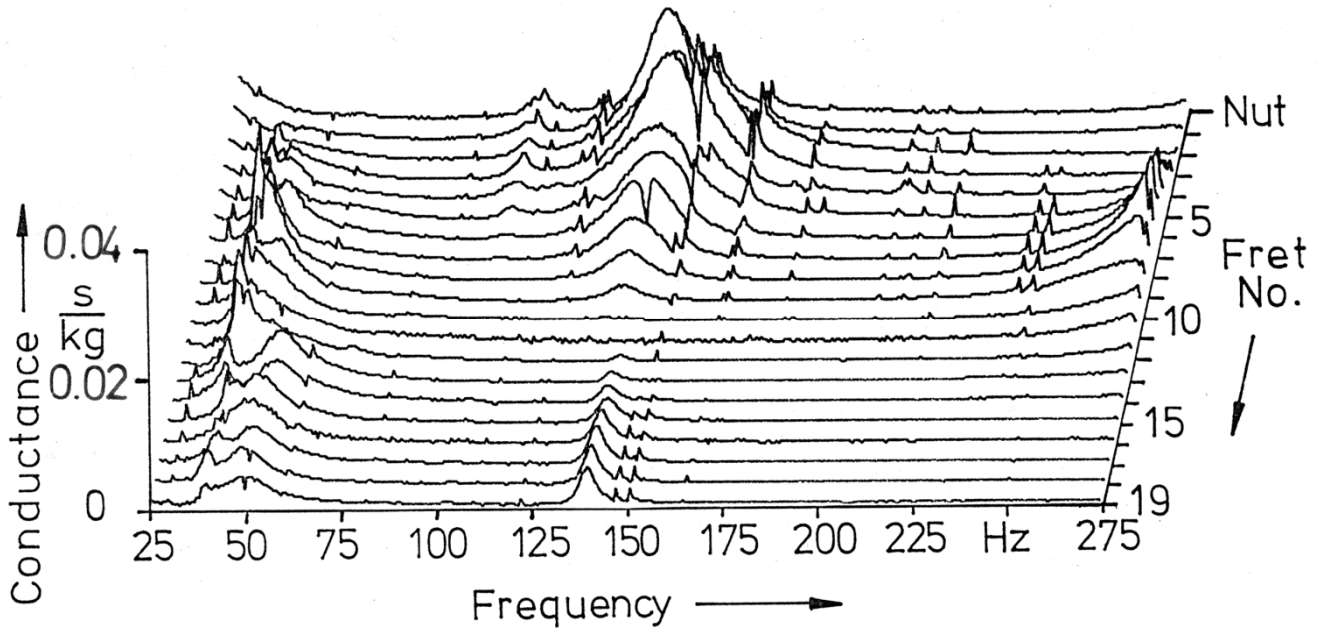


Fig. 31. Conductance at the nut and the first nineteen frets of the Music Man Bass No. 2 as a function of frequency measured along the centre line of the fingerboard between the  $E_1$  and  $A_2$  strings.

#### 6.4. Results of the Dyna Bass

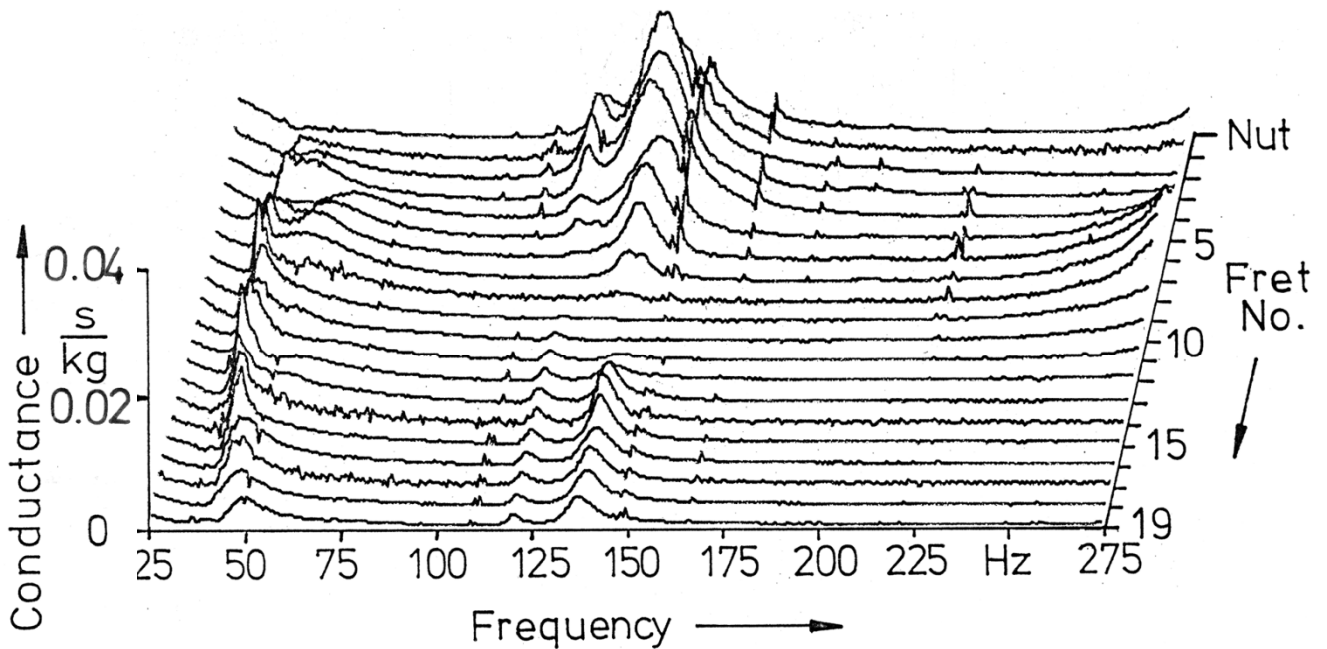


Fig. 32. Conductance at the nut and the first nineteen frets of the Dyna Bass No. 3 as a function of frequency measured along the centre line of the fingerboard between the  $A_1$  and  $D_2$  strings.

The overall-appearance of the conductance landscapes in the Figs. 32 (Dyna Bass No. 3) and 31 (Music Man Bass No. 2) is very similar. The ODS I of the Dyna Bass (cf. Fig. 18) is reflected by a mountain chain between 40 Hz and 50 Hz. Fig. 32 exhibits one pronounced mountain chain in the vicinity of 140 Hz that is related to the ODS II. In the region of the lower frets the conductance is high. Hence, no clipping is observed which indicates that the maximum of 20 ms/kg is never exceeded.

## 6.5. Results of the Carvin Bass

The conductance landscape on the neck of the instrument No. 4 is displayed in Fig. 33. The first bending pattern (ODS I; cf. Fig. 19) becomes visible as a well-pronounced mountain chain at about 50 Hz. The low-frequency motion, which was observed at 29 Hz in the vibration measurement (ODS 0 in Fig. 19), plays only a minor role in the conductance. Comparable to e.g. the Dyna Bass No. 3 (cf. Fig. 32), the Carvin Bass exhibits not such a wide frequency separation of the variants of the ODS II as it is observed for the Action Bass No. 1 (cf. Fig. 30). Nevertheless, at least two crests show up in the mountain chain around 150 Hz. For frequencies close to 50 Hz, in the vicinity of the 8<sup>th</sup> fret maxima higher than 20 ms/kg may occur.

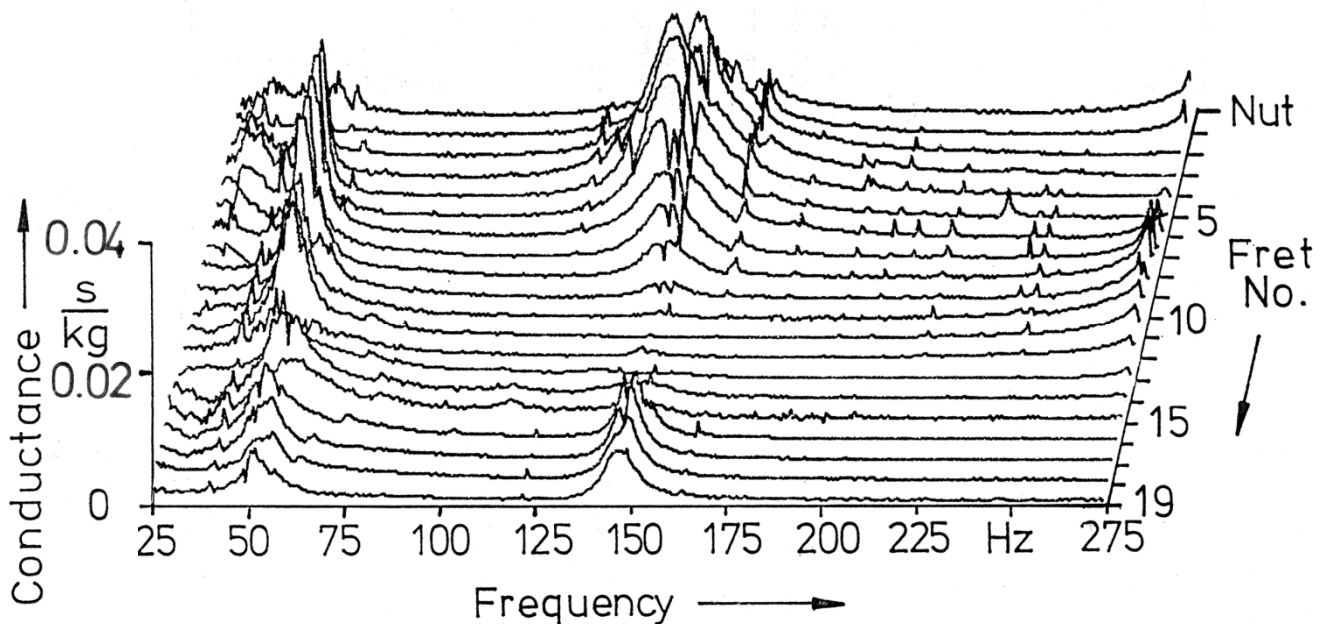


Fig. 33. Conductance at the nut and the first nineteen frets of the Carvin Bass No. 4 as a function of frequency measured along the centre line of the fingerboard between the  $A_1$  and  $D_2$  strings.

## 6.6. Results of the Riverhead Bass

While the conductance landscapes of the first four basses are rather similar, the Riverhead Bass No. 5 (Fig. 34) exhibits a basically different behaviour. The conductance diagram shows a multitude of mountain chains, which are closely related to the various ODSs in Fig. 20. (The smaller regular peaks at 50 Hz and multiples are suspected to originate from the hum of power supplies.) The conductance reflects the following vibration patterns: The rigid body motion (ODS 0 in Fig. 20) with an antinode at the nut for 40 Hz, the first bending pattern (ODS I) around 70 Hz and the second

bending pattern (ODS II) between 200 Hz and 220 Hz. In the vicinity of the ODS I as well as ODS II there are relatively wide regions of high conductance. Some maxima (at the 4<sup>th</sup>, 5<sup>th</sup> and 6<sup>th</sup> fret) at about 210 Hz are clipped indicating that the conductance happens to exceed 20 ms/kg.

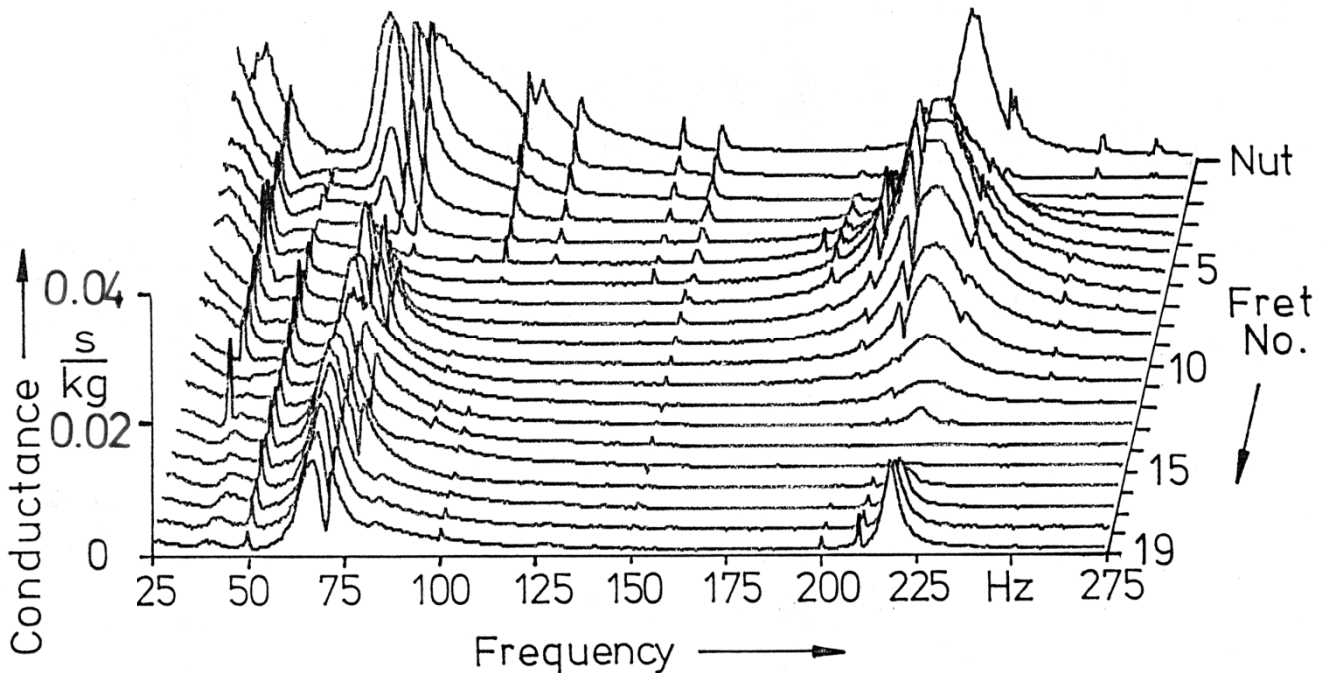


Fig. 34. Conductance at the nut and the first nineteen frets of the Riverhead Bass No. 5 as a function of frequency measured along the centre line of the fingerboard between the  $A_1$  and  $D_2$  strings.

## 6.6. Concluding Remarks

There are two basic variants of basses in the ensemble of the instruments under consideration. The first one comprises exclusively the headless carbon fibre bass No. 5. This instrument differs considerably from the other basses and does not fit into the common scheme. The second variant includes the remaining instruments No. 1 through No. 4, which are conventionally designed and manufactured from wood. In spite of some differences in detail, the conductance diagrams of these four instruments prove as relatively similar. They usually exhibit a mountain chain at low frequencies (between 40 Hz and 50 Hz) with very small conductances at the lower frets close to the nut and high values in the vicinity of the 8<sup>th</sup> fret. Additionally, these four basses have in common a second (single-peaked or multiple-peaked) mountain chain, which shows very high values in the region of the lower frets. On this part of the fingerboard, for frequencies in the region around 150 Hz the conductance happens to reach and even exceed 20 ms/kg. Thus, in the extreme case, the conductance at the neck termination of a bass string may amount to several percent of the characteristic admittance (cf. the following chapter).

In consequence, an additional flow of vibration energy from the string to the instrument structure via the neck is expected. Whether it shall be principally relevant for musical practice, can be checked using the overlay chart of Fig. 29 which, in a transparent version, is added to each copy of this report. The dots indicate the string-fret combinations for a bass with four, five or six strings in standard tuning. The transparent chart is laid in the conductance landscape. For each string-fret

combination the conductance is checked. A high conductance serves as a qualitative indicator for a dead spot. Since the quantitative relations are not yet known in detail, the different mechanisms of damping, including the damping by mobile supports, shall be considered in the next chapter.

## 7. DAMPING AND DECAY OF STRING VIBRATIONS

The scope of this chapter is to consider theoretically the different mechanisms, by which string vibrations may be damped. Comprehensive foundations are compiled by Nashif et al. (1985). Corresponding work on strings is documented by Fletcher (1976, 1977), Cuesta and Valette (1990) as well as Fletcher and Rossing (1998). While Cuesta and Valette (1988) make use of empirical damping parameters, determined by experiments on real strings, Fletcher deals with the theory of different damping mechanisms. A similar procedure is used in the following. Damping due to energy loss via the electromagnetic pick-ups shall be not considered. Based on experience accumulated in numerous damping measurements by means of a Complex Modulus Apparatus B&K 3930, which includes an electromagnetic transducer, this influence was neglected.

### 7.1. Vibration of the String

Classical theory, as treated in textbooks, assumes physical and geometrical linearity, *i.e.* small deflections and proportionality of force and displacement. Provided that there is no damping, the vibrations of a stretched string with constant parameters are governed by the linear partial differential equation of second order

$$S \frac{\partial^2 w}{\partial x^2} + q = \mu \frac{\partial^2 w}{\partial t^2} \quad (1)$$

with

- $S$     tensional force,
- $\mu = \rho_{st} A$     linear density, mass per unit length with  $\rho_{st}$  density and  $A$  cross-section area,
- $q$     loading force per length unit,
- $w$     displacement perpendicular to the axis of the unformed string,
- $x$     co-ordinate of the string axis and
- $t$     time.

For free vibrations ( $q = 0$ ) Eq. (1) simplifies to

$$c^2 \frac{\partial^2 w}{\partial x^2} = \frac{\partial^2 w}{\partial t^2} \quad (2)$$

where

$$c = \sqrt{S/\mu} \text{ speed of transverse waves on a string.}$$

The general (Bernoulli) solution is

$$w(x,t) = \sum_{j=1}^{\infty} \left( A_j \cos \frac{\omega_j}{c} x + B_j \sin \frac{\omega_j}{c} x \right) (C_j^* \cos \omega_j t + D_j^* \sin \omega_j t) \quad (3)$$

The ratio of the constants  $A_j$  and  $B_j$  as well as the characteristic equation, which yields the eigenvalues, are determined by means of the boundary conditions.

A string of length  $l$  fixed by rigid supports at both terminations ( $x = 0$  and  $x = l$ ) is characterised by

$$w(0,t) = 0 \text{ and}$$

$$w(l,t) = 0 \quad . \quad (4)$$

Inserting the boundary conditions given by Eq. (4) into Eq. (3) leads to the characteristic equation which yields the eigenvalues  $j\pi$ , the eigenfunctions

$$\hat{w}_j = \sin j\pi \frac{x}{l} \quad (5)$$

and the corresponding angular eigenfrequencies

$$\omega_j = \frac{j\pi}{l} \sqrt{\frac{S}{\mu}} \quad (6)$$

or the eigenfrequencies

$$f_j = \frac{j}{2l} \sqrt{\frac{S}{\mu}} \quad . \quad (7)$$

In this ideal undamped case, the eigenfrequencies  $f_j$  are harmonically related, *i.e.*  $f_j = j f_1$  with  $j$  an integer. At a given location  $x_0$  on the string the displacement is

$$w(x_0,t) = \sum_{j=1}^{\infty} (\sin j\pi \frac{x_0}{l}) (C_j \cos \omega_j t + D_j \sin \omega_j t) \quad . \quad (8)$$

The constants  $C_j$  and  $D_j$  of the time function are determined by evaluating the initial conditions. If the velocity is studied, the temporal derivation of Eq. (8) yields

$$v(x_0,t) = \sum_{j=1}^{\infty} (\sin j\pi \frac{x_0}{l}) (G_j \cos \omega_j t + H_j \sin \omega_j t) \quad (9)$$

with the modified constants

$$\begin{aligned} G_j &= \omega_j D_j \quad \text{and} \\ H_j &= -\omega_j C_j \quad . \end{aligned} \quad (10)$$

Compared to the displacement  $w(x_0,t)$ , the ratios of the partial amplitudes of the velocity  $v(x_0,t)$  increase proportionally to  $\omega_j$ .

Eqs. (8) and (9) predict that the amplitudes remain constant and do not decay. This is no longer true if damping is taken into account. In a real string energy is lost within the material, at the interface to the surrounding medium and at the contact points at the end supports. The consequences are that

- the frequencies of the partial vibrations are no longer in strictly harmonic relations and
- the amplitudes of the partial vibrations decrease as a function of time.

The latter effect is considered in the following and characterised by an additional exponential term

$$e^{-\delta_j t} = e^{-t/\tau_j} \quad (11)$$

where

- $\delta_j$  damping constant and
- $\tau_j = 1/\delta_j$  time constant

of the  $j^{\text{th}}$  partial of the string vibration. The time function of the displacement is extended by the exponential decay according to Eq. (11). For a fixed location  $x_0$  on the string Eq. (8) now writes as

$$w(x_0, t) = \sum_{j=1}^{\infty} K_j e^{-t/\tau_j} \cos(2\pi f_j^* t + \varphi_j) \quad (12)$$

with

- $K_j$  a constant which depends on the location on the string and the initial conditions,
- $f_j^* = \sqrt{f_i^2 - (\delta_j/2\pi)^2}$  frequency of the damped vibration and
- $\varphi_j$  phase angle, derived from the constants  $C_j$  and  $D_j$ , *i.e.* depending on the initial conditions.

The inharmonicity, which may originate from damping, is not considered in this report. The main scope is to analyse the decay of the vibrations. In the experiments on basses (Fleischer and Zwicker (1996, 1997)) and guitars (Fleischer (1998), Fleischer and Zwicker (1999)), the decaying of the string signals was characterised by the decay time  $T_{30}$ . This parameter is defined as the time within which the level of the (total) string signal decreases by 30 dB. It is related to the time constant  $\tau$ , *i.e.* the time within which the amplitude decreases by a factor of Euler's number  $e$ , by

$$T_{30} = 3.45 \tau \quad (13)$$

As can be taken from Eq. (12), the time constant  $\tau_j$  is defined in terms of the displacement (or velocity, or acceleration). This definition deviates from Fletcher's, where the decay of energy is considered; cf. Fletcher (1977) p. 141. Consequently, our time constants may differ from Fletcher's by a factor of two. In the following paragraphs, three different damping mechanisms (cf. Fletcher and Rossing (1998) pp. 53 - 56) shall be taken into account.

## 7.2. Air Damping

In the frequency range under consideration, a bass string is a poor acoustic radiator, which means that radiation damping is of minor importance. As a more prominent effect, viscous damping of the string motion by interaction with the surrounding fluid is considered. The string is modelled as a cylinder and the retarding force calculated according to the formula given by Stokes (1851). Eq. (1) has to be extended by an additional term comprising  $\partial w/\partial t$ . Work on this topic is reported for instance by Hancock (1982; cello strings) or Cuesta and Valette (1988, harpsichord strings). Alternatively, from the ratio of the respective energies a time constant is derived which characterises the decay of the displacement (or velocity, or acceleration) of the string vibration due to viscous damping in air. Considering the factor of 2 originating from the alternative definition based on the motion instead on the energy (Fletcher (1977)), this time constant is given by

$$\tau_{\text{air}} = \frac{\rho_{\text{st}}}{\pi \rho_{\text{air}}} \frac{2 M^2}{2\sqrt{2} M + 1} \frac{1}{f} \quad (14)$$

where

- $\rho_{\text{st}}$  density of the string (metal bass strings: 6000 ... 7000 kg/m<sup>3</sup>),
- $\rho_{\text{air}}$  density of the air (1.2 kg/m<sup>3</sup>) and
- $f$  frequency.

The parameter  $M$  is calculated from

$$M = \frac{R}{2} \sqrt{\frac{2\pi f}{\eta_{\text{air}}}} \quad (15)$$

with

$R$  string radius

$\eta_{\text{air}}$  kinematic viscosity of air.

For  $\eta_{\text{air}} = 1.5 \cdot 10^{-5} \text{ m}^2/\text{s}$  Eq. (15) is written as

$$M = 324 R \sqrt{f} \quad . \quad (16)$$

The radii  $R$  of typical bass strings were measured. The mean values of these own measurements as compiled in the first row of Tab. III are used for the calculations. They are inserted into Eq. (16) and lead to specific formulae of  $M_B \dots M_C$  for the different strings; see lower row of Tab. III.

String	B <sub>0</sub>	E <sub>1</sub>	A <sub>1</sub>	D <sub>2</sub>	G <sub>2</sub>	C <sub>3</sub>
$R/\text{mm}$	1.6	1.2	1.0	0.7	0.5	0.4
$M$	$0.52\sqrt{f}$	$0.39\sqrt{f}$	$0.32\sqrt{f}$	$0.23\sqrt{f}$	$0.16\sqrt{f}$	$0.13\sqrt{f}$

Tab. III. Radius  $R$  in mm and formula for the parameter  $M$  of typical bass strings.

The parameter  $M$  depends on the square root of the frequency  $f$ . In Tab. IV the frequencies of the fundamentals ( $j = 1$ ) are given for both the open strings and the strings fingered at the 12<sup>th</sup> fret, *i.e.* one octave higher. The column on the right side shows the  $M_1$  values calculated for the fundamental frequencies by the formulae given in the lower row of the above Tab. III. The parameter  $M_1$  ranges from 1.5 (open C string) to 4.1 (B string 12<sup>th</sup> fret) which is within the limits of validity of Eq. (14). For electric basses the parameter  $M_1$  can be estimated to be about a factor of five greater than for harpsichords as given by Fletcher (1977).

String	Frequency $f_1/\text{Hz}$	$M_1$
B open	30.9	2.9
B 12 <sup>th</sup>	61.8	4.1
E open	41.2	2.5
E 12 <sup>th</sup>	82.4	3.5
A open	55	2.4
A 12 <sup>th</sup>	110	3.4
D open	73.4	1.9
D 12 <sup>th</sup>	146.8	2.7
G open	98	1.6
G 12 <sup>th</sup>	196	2.3
C open	130.9	1.5
C 12 <sup>th</sup>	261.8	2.1

Tab. IV. Fundamental frequencies  $f_1$  and corresponding  $M_1$  values of typical bass strings, open and fingered at the 12<sup>th</sup> fret.

For a rough estimation of the time constant and its dependence on frequency,  $M \gg 1/(2\sqrt{2})$  is assumed. Eq. (14) then turns to

$$\tau_{\text{air}} \approx \frac{\rho_{\text{st}}}{\sqrt{2} \pi \rho_{\text{air}}} M \frac{1}{f} \quad (17)$$

From the densities

$$\rho_{\text{st}} = 6000 \text{ kg/m}^3 \text{ and}$$

$$\rho_{\text{air}} = 1.2 \text{ kg/m}^3$$

follows the ratio  $\rho_{\text{st}}/\rho_{\text{air}} = 5000$ , *i.e.*

$$\tau_{\text{air}} \approx 1125 M \frac{1}{f} \quad (18)$$

A comparison to the exact values reveals that the deviation amounts to maximally 24 % ( $M_1 = 1.5$ ; open C string). The smallest difference is less than 9 % ( $M_1 = 4.1$ ; B string 12<sup>th</sup> fret). The deviations decrease with increasing thickness of the string and with increasing fret number. The approximation is judged as sufficient for an estimation.

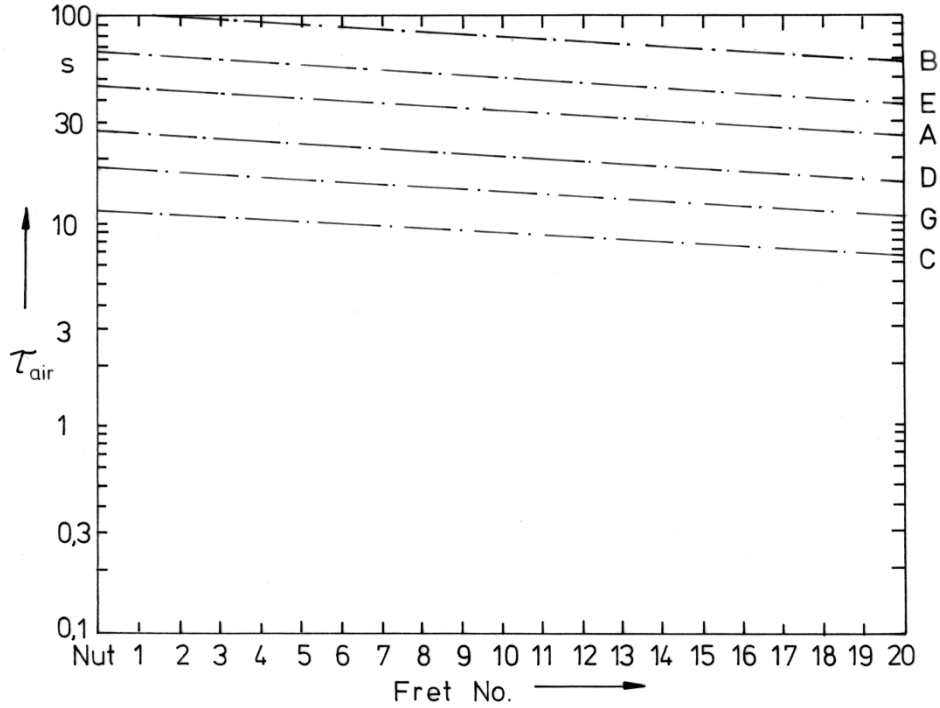


Fig. 35. Time constant  $\tau_{\text{air}}$ , caused by viscous air damping, as a function of the fret number for the fundamental vibrations of typical bass strings in standard tuning.

In order to elaborate the dependence of the time constant on frequency, Eq. (16) is inserted into Eq. (18) resulting in

$$\tau_{\text{air}}/\text{s} = 364 \frac{1}{\sqrt{f/\text{Hz}}} R/\text{mm} \quad (19)$$

the time constant  $\tau_{\text{air}}$  resulting in seconds if the radius  $R$  is inserted in millimetres and the frequency  $f$  in Hertz. Eq. (19) shows

- a direct proportionality of the time constant  $\tau_{\text{air}}$  on the radius  $R$  of the string and
- an inverse proportionality on the square root of the frequency  $\sqrt{f}$ .

Thus, if only viscous damping acts on a given string, the time constant decreases to the same extent as the root of the frequency increases. For example, a string shall decay about 40 % faster if fingered at the 12<sup>th</sup> fret as compared to the open string. The quantitative relations can be taken from Fig. 35.

In Fig. 35 the time constant  $\tau_{\text{air}}$  is plotted as a function of the fret number. Each fret step corresponds to a musical semitone, *i.e.* to a constant frequency ratio of about 1.06. Therefore, with respect to the time constant and the frequency, a log-log representation is created which simplifies the curves to straight lines. The time constant  $\tau_{\text{air}}$  is plotted for metal strings with radii as given in Tab. III. The global result is that viscous air damping causes bass strings to decay relatively slow. For a normal four-string bass ( $E_1$  through  $G_2$ ) the time constants are always greater than 10 s. For the low  $B_0$  string, which may be mounted on a five- or six-string bass, the time constant even proves as always greater than about 60 s. Obviously, for thick and heavy strings the effect of viscous air damping is minor. From this tentative consideration follows that air damping is not expected to be a substantial cause for the decay of bass strings.

### 7.3. Internal Damping

The next step is dedicated to internal damping. Internal damping results from the viscoelastic properties of the string material itself and should additionally account for effects which are a consequence of the fact that bass strings are made of a steel core and a compound winding. It is common knowledge that the sustain of a wound steel string deteriorates in the course of its lifetime; physical experiments were given *e.g.* by Hanson (1987). Experimental investigations of the influence of ageing on string sounds based on modern aurally-adequate methods are reported by Valenzuela (1999). Oxidation of the winding due to contact with the player's fingers and even air humidity are the causes. Effects originating from viscoelasticity as well as internal friction between the core and winding of the string are subsumed to internal damping. Cuesta and Valette (1988) as well as Chaigne (1991) report detailed considerations and experimental results.

While Allen (1976) gives an inverse quadratic dependence of the time constant on frequency, the calculations of Fletcher (1976) and Fletcher and Rossing (1998) lead to an inverse linear relation. Viscoelastic behaviour of the string material may be characterised by a complex Young's modulus

$$E = E_1 + i E_2 \quad (20)$$

where

$E_1$  storage modulus,

$E_2$  loss modulus and

$E_2/E_1 = \eta$  loss factor.

Bending stiffness has to be considered in Eq. (1). Internal damping is represented by a term with  $\partial^3 w / (\partial x^2 \partial t)$ , *i.e.* proportional to velocity  $\partial w / \partial t$  and curvature  $\partial^2 w / \partial x^2$ . Solving the modified differential equation or calculating the ratio of the reversible energy and the loss energy yields the time constant (cf. Cremer and Heckl (1986))

$$\tau_{\text{int}} = \frac{1}{\pi \eta f} \quad (21)$$

which in the present case is

$$\tau_{\text{int}} = \frac{E_1}{\pi E_2} \frac{1}{f} \quad (22)$$

The time constant  $\tau_{\text{int}}$  due to internal damping proves as proportional to the inverses of the

- loss factor  $\eta = E_2/E_1$  and

- frequency  $f$ .

If the loss factor of a metal string is supposed not to depend on frequency and tentatively estimated to 0.001, Eq. (22) turns to the preliminary formula

$$\tau_{\text{int}}/\text{s} = 318 \frac{1}{f/\text{Hz}} \quad (23)$$

which yields the time constant  $\tau_{\text{int}}$  in seconds if the frequency  $f$  is inserted in Hertz. Results for the fundamental frequencies of six bass strings are illustrated by Fig. 36.

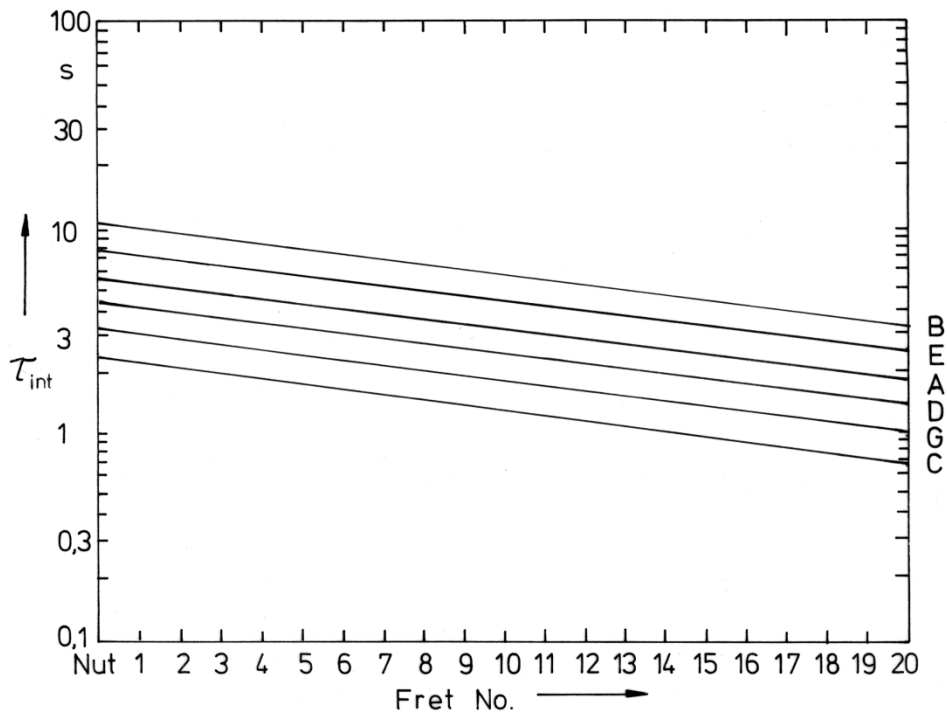


Fig. 36. Time constant  $\tau_{\text{int}}$ , caused by internal damping, as a function of the fret number for bass strings in standard tuning. The loss factor is  $E_2/E_1 = 0.001$ .

In Fig. 36 the time constant  $\tau_{\text{nit}}$  due to internal damping is given in the log-log representation for the loss factor 0.001. It is plotted as a function of the fret number including the nut for six bass strings in standard tuning. Again, only the fundamental vibration is considered. According to Eq. (23) the time constant decreases by  $f^{-1}$ . This is in contrast to Chaigne (1991), who found a  $f^{-3}$ -law for the time constant due to internal losses in nylon guitar strings. The higher the string is tuned, the more rapidly decays the fundamental. Correspondingly, the higher the fret is, at which the string is fingered, the more rapidly decays the vibration. The time constant, obeying the  $1/f$ -law, decreases by a factor of two per octave. The time constants in Fig. 36 range from about 0.8 s ( $C_3$  string 20<sup>th</sup> fret) to slightly more than 10 s (open  $B_0$  string). This tentative consideration on the basis of a realistically estimated loss factor indicates that internal damping is most probably more relevant for the decay of bass strings than viscous air damping.

## 7.4. Damping Due to Energy Loss via a Support

In a final step, the damping caused by the flow of vibration energy from one termination of the string to the instrument structure is considered. To account for the "worst case", the termination is assumed as purely resistive without a reactive part which is only true in the resonance case. Different approaches can be used to determine the corresponding time constants. One (cf. for instance Hagedorn (1989)) is to modify Eq. (3) by the exponential term Eq. (11). The boundary condition at  $x = l$  does no longer obey Eq. (4) but characterises damping now and is expressed by

$$S \frac{\partial w}{\partial x} \Big|_{x=l} = - \frac{1}{G} \frac{\partial w}{\partial t} \Big|_{x=l} \quad (24)$$

where

$S$  tensional force and

$G$  conductance, *i.e.* real part of the mechanical point admittance at the termination of the string at  $x = l$ .

This boundary condition is inserted in order to ascertain the eigenvalues and -functions. The eigenvalues become complex and contain the damping constant  $\delta_j$ .

In the following, the string is considered as a waveguide with characteristic impedance  $Z_{\text{st}}$ . A transverse wave is travelling toward the termination, which is represented by the conductance  $G$ . The susceptance is not taken into account. One part of the wave is reflected and the other one absorbed.

The reflection factor is

$$r = \frac{Z_{\text{term}} - Z_{\text{st}}}{Z_{\text{term}} + Z_{\text{st}}} \quad (25)$$

or, replacing the (real) impedance  $Z_{\text{term}}$  at the termination, which is assumed as purely real, by  $1/G$

$$r = \frac{1 - Z_{\text{st}} G}{1 + Z_{\text{st}} G} \quad (26)$$

The absorption coefficient writes as

$$\alpha = 1 - r^2 \quad (27)$$

The part of the incident energy  $E_{\text{inc}}$  absorbed at the termination is

$$E_{\text{abs}} = \alpha E_{\text{inc}} \quad (28)$$

the part reflected at the termination is

$$E_{\text{refl}} = (1 - \alpha) E_{\text{inc}} \quad . \quad (29)$$

After Cremer et al. (1973) as well as Cremer and Heckl (1986) the loss factor is

$$\eta = \frac{E_{\text{abs}}}{2\pi E_{\text{refl}}} \quad . \quad (30)$$

Inserting Eqs. (28) and (29) into Eq. (30) yields

$$\eta = \frac{\alpha}{2\pi(1 - \alpha)} \quad (31)$$

or with Eq. (27)

$$\eta = \frac{1}{2\pi} \left( \frac{1}{r^2} - 1 \right) \quad . \quad (32)$$

Substituting the reflection factor  $r$  by means of Eq. (26) leads to

$$\eta = \frac{1}{2\pi} [(1 + Z_{\text{st}}G)^2 (1 - Z_{\text{st}}G)^{-2} - 1] \quad . \quad (33)$$

Since the conductance at the termination is very small compared to the inverse of the characteristic impedance of the string, *i.e.*  $Z_{\text{st}}G \ll 1$ , a Taylor series can be used to expand the parenthesis terms with the exponents 2 and -2 in Eq. (33), which leads to

$$\eta = \frac{2}{\pi} Z_{\text{st}}G \quad . \quad (34)$$

From this loss factor the time constant can be calculated using Eq. (21) with the result

$$\tau_{\text{sup}} = \frac{1}{2} \frac{1}{Z_{\text{st}}G} \frac{1}{f} \quad . \quad (35)$$

The time constant  $\tau_{\text{sup}}$  depends on the inverses of the characteristic impedance  $Z_{\text{st}}$  of the string, of the conductance  $G$  at the support and of the frequency  $f$ . If the characteristic impedance is substituted by its inverse, the characteristic admittance  $Y_{\text{st}} = 1/Z_{\text{st}}$ , Eq. (35) shows that the time constant is proportional to  $Y_{\text{st}}/G$ . This means that  $\tau_{\text{sup}}$  is directly dependent on the ratio of the characteristic string admittance and the conductance at the support.

The characteristic impedance may be calculated from the parameters of the open string (cf. Fleischer (1999b))

$$Z_{\text{st}} = 2 m_{\text{open}} f_{\text{open}} \quad , \quad (36)$$

where

$m_{\text{open}}$  mass of the speaking part and  
 $f_{\text{open}}$  fundamental frequency of the open string.

As can be taken from Tab. V, the characteristic impedance of bass strings ranges from somewhat less than 0.7 kg/s ( $C_3$  string) up to 2.5 kg/s ( $B_0$  string) and may differ for different sets of strings.

String	Frequency $f_{\text{open}}/\text{Hz}$	Mass $m_{\text{open}}/\text{g}$	$Z_{\text{st}}/\text{kg s}^{-1}$	$Y_{\text{st}}/\text{mskg}^{-1}$
B	30.9	41	2.5	400
E	41.2	23	1.9	530
A	55	15.3	1.7	590
D	73.4	6.8	1.0	1000
G	98	3.9	0.76	1310
C	130.9	2.6	0.68	1470

Tab. V. Fundamental frequency  $f_{\text{open}}$ , mass  $m_{\text{open}}$  of the speaking part, characteristic impedance  $Z_{\text{st}}$  and characteristic admittance  $Y_{\text{st}}$  of typical bass strings.

Inserting Eq. (36) into Eq. (35) yields the time constant induced by energy losses at the termination

$$\tau_{\text{sup}} = \frac{1}{4 m_{\text{open}} f_{\text{open}}} \frac{1}{G} \frac{1}{f} \quad (37)$$

which differs by a factor of two from the formula given by Fletcher (1976, 1977 and 1998) due to a different definition of the time constant but coincides with formula (2.21) by Gough (1981). With respect to the slope, it has to be compared to the curve for  $\tau_2$  in Fig. 3(a) by Fletcher (1977), which refers to  $l \sim 1/f$  and  $R = \text{const.}$  Only for open strings ( $f = f_{\text{open}}$ ) having constant mass ( $m_{\text{open}} = \text{const.}$ ), Eq. (37) shows an inverse proportionality of the time constant on the squared frequency  $f_{\text{open}}$ . This special case is considered by Fletcher (1976) as  $\tau_1$  in Fig. 2 and by Fletcher and Rossing (1998) as  $\tau_3$  in Fig. 2.16, which are valid for  $l = \text{const.}$  and  $R = \text{const.}$

For the fingered strings of the bass, Eq. (37) has to be evaluated on the basis of the data compiled in Tab. V. Again, the consideration shall be restricted to the fundamentals of the complex string vibrations. The time constant  $\tau_{\text{sup}}$  is inversely proportional to the

- mass  $m_{\text{open}}$  and frequency  $f_{\text{open}}$  of the open string,
- conductance  $G$  at the support and
- frequency  $f$ .

Thus, the time constant  $\tau_{\text{sup}}$  depends on frequency  $\sim 1/f$  in the same way as the time constant  $\tau_{\text{int}}$  due to internal damping does.

If Eq. (37) is modified to

$$\tau_{\text{sup}} = \frac{1}{4 m_{\text{open}} f_{\text{open}}^2} \frac{1}{G} \frac{f_{\text{open}}}{f} \quad (38)$$

and the data from Tab. V inserted, a good mean value for all strings is estimated by

$$\tau_{\text{sup}}/\text{s} = \frac{6}{G/(\text{ms/kg})} \frac{f_{\text{open}}}{f} \quad (39)$$

The units are milliseconds per kilogram (for the conductance  $G$ ), Hertz (for the frequencies  $f_{\text{open}}$  of the open string as well as  $f$  of the string fingered at the fret under consideration) resulting in seconds for the time constant  $\tau_{\text{sup}}$ . Fig. 37 shows results for three different conductance values, which were assumed as independent on frequency. *E.g.* the conductance  $G = 1 \text{ ms/kg}$  (mid curve) leads to a time

constant of 6 s as long as the string is played open. The time constant decreases by a factor of two per octave. This means that, provided that the conductance remains the same, the time constant is only 3 s if the string is stopped at the 12<sup>th</sup> fret. As a consequence of the  $1/G$ -law, the time constant is highly sensitive to the conductance. The upper curve in Fig. 37 refers to 0.1 ms/kg and yields time constants by a factor of ten longer. A conductance of 10 ms/kg, which according to the experimental results is not uncommon for bass necks, lowers the time constant to fractions of a second.

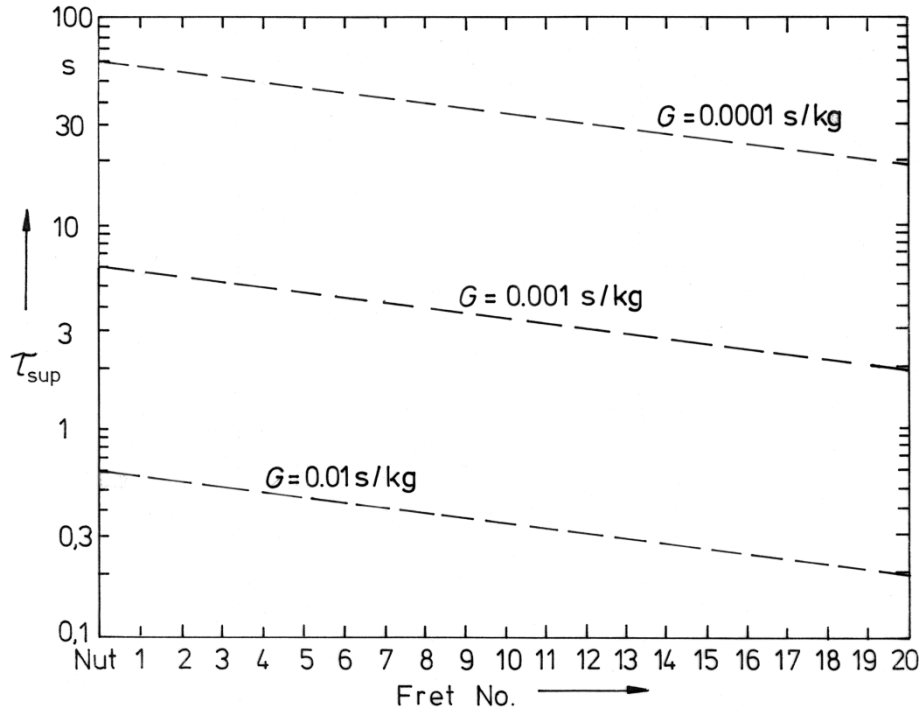


Fig. 37. Time constant  $\tau_{sup}$  due to the energy loss as determined by the conductance  $G$  at a termination, as a function of the fret number for an average bass string.

## 7.5. "Addition" of Time Constants

Each damping mechanism contributes an exponential term; cf. Eq. (11). If all three mechanisms are taken into account, the decay of the vibration is given by

$$e^{-\delta_{res} t} = e^{-t/\tau_{res}} = e^{-t/\tau_{air}} \cdot e^{-t/\tau_{int}} \cdot e^{-t/\tau_{sup}} = e^{-t(1/\tau_{air} + 1/\tau_{int} + 1/\tau_{sup})} \quad (40)$$

where

- $\delta_{res}$  resulting damping constant,
- $\tau_{res}$  resulting time constant,
- $\tau_{air}$  time constant for viscous air damping; cf. Eq. (19),
- $\tau_{int}$  time constant for internal damping; cf. Eq. (22) and
- $\tau_{sup}$  time constant for energy loss via an end support; cf. Eq. (37).

From Eq. (40) follows

$$\tau_{\text{res}}^{-1} = \tau_{\text{air}}^{-1} + \tau_{\text{int}}^{-1} + \tau_{\text{sup}}^{-1} \quad (41)$$

If all partial time constants have the same value, according to Eq. (41) the resulting time constant is only one third of this value. If the partial time constants are different, the resulting time constant is dominated by the smallest of the partial time constants. For an assessment of the role, which the different mechanisms play, the summation of the inverses after Eq. (41) shall not be executed. It seems to be sufficient for an estimation to identify the most prominent effect and to examine only the smallest time constant.

Furthermore, it should be kept in mind that the calculations of this chapter were restricted to the fundamental vibration. A complex vibration, as that of a plucked bass string, contains numerous partials. Each partial is damped in a different way. The normal case is that the fundamental has a great amplitude and decays slower than the higher partials. Consequently, the decay of the fundamental is most important for the decay of the total signal. Tentatively, this simplified image is taken as granted. The preliminary model used in the following assumes that

- the decay of the total signal is governed by the fundamental vibration and
- one damping mechanism dominates such far that the other ones may be neglected.

## 7.6. Comparison of the Time Constants for Bass Strings

In this paragraph, the time constants as derived in the preceding paragraphs of this chapter are compared. Each individual string of a bass is considered separately on the basis of realistic parameters. For this purpose,

- $\tau_{\text{air}}$  for viscous air damping is calculated by means of Eq. (19) for the radii according to Tab. III,
- $\tau_{\text{int}}$  for internal damping is calculated by Eq. (23), *i.e.* for an estimated loss factor of 0.001 and
- $\tau_{\text{sup}}$  for energy loss via a support is calculated by Eq. (37). The masses for the individual strings are taken from Tab. V. Curves for three values  $G = 0.0001 \dots 0.01$  s/kg in steps of one order of magnitude are plotted.

### 7.6.1. Normal Bass Strings

The bottom string of a conventional four-string bass is  $E_1$ ; see Fig. 38. As can be taken from the upper abscissa, the (rounded) frequencies of the fundamental vibrations range from 41 Hz (open) to 131 Hz (20<sup>th</sup> fret) and comprise a factor of 3.2. Because the "addition" of time constants is not considered, the predominant effect is discussed on the basis of the curve that yields the smallest time constants. Air damping (broken dotted line, which according to  $f^{-1/2}$  only weakly depends on frequency) is characterised by a too high time constant to influence the resulting time constant. Internal damping (solid line, decreasing by  $f^{-1}$ ) is in the order of 3 s to 7 s. Since the conductance, which characterises the damping at the support, may vary to a large extent, three broken curves for different  $G$  values are included in each diagram. They obey the same  $1/f$ -law as known from internal damping. Two of them, the curves for  $G = 0.0001$  s/kg and  $G = 0.001$  s/kg, respectively, bracket the time constant for internal damping.

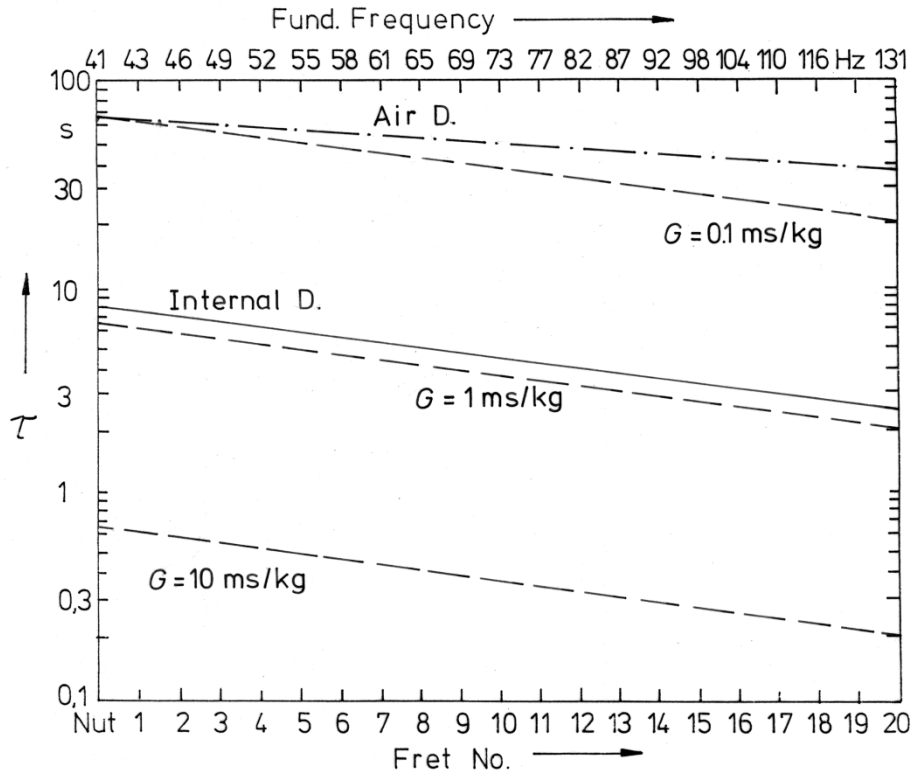


Fig. 38. Time constants  $\tau_{air}$  (broken dotted line),  $\tau_{int}$  (solid line) and  $\tau_{sup}$  (broken lines) as a function of the fret number and the fundamental frequency for a typical  $E_1$  string.

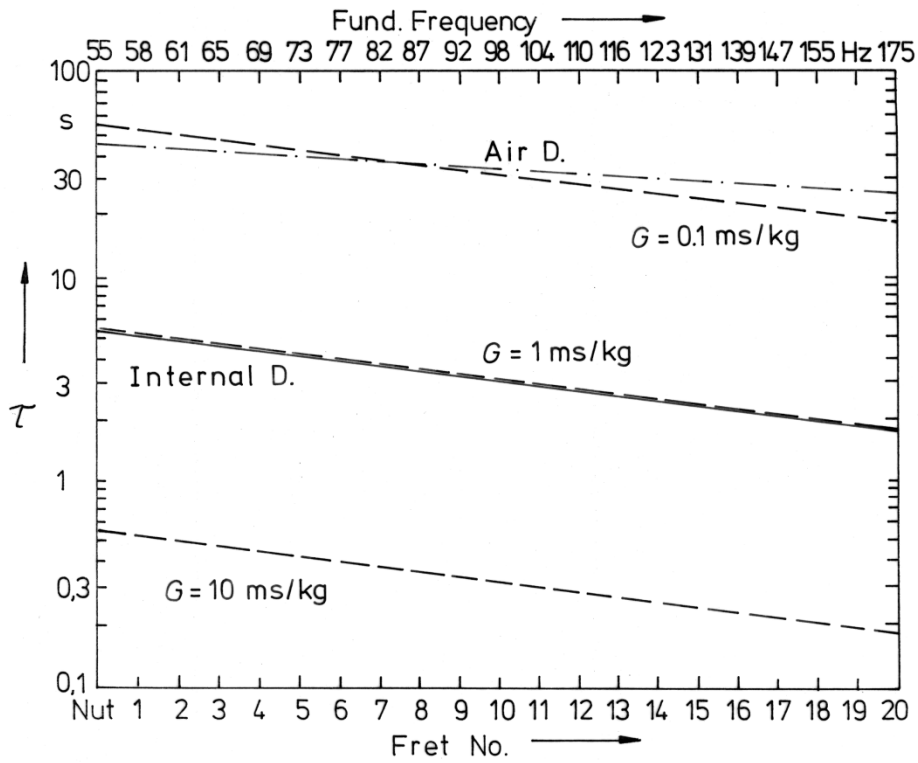


Fig. 39. Time constants  $\tau_{air}$  (broken dotted line),  $\tau_{int}$  (solid line) and  $\tau_{sup}$  (broken lines) as a function of the fret number and the fundamental frequency for a typical  $A_1$  string.

In Fig. 39 the frequency ranges from 55 Hz to 175 Hz for the  $A_1$  string. While the curves for the support damping are similar to those of the other strings, the curves for air damping (somewhat less than 30 s ... 45 s) and internal damping (about 2 s ... 6 s) are shifted downward compared to the E string. Air damping remains irrelevant, internal damping grows in importance in relation to support damping which can be seen from the coincidence of the time constants  $\tau_{int}$  for internal damping (loss factor  $E_2/E_1 = 0.001$ ) and  $\tau_{sup}$  due to a support conductance  $G = 0.001$  s/kg.

This tendency continues in Fig. 40 for the  $D_2$  string (73 Hz through 233 Hz). Again, the time constant for air damping is about one order of magnitude greater than for internal damping. Both curves ( $\tau_{air}$  and  $\tau_{int}$ ) are lower than observed for the E and A strings. The curves for support damping, however, almost remain the same with the consequence that the weights are gradually shifted. For instance, internal damping ( $E_2/E_1 = 0.001$ ) now leads to a smaller time constant than support damping by a conductance of  $G = 0.001$  s/kg.

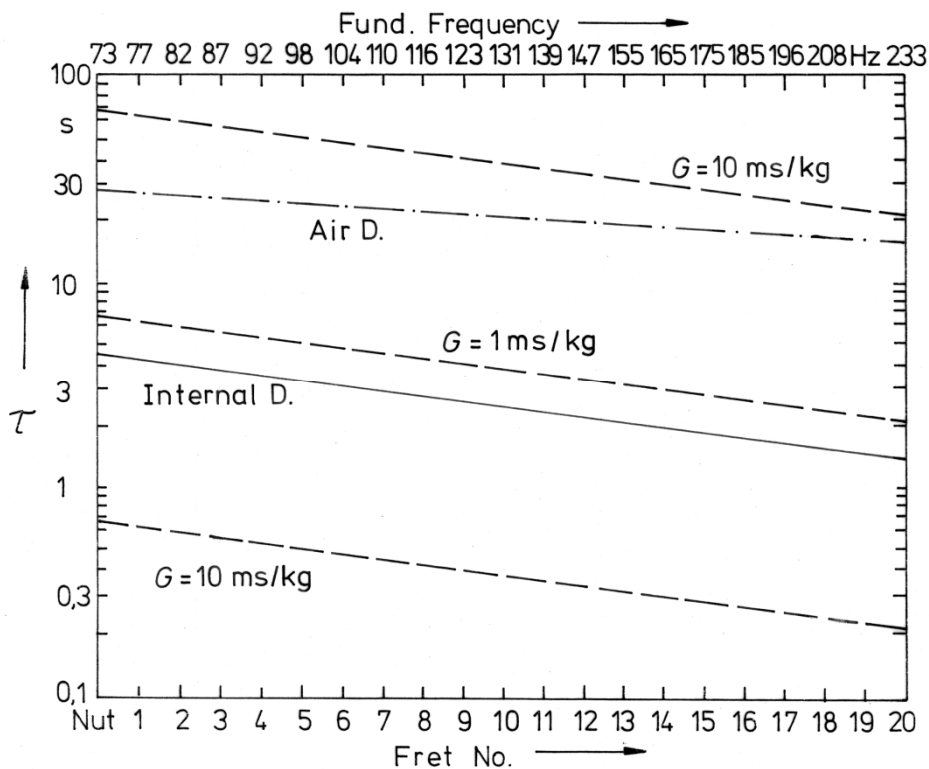


Fig. 40. Time constants  $\tau_{air}$  (broken dotted line),  $\tau_{int}$  (solid line) and  $\tau_{sup}$  (broken lines) as a function of the fret number and the fundamental frequency for a typical  $D_2$  string.

The top string of a normal bass is represented by Fig. 41. The fundamental frequencies are between  $G_2 \cong 98$  Hz and 310 Hz. The time constant for air damping is always higher than 10 s. Internal damping ranges between about 1 s and 3 s. The corresponding curve is bracketed by the curves for support damping characterised by the conductances  $G = 0.001$  s/kg and 0.01 s/kg, respectively. Air damping with an average time constant in the order of 15 s proves as less relevant than internal damping with an average time constant in the order of 2 s. These string-immanent mechanisms both tend to lose their dominance as soon as the (instrument-immanent) conductance exceeds a value of about  $G = 0.002$  s/kg.

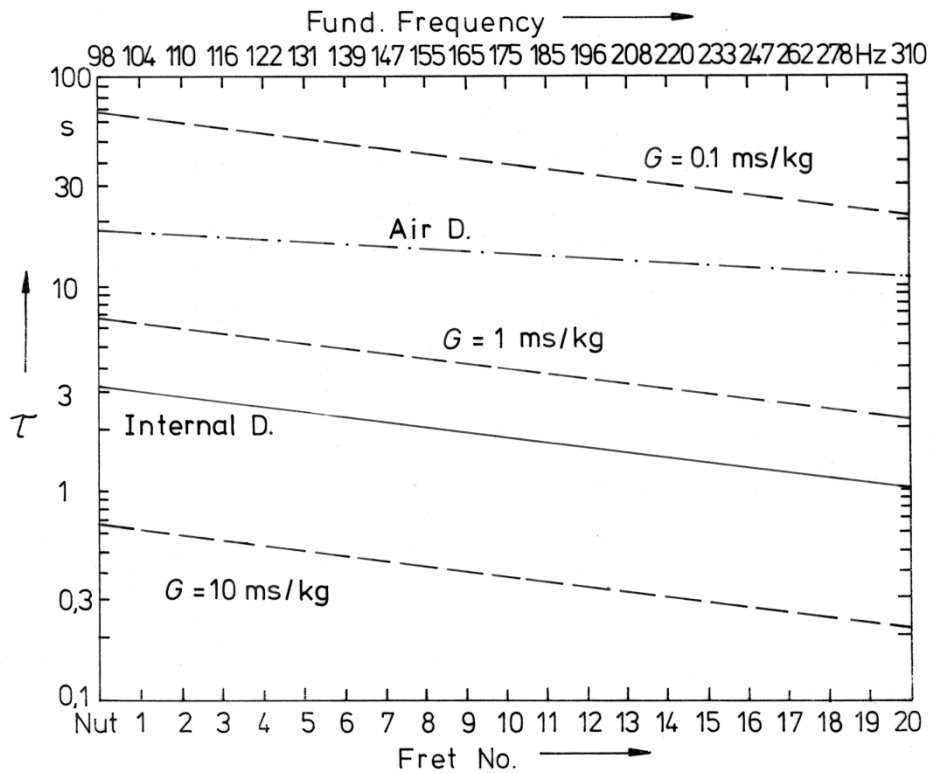


Fig. 41. Time constants  $\tau_{air}$  (broken dotted line),  $\tau_{int}$  (solid line) and  $\tau_{sup}$  (broken lines) as a function of the fret number and the fundamental frequency for a typical  $G_2$  string.

### 7.6.2. Extreme Cases

By regarding the bottom and top strings of a six-string bass, extreme values are elaborated and the tendencies emphasised. Fig. 42 refers to the  $B_0$  string (31 Hz through 98 Hz), which is used on the basses No. 2 and No. 4. As in the other examples, a loss factor of 0.001 is used for the estimation of internal damping (solid lines). Broken dotted lines characterise air damping, and the broken lines mark the damping due to energy flow through the support.

Since the time constant  $\tau_{air}$  (broken dotted line) is always greater than 50 s, it is in the upper ordinate range of Fig. 42 and therefore intrinsically irrelevant for the lowest bass string. The solid curve for internal damping (assumed loss factor  $E_2/E_1 = 0.001$ ), which reflects the inverse proportionality on frequency ( $\sim 1/f$ ), ranges from about 10 s (open string) to about 3 s (20<sup>th</sup> fret). Since internal damping marks an upper limit for the resulting time constant, the region in Fig. 42 above the corresponding curve is shaded. Only time constants outside the shaded area may substantially lower the resulting time constant. Internal damping dominates, as long as the support damping is represented by values within the shaded area, *i.e.* as long the conductance does not exceed about  $G = 0.0006$  s/kg. Compared to the experimental data, this value is relatively low. Obviously, the lower a bass string is tuned, the more sensitive it is to damping by the support.

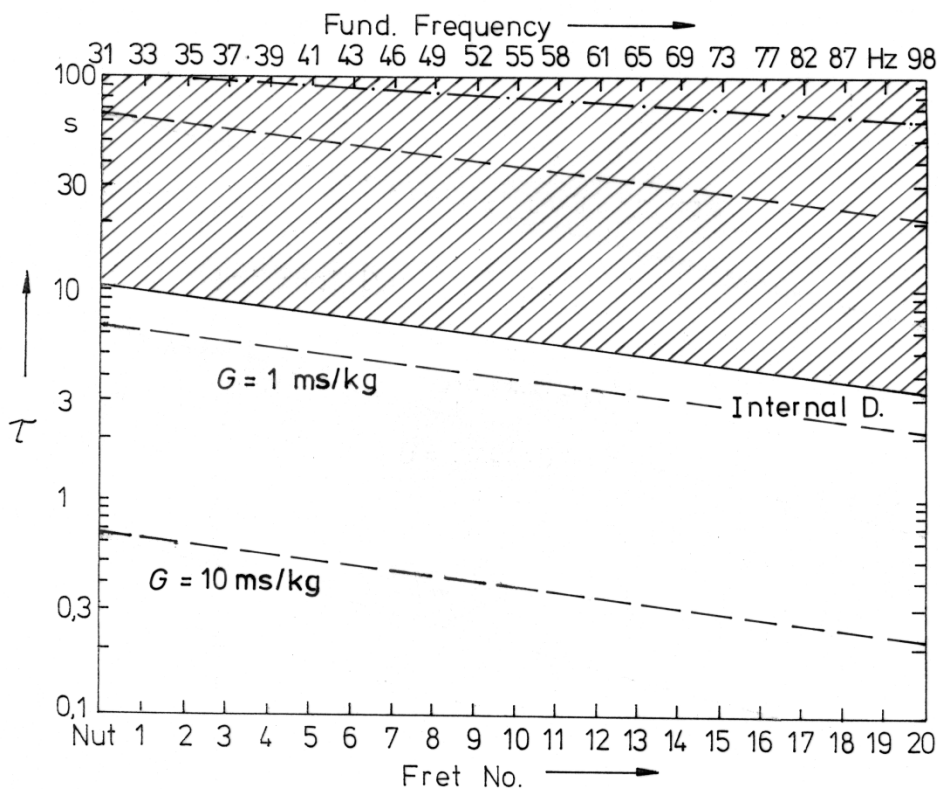


Fig. 42. Time constants  $\tau_{\text{int}}$  (solid line) and  $\tau_{\text{sup}}$  (broken lines) as a function of the fret number and the fundamental frequency for a typical  $B_0$  string.

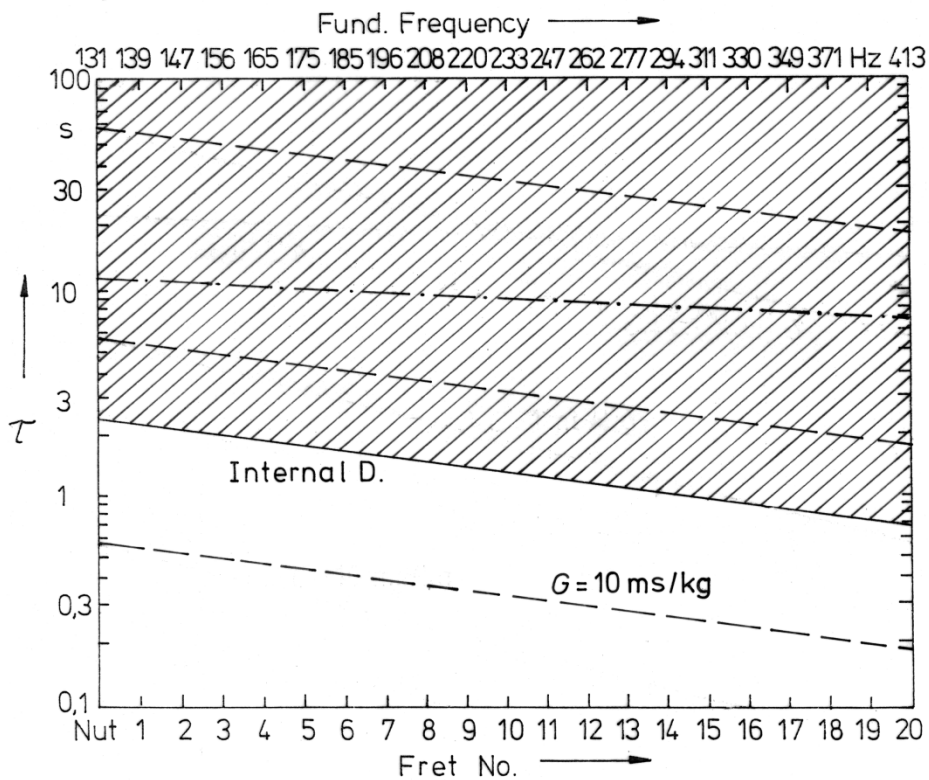


Fig. 43. Time constants  $\tau_{\text{air}}$  (broken dotted line),  $\tau_{\text{int}}$  (solid line) and  $\tau_{\text{sup}}$  (broken lines) as a function of the fret number and the fundamental frequency for a typical  $C_3$  string.

The highest-tuned bass string is  $C_3$ ; it is used on the bass No. 4. Fig. 43 shows that the fundamental frequencies range from 131 Hz to 413 Hz. It serves to illustrate the other extreme. Air damping (broken dotted line) results in an average time constant of about 10 s. This is much smaller than for the  $B_0$  string, but almost an order of magnitude greater than the time constant due to internal damping (solid line). The region is shaded in which the resulting time constant is dominated by internal damping. The shaded area is larger in Fig. 43 than in Fig. 42, which reflects the tendency that the higher a string is tuned the faster it decays. Support damping becomes important for a conductance higher than about  $G = 0.002$  s/kg.

Air damping is represented by a curve within the shaded area indicating that even for the highest tuned and highest fingered bass strings the friction with the viscous air has no relevance. The limiting factor, which marks the greatest possible time constant, is internal damping. The higher the tuning of a bass string is, the more important becomes this (string-immanent) damping mechanism compared to the external (instrument-immanent) support damping. Or in other words: A low-B string is more sensitive to the influence of the support since internal damping defines a relatively slow decay. In contrast to this, a high-C string is less prone to the supports because its decay is widely determined by internal damping.

## 7.7. Concluding Remarks

Three damping mechanisms have been treated which are suspicious to contribute to the decay of the vibrations of plucked bass strings. They are of "mechanical" origin in contrast to the damping due to electromagnetic interaction with the pick-ups, which was not considered. Because the inharmonicity of the partial frequencies as well as the eigenfunctions of the strings are not relevant for this task, no consequent holistic approach on the basis of the complete differential equation and dissipative boundary conditions was chosen. In a simplified procedure the three mechanisms were separately treated. They include

- damping due to viscous friction between the string surface and the surrounding air,
- internal damping and
- damping as a result of energy flow from the vibrating string to the instrument as defined by the conductance.

While internal damping as well as air damping are properties of the string itself, the energy flow through the support represents an effect which originates from the instrument structure. Air damping proves as irrelevant for bass strings which means that only two mechanisms (the string-immanent internal damping and the structure-immanent support damping) have to be taken into further account. The upper limit of the resulting time constant is always defined by internal damping. It should be kept in mind that the relations have been estimated on the basis of realistic, but assumed parameters. To interpret experimental data, the remaining two mechanisms shall be considered and the damping parameters determined in the next chapter.

## 8. DECAYING OF BASS STRINGS

This chapter deals with experiments in which the decay of bass signals was measured. The experimental results are discussed by means of the theoretical results derived in the precedent chapter. This way, the mechanisms underlying the generation of dead spots are investigated in detail.

### 8.1. Quantifying the Decay

#### 8.1.1. Measuring Procedure

The string signals of an electric bass are easily obtained via the electric output socket of the built-in electromagnetic pick-ups. For the measurement the tone and volume knobs were turned to their maximum positions. If different pick-ups can be chosen, which is the case for the Dyna Bass No. 3, the pick-up closest to the neck was switched to the output. The sustain was quantified by evaluating the decay of the total signal. The bass under consideration was handled by the author in sitting playing position. No artificial plucking mechanism was used. The player plucked the string in the "natural" way by means of his thumb such that the string vibrated both in and out of the finger-board-body plane. The total output signal was fed to a level recorder (B&K 2305) and the level registered. A 50-dB potentiometer and a paper speed of 3 mm/s were chosen.

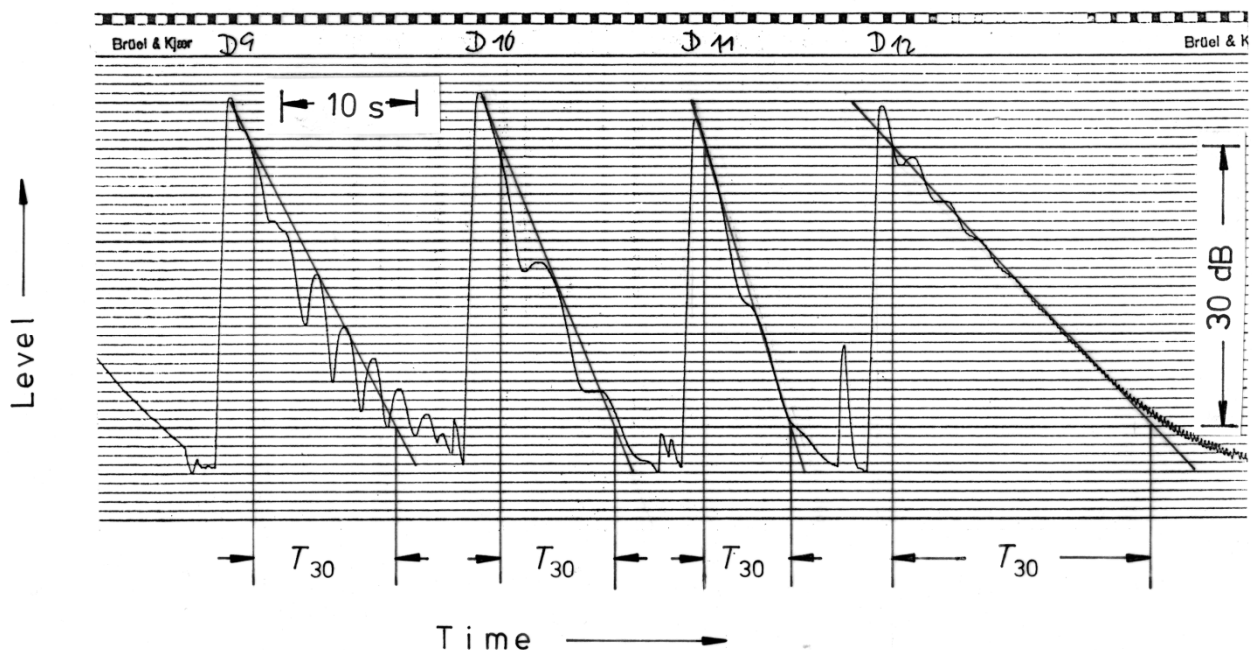


Fig. 44. Decay curves at the 9<sup>th</sup> (left) through 12<sup>th</sup> fret on the D string of the Action Bass No. 1. Sloping lines are inserted for the determination of the decay time  $T_{30}$ .

Since it was judged as more realistic for the musical action of a bass, the decay of the total signal was investigated in our study. This is in contrast to Heise's (1993) experiments who restricted his considerations to the fundamental vibration by filtering the signal. A sample of an original plot for four different fingering positions on the D string of the Action Bass No. 1 is given in Fig. 44. In

many cases, the level of the output signal does not decay monotonically but shows a more or less pronounced ripple. Most probably the cause is that the signal contains two partials with similar amplitudes and decay rates but with frequencies which are not in exact harmonic relations. Fluctuations of the total level, as visible in Fig. 44, are the result. The paper records were evaluated manually. Auxiliary straight lines (see Fig. 44) were used to characterise the average decay. The time difference was ascertained during which the total level had decreased by 30 dB. The result is denoted decay time  $T_{30}$  and amounts to half the reverberation time  $T_{60}$ , which is commonly used in room acoustics. The level difference of 30 dB, which defines  $T_{30}$ , corresponds roughly to a decrease of the loudness sensation by a factor of eight; cf. Zwicker and Fastl (1999). As given by Eq. (13)

$$T_{30} = 3.45 \tau$$

the decay time  $T_{30}$  is related to the time constant  $\tau$ , which was used in the theoretical considerations, by a numerical factor. Both parameters shall be simultaneously used in the following.

### 8.1.2. Decay of the Total Signal

Accordinging this criterion the decay time was determined for each fret of each string of two instruments (Action Bass No. 1 and Dyna Bass No. 3). After some time, the measurements were repeated and the results arithmetically averaged. Fig. 45 gives an example.

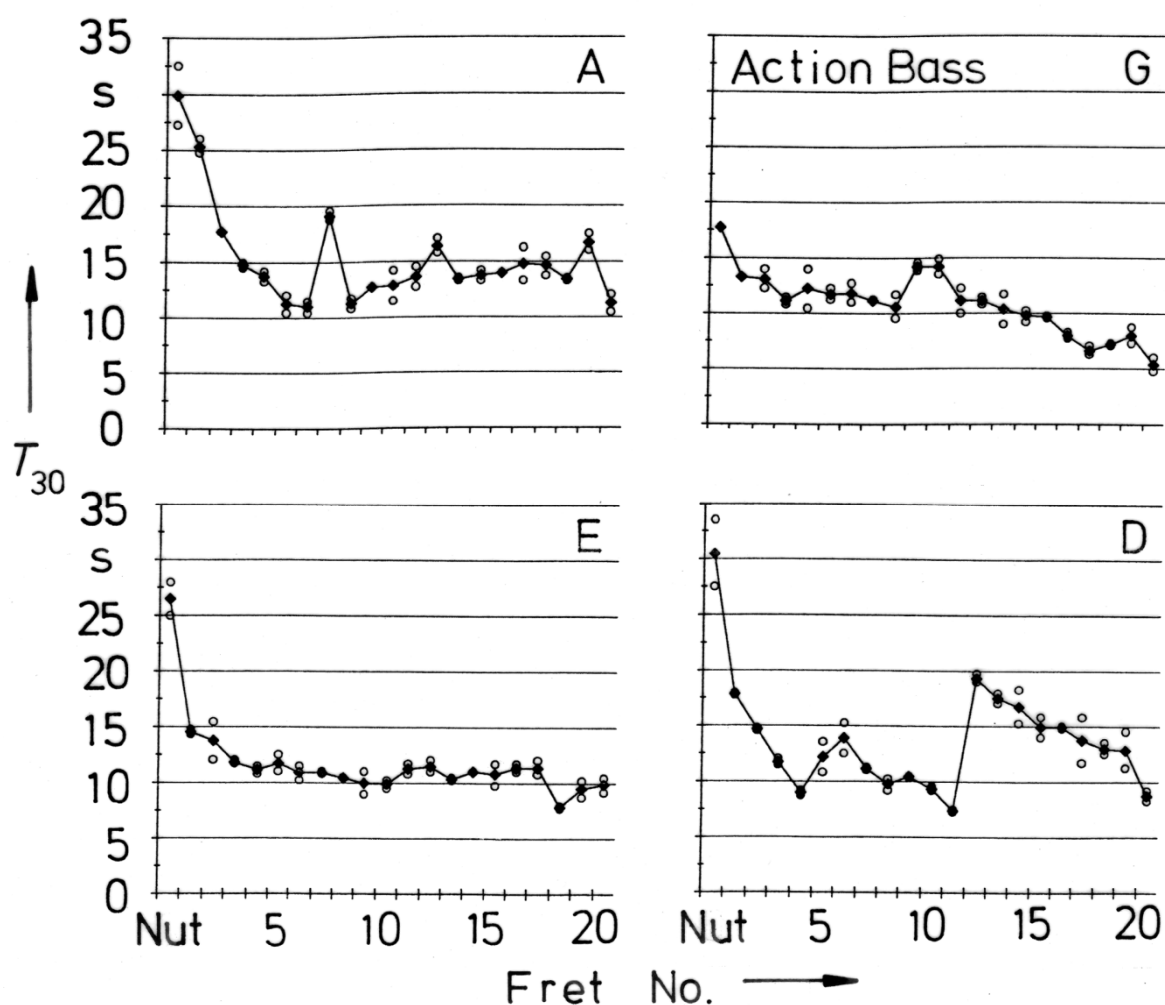


Fig. 45. Decay time  $T_{30}$  for the Action Bass No. 1.

The decay time for all strings of the Action Bass No. 1 is plotted in Fig. 45 versus the number of the fret at which the string is fingered. The open circles indicate single plucks and filled circles the linear average. In most cases, the decay times obtained by the two measurements coincide satisfactorily. Discrepancies, which are observed, may be the consequence of differing plucking in the two measurement series. It is a well-known fact that the manner and location of plucking affect the result. In this context, especially the direction plays an important role. As *e.g.* Fig. 23 has shown, the conductance is different in and out of the fingerboard plane which means that damping due to energy loss through a support depends on the polarisation of the string vibration.

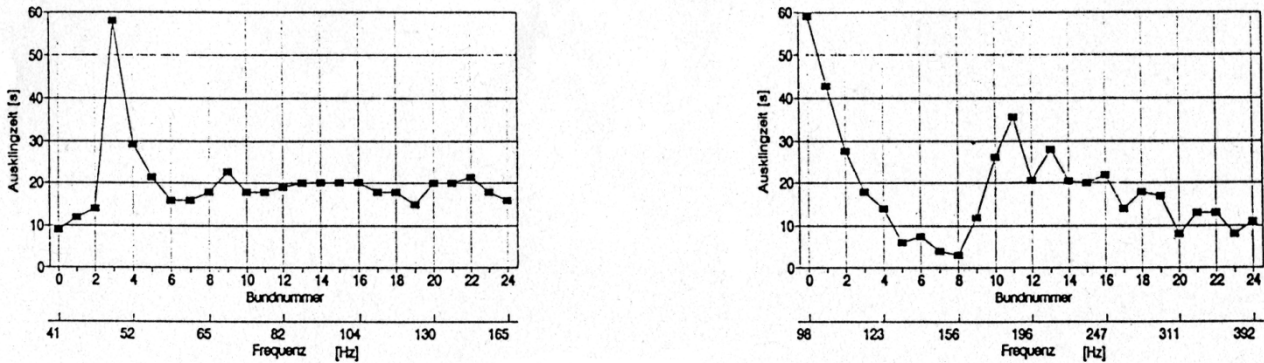


Fig. 46. Decay of the fundamental component after Heise (1993). The reverberation time ( $= 2 T_{30}$ ) is plotted versus the fret number and versus frequency for the E string (left) and G string (right).

The results indicate that it takes between about 5 s and 30 s for the string signal to decay by 30 dB. On the whole, the mean values (filled circles) tend to become smaller with increasing fret number. However, several exceptions to a steady decrease become evident. Unusually short decay times indicating dead spots are *e.g.* observed at the 5<sup>th</sup> and 6<sup>th</sup> fret of the A string and at the 11<sup>th</sup> fret of the D string; for the latter see also the original curve in Fig. 44. Examples of a relatively long decay suggesting the contrary, denoted live spots, occur for instance at the 7<sup>th</sup> fret of the A string and at the 12<sup>th</sup> fret of the D string. Again, for the latter cf. Fig. 44. On the average, the values of Fig. 45 for the decay of the total signal coincide well to the data given by Heise (1993) for the fundamentals of the E and G string signals. A remarkable discrepancy, however, is that the difference between the longest and shortest decay is much greater if only the fundamental is considered. For instance, according to Fig. 46 Heise finds that the fundamental decays by almost a factor of 20 faster at the 8<sup>th</sup> fret than the for the open G string. If the total signal is studied, the range of the decay times on a string is considerably smaller and comprises a factor of maximally five.

### 8.1.3. Decay of the Partial

With respect to the actual playing situation of a bass, it is regarded as representative to characterise the decay by the total signal as defined in the precedent paragraph. For the interpretation of the results, however, it has to be kept in mind that the vibration of a plucked string consists in a series of partial vibrations each of which, according to Eq. (12), decays by its individual rate. To get insight into the underlying details, in an additional measurement the string signals were decomposed and the decay behaviour of the single partial vibrations visualised. Each string was played both open and fingered at the 12<sup>th</sup> fret. The output of the pick-ups was fed to an FFT analyser (Ono Sokki CF 350), stored in the internal memory and analysed. Corresponding to the 1 kHz-bandwidth used in the experiments each time window was 0.4 s long.

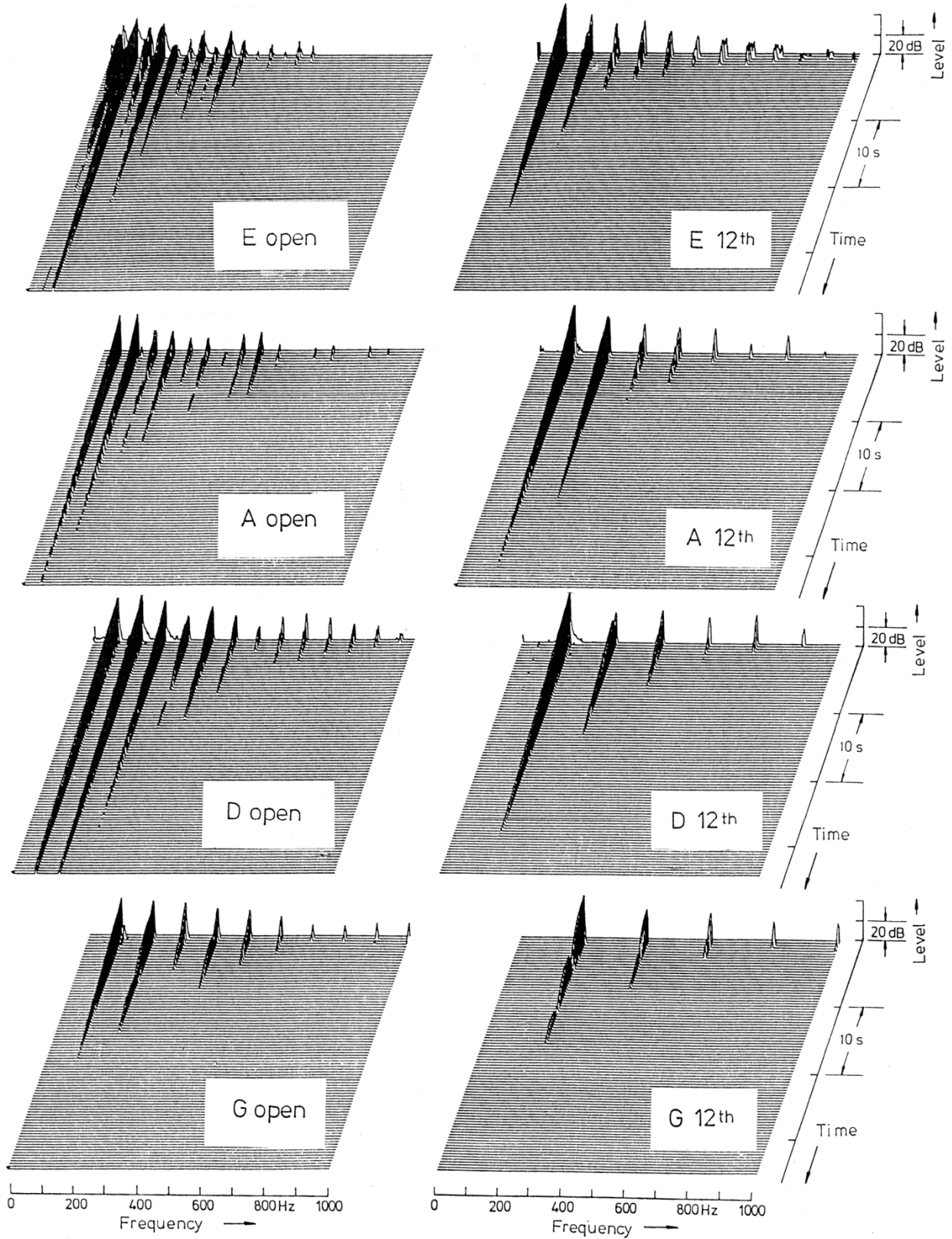


Fig. 47. Signals of the four strings of the Action Bass No. 1 as measured at the output plug. The level is plotted versus frequency and time.

The output signals of the Action Bass No. 1 are given as an example in Fig. 47. The level is plotted as a function of frequency and time. This representation visualises the single partials including their

individual decays. Generally, the fundamental tone is high in level and, as a rule, sustains for a longer time than the higher partials. This means that, in the normal case, the fundamental vibration determines the decay of the total signal. As can be taken from Fig. 47, the signals tend to decay the faster

- the higher a string is tuned ( $E_1$  through  $G_2$ ) and
- the higher the fret is where it is fingered (open and 12<sup>th</sup> fret, respectively).

Some of the diagrams in Fig. 47 emphasise, however, that under certain circumstances these simple rules do no longer hold. For the open E string, for example, the first partial tone decays unusually fast. Consequently, the fundamental vibration does no longer govern the decay of the total signal. In this special case, the decay of the second partial vibration is dominant. Nevertheless, in a first stage the decay of the total signal shall be tentatively explained in terms of the decay of the fundamental component, the remaining partials being ignored.

## 8.2. Comparing Experimental Data and Theoretical Decay of the Fundamental

In the following, experimental data are compared to theoretical ones. For the basses No. 1 and No. 3 the sustain, as determined by experiment, is characterised by the decay time of the total signal (cf. paragraph 8.1.1), averaged from two measurements. The results of experiments are compared to calculations from Chapter 7. Since a common relationship becomes obvious, corresponding strings of both instruments are treated together. The results of the decay measurements are plotted on a logarithmic scale as a function of the fret number. With respect to the frequency, this corresponds to a log-log representation. The double ordinate, which shows as well the time constant  $\tau$  as the decay time  $T_{30}$ , comprises one and a half decades.

### 8.2.1. Internal Damping and Support Damping

Based on the theoretical considerations of the precedent chapter, two damping mechanisms are discussed to interpret the experimental results:

- Internal damping is assumed to yield the upper limit for the time constant/decay time and
- damping due to energy loss via a support is assumed to account for uncommonly short time constants/decay times.

The curves for the time constants due to internal damping as given by Eq. (22)

$$\tau_{\text{int}} = \frac{E_1}{\pi E_2} \frac{1}{f_1}$$

and due to support damping by Eq. (37)

$$\tau_{\text{sup}} = \frac{1}{4 m_{\text{open}} f_{\text{open}}} \frac{1}{G} \frac{1}{f_1}$$

represent the upper and lower limit, respectively. Both obey a  $1/f_1$ -law. As a basic simplification, the theoretical treatment is restricted to the fundamental vibration (frequency  $f_1$ ). The individual parameters  $E_2/E_1$  and  $G$  are derived from the best fit of the experimental data. This means that, in this first step, experimental data, measured for the total signal, are approximated by theoretical curves, which refer to only one component of the complex signal.

### 8.2.2. Decay of the E String

Figs. 48 and 49 show the results for the  $E_1$  strings of both the Action Bass and the Dyna Bass. The upper limit of the experimental data is given by the solid curves, *i.e.* by internal damping with a loss factor  $E_2/E_1 = 0.0009 \dots 0.001$ . The lower limit is defined by the broken lines. Assuming support damping, the curves are related to a conductance  $G = 0.0017 \text{ s/kg} \dots 0.0021 \text{ s/kg}$ .

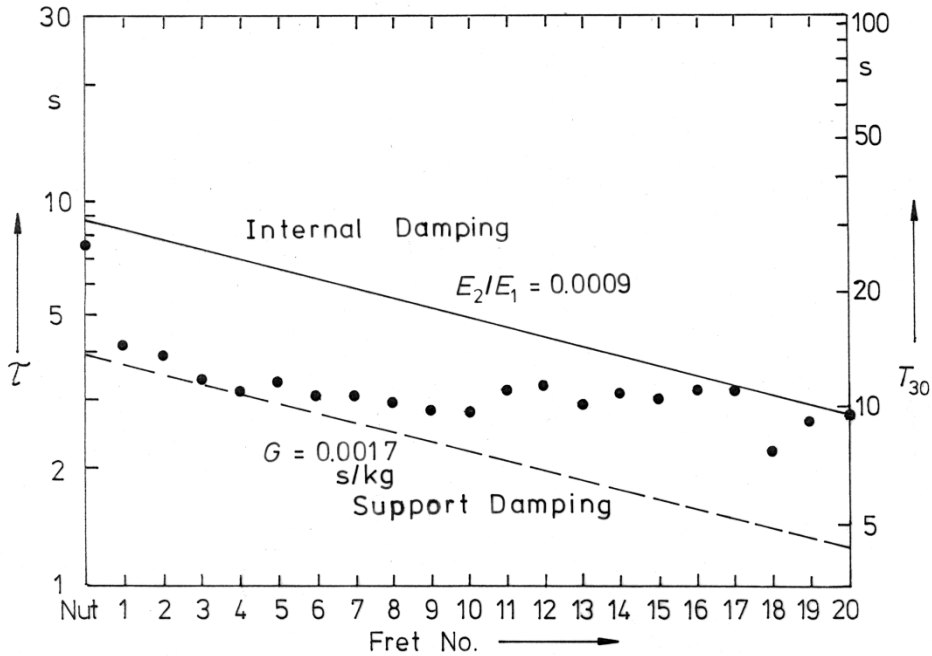


Fig. 48. Time constant  $\tau$  and decay time  $T_{30}$  at the different frets of the  $E_1$  string of the Action Bass No. 1. The experimental results (dots) are bracketed by the theoretical curves for internal damping (solid line) and support damping (broken line) of the fundamental component.

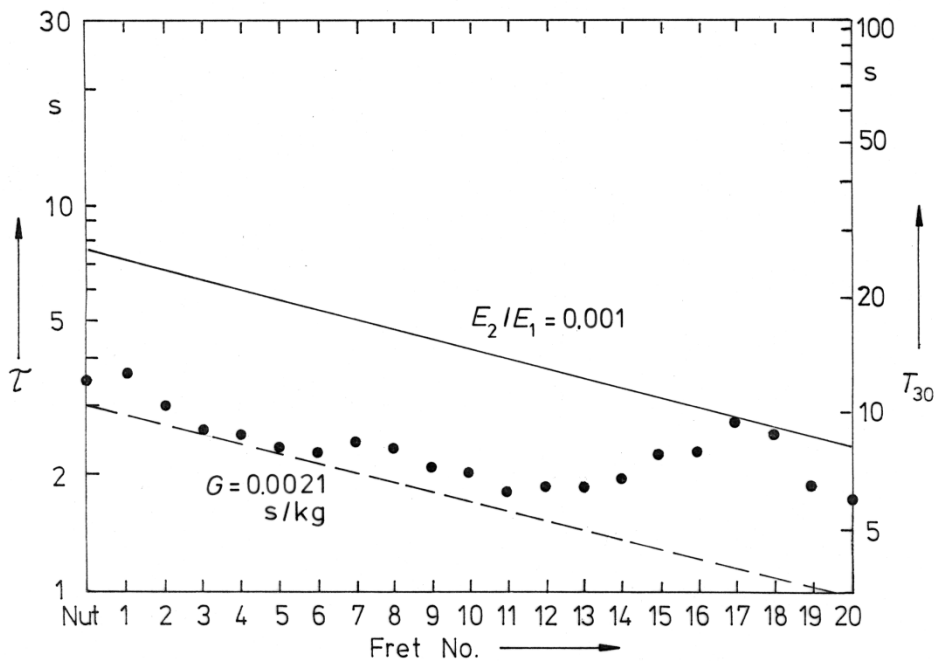


Fig. 49. Time constant  $\tau$  and decay time  $T_{30}$  at the different frets of the  $E_1$  string of the Dyna Bass No. 3. The experimental results (dots) are bracketed by the theoretical curves for internal damping (solid line) and support damping (broken line) of the fundamental component.

### 8.2.3. Decay of the A String

Figs. 50 and 51 give the results for the  $A_1$  strings of both basses. The upper limit for the experimental data is determined by internal damping with a loss factor  $E_2/E_1 = 0.0005 \dots 0.0006$ . The other limit is defined by the broken lines for support damping, the curves being related to the conductance  $G = 0.0013 \text{ s/kg} \dots 0.0019 \text{ s/kg}$ .

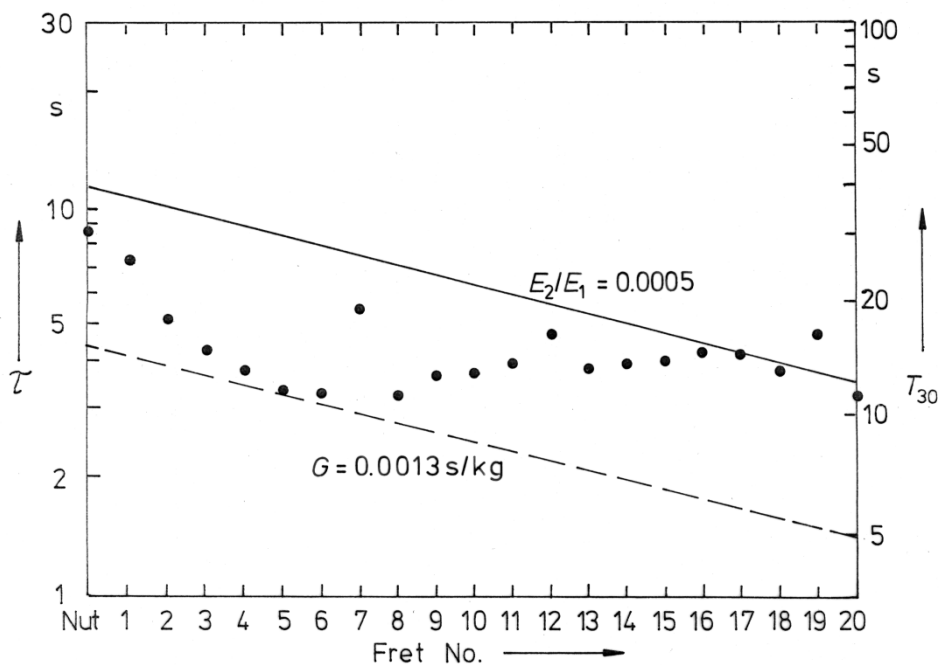


Fig. 50. Time constant  $\tau$  and decay time  $T_{30}$  at the different frets of the  $A_1$  string of the Action Bass No. 1. The experimental results (dots) are bracketed by the theoretical curves for internal damping (solid line) and support damping (broken line) of the fundamental component.

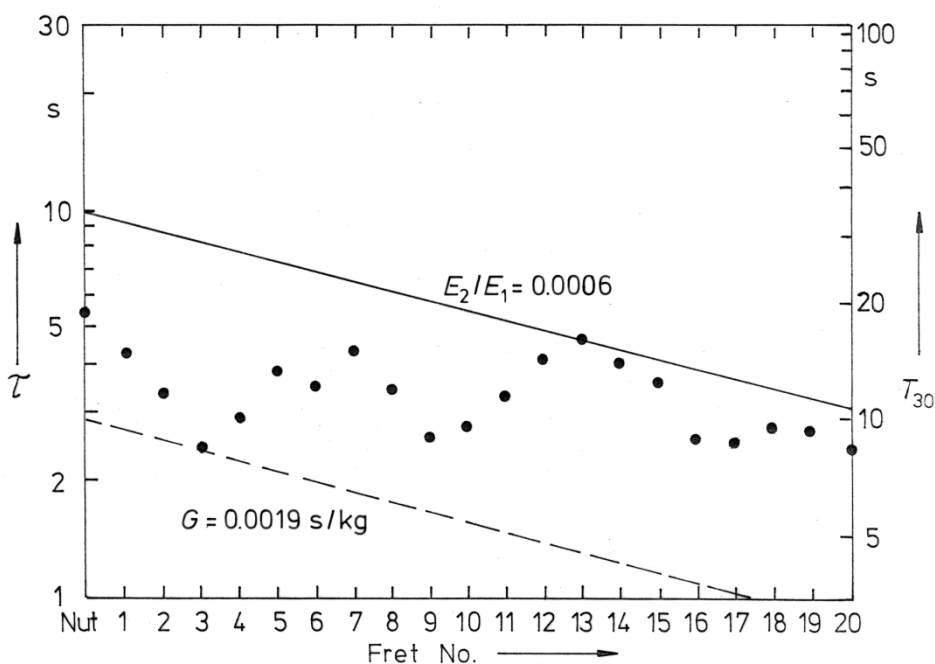


Fig. 51. Time constant  $\tau$  and decay time  $T_{30}$  at the different frets of the  $A_1$  string of the Dyna Bass No. 3. The experimental results (dots) are bracketed by the theoretical curves for internal damping (solid line) and support damping (broken line) of the fundamental component.

### 8.2.4. Decay of the D String

In Figs. 52 and 53 the experimental results for the  $D_2$  strings are compiled and the theoretical curves included. Internal damping is represented by the loss factor  $E_2/E_1 = 0.00035 \dots 0.0004$ , while support damping is defined by the conductance  $G = 0.0017 \text{ s/kg} \dots 0.0021 \text{ s/kg}$ .

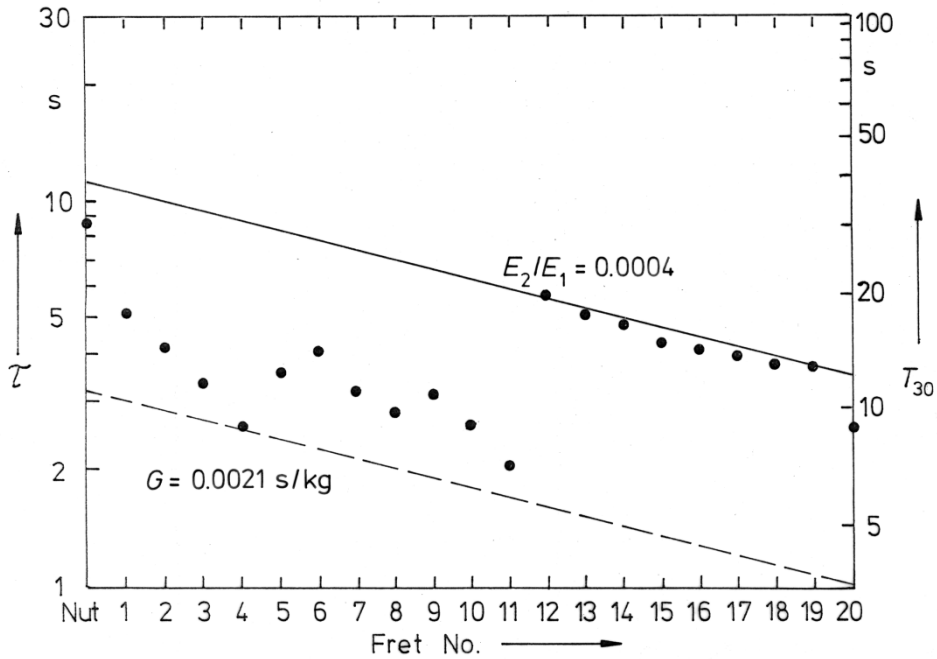


Fig. 52. Time constant  $\tau$  and decay time  $T_{30}$  at the different frets of the  $D_2$  string of the Action Bass No. 1. The experimental results (dots) are bracketed by the theoretical curves for internal damping (solid line) and support damping (broken line) of the fundamental component.

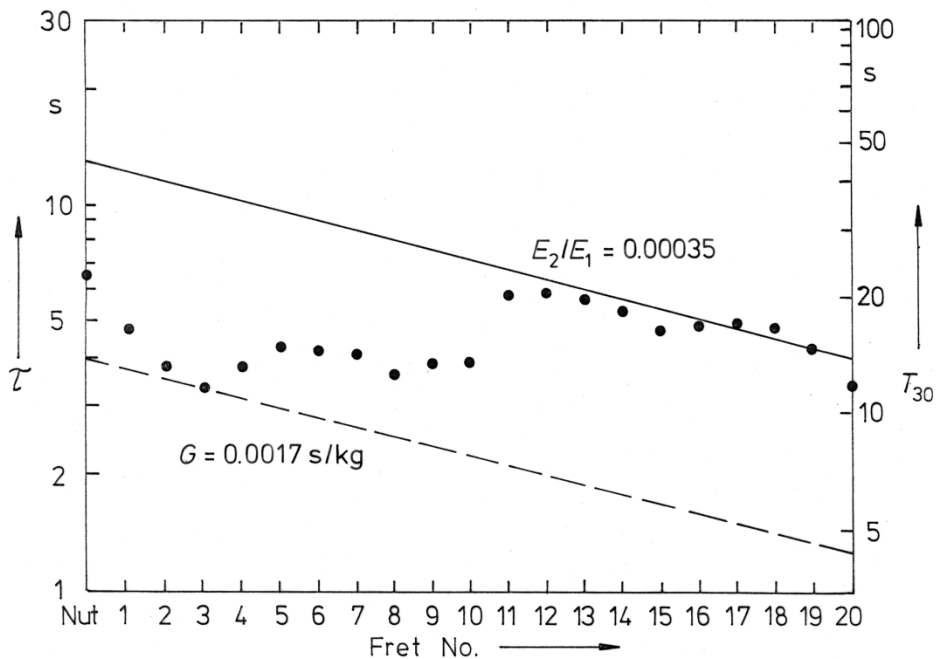


Fig. 53. Time constant  $\tau$  and decay time  $T_{30}$  at the different frets of the  $D_2$  string of the Dyna Bass No. 3. The experimental results (dots) are bracketed by the theoretical curves for internal damping (solid line) and support damping (broken line) of the fundamental component.

### 8.2.5. Decay of the G String

Figs. 54 and 55 refer to the results for the  $G_3$  strings of the basses. For the top string, internal damping is given by a loss factor  $E_2/E_1 = 0.00045 \dots 0.00047$ . The lower limit due to support damping is characterised by the conductance  $G = 0.0018 \text{ s/kg} \dots 0.0022 \text{ s/kg}$ .

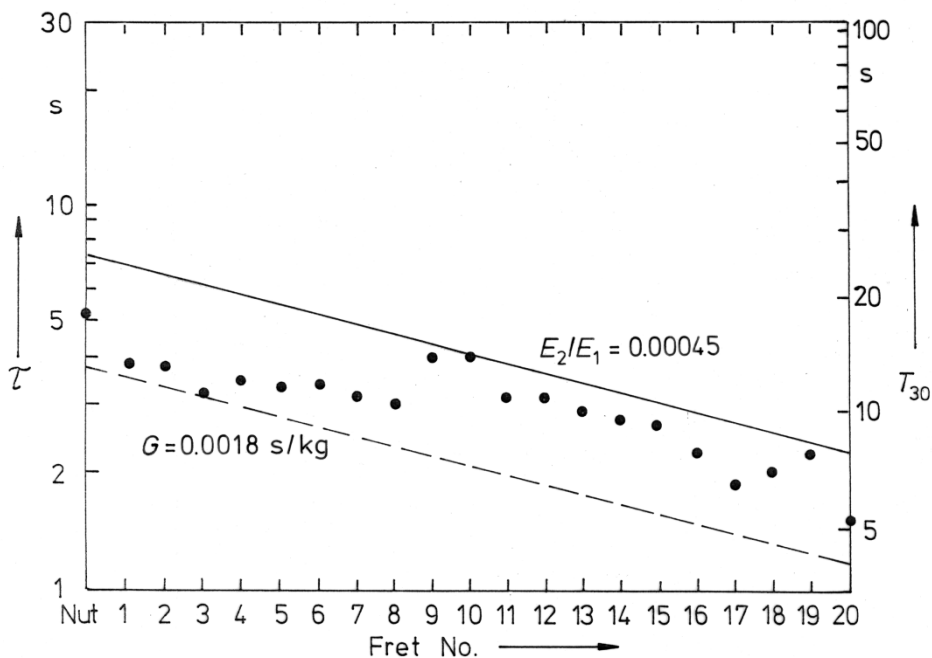


Fig. 54. Time constant  $\tau$  and decay time  $T_{30}$  at the different frets of the  $G_2$  string of the Action Bass No. 1. The experimental results (dots) are bracketed by the theoretical curves for internal damping (solid line) and support damping (broken line) of the fundamental component.

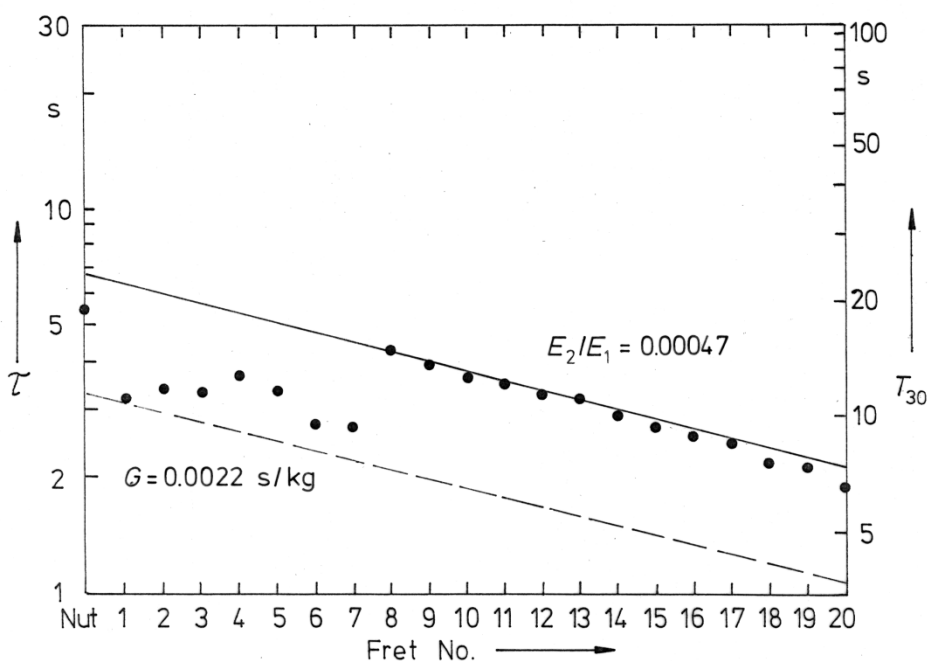


Fig. 55. Time constant  $\tau$  and decay time  $T_{30}$  at the different frets of the  $G_2$  string of the Dyna Bass No. 3. The experimental results (dots) are bracketed by the theoretical curves for internal damping (solid line) and support damping (broken line) of the fundamental component.

### 8.2.6. Evaluation

The individual data, which determine the limiting curves in Figs. 48 through 55, are assembled in Tab. VI. The upper limit is defined by internal damping and represented by a loss factor between less than  $E_2/E_1 = 0.0005$  for the top and mid strings up to  $E_2/E_1 = 0.001$  for the bottom strings. This range appears reasonable. Although the values are about one order of magnitude smaller than those given by Chaigne (1991) for nylon guitar strings are, they are in accordance with usual loss factors for metals. In addition to a realistic magnitude, the theoretical curves exhibit the same slope as the experimental data obtained if the player stops the strings in the high-fret region of the fingerboard. Evidently, this part of the interpretation of the experimental data, which refers to "live spots", is realistic and appears justified.

Fitted Parameter	Action Bass No. 1		Dyna Bass No. 3	
	$E_2/E_1$	$G/\text{ms kg}^{-1}$	$E_2/E_1$	$G/\text{ms kg}^{-1}$
E String	0.0009	1.7	0.001	2.1
A String	0.0005	1.3	0.0006	1.9
D String	0.0004	2.1	0.00035	1.7
G String	0.00045	1.8	0.00047	2.2

Tab. VI. Best-fit parameters representing internal damping ( $E_2/E_1$ ) and damping due to the conductance  $G$  at a support.

In contrast to the upper limit, the lower one characterising "dead spots" is left open for further discussion. Undoubtedly, it makes sense to attribute an uncommonly short decay time to an uncommonly high conductance at the corresponding fret. However, the fitting of the experimental data by the corresponding theoretical curves leads to a value  $G \approx 2 \text{ ms/kg}$ . As can be taken from Chapters 5 and 6, the conductance may reach values up to about 20 ms/kg, which is a factor of 10 higher than the parameter of the above fitting curves. If the conductance were a direct measure for the decay, the corresponding decay times should be less than one second and out of the range observed in the experiments.

This is the moment to recall in mind that the theoretical considerations refer to the fundamental component in contrast to the measurements, which are valid for the total signal. In order to study the behaviour of the fundamental on the basis of our model, the results after Heise (1993) are plotted in the same scale and fitted by the theoretical curves. Heise made use of a filter to reject the higher partials and ascertained the decay of the fundamental only. His results for the  $E_1$  and  $G_2$  strings are given in Fig. 56. The upper limit for the time constant/decay time is supposed to be defined by internal damping. For the fundamental of the  $E_1$  string (top diagram) the fit leads to the loss factor  $E_2/E_1 = 0.0008$ , which is close to the corresponding values in Tab. VI. The bottom diagram in Fig. 56 refers to the  $G_2$  string; a good fit is found for the loss factor  $E_2/E_1 = 0.00032$ . This value is somewhat smaller than the values in Tab. VI but comparable to such an extent that a different state or age of the strings can explain the discrepancy. On the whole, there is no obvious difference between the decay of the total signal and the isolated fundamental vibration.

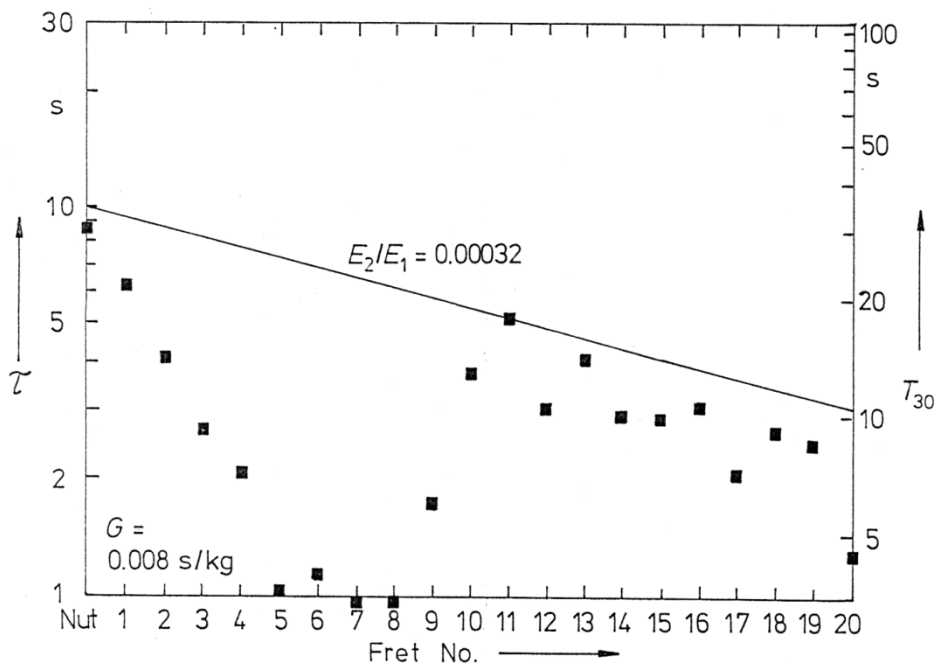
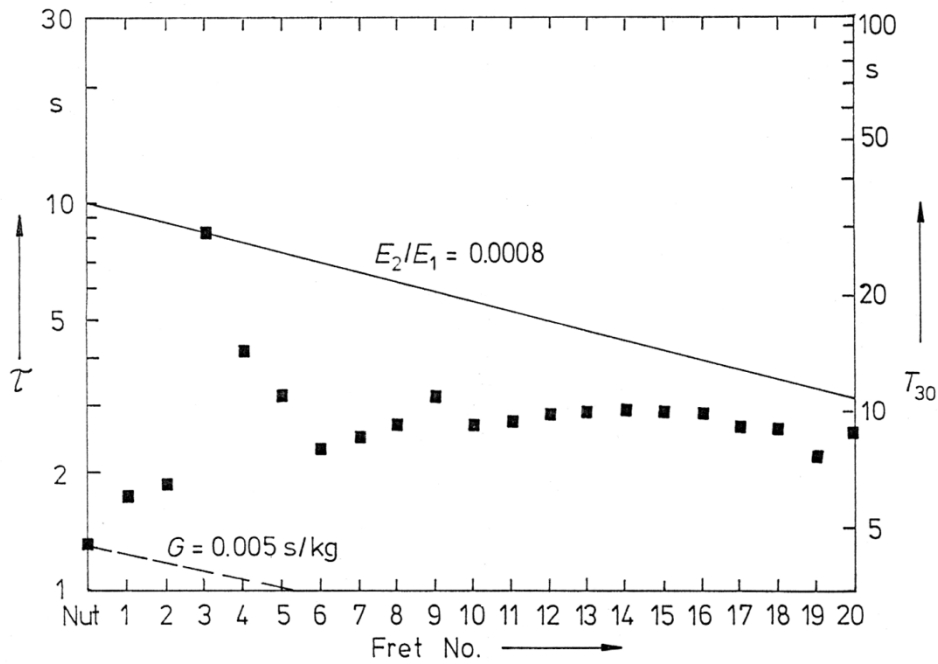


Fig. 56. Time constant  $\tau$  and decay time  $T_{30}$  of the fundamental on the  $E_1$  string (top) and  $G_2$  string (bottom) after Heise (1993). The experimental results (squares) are bracketed by the theoretical curves for internal damping (solid line) and support damping (broken line).

Much more pronounced differences can be taken from the lower limits; the broken line represents support damping. For the  $E_1$  string the conductance  $G = 5$  ms/kg is derived from the fitting curve.

The corresponding curve for the  $G_2$  string is no longer within the range of the diagram and is defined by the conductance  $G = 8 \text{ ms/kg}$ . These values are about three to four times as large as the values according to Tab. VI. This means that the "dynamic range" between the two limiting curves increases considerably if the fundamental rather than the total signal is considered. Obviously, dead spots of the total signals appear less "dead" compared to dead spots of the filtered fundamental.

This is a hint that it might be a too strong simplification to discuss the decay of the total signal merely in terms of the fundamental vibration. In the ideal case, *i.e.* as long as the supports do not accept vibration energy, the fundamental is the most prominent partial and governs the decay of the total signal. In the cases, which are in the focus of interest of this report, the fundamental obviously happens to decay so fast that it no longer dominates the total signal. Consequently, the decay of further partials has to be taken into additional account. This shall be the scope of the following paragraph.

### 8.3. Comparing Experimental Data and Theoretical Decay of Partial

As in the preceding paragraph, the results of the decay measurements on the two instruments are presented and compared to calculations. The refined theoretical model is primarily based on internal damping and accounts for the higher partials.

#### 8.3.1. Internal Damping of the Partial

In this advanced study, the fact is considered that the string signal consists of a series of partials. In accordance with the preceding paragraph, the model is based on the idea that the decay of the total signal is governed by the partial with the greatest decay time. In contrast to the preceding paragraph, damping by energy flow via a support is no longer regarded as a proportional measure for the decay of the total signal but has the function of a switch.

An individual time constant  $\tau_{\text{int},j}$  is calculated for the single partial by means of

$$\tau_{\text{int},j} = \frac{E_1}{\pi E_2} \frac{1}{j f_1} \quad (42)$$

where

- $E_2/E_1$  loss factor,
- $j$  number of the partial tone ( $j = 1, 2, 3$  in this study) and
- $f_1$  frequency of the fundamental ( $j = 1$ ).

Inharmonicity ( $f_j \neq j f_1$ ) is ignored and the loss factor assumed not to depend on frequency. If the decay time  $T_{30}$  is used instead of the time constant, according to Eq. (13)  $\tau_{\text{int},j}$  has to be multiplied by 3.45.

The hypothesis is as follows. Internal damping is the primary mechanism, which acts on all partials. Support damping is the secondary mechanism and acts selectively. The conductance serves no longer as a direct (inverse) measure for the resulting time constant/decay time, but as a criterion to discriminate different cases:

- If the conductance at the support is sufficiently small for the fundamental, the decay of the total signal is determined by the decay of this first partial ( $j = 1$ ; frequency  $f_1$ ).

- If the conductance exceeds a certain limit for the fundamental, the decay of the total signal is determined by the decay of the second partial ( $j = 2$ ; frequency  $2f_1$ ).
- If the conductance exceeds a certain limit for both the fundamental and second partial, the decay of the total signal is determined by the decay of the third partial ( $j = 3$ ; frequency  $3f_1$ ).

This series might be continued. For the data obtained in the own experiments it proves as sufficient to consider the first three partials.

Thus, as in Paragraph 8.2, internal damping of the fundamental yields the upper limit for the time constant/decay time. In contrast to this paragraph, damping due to energy loss via a support is no longer treated as an analog measure for the damping of the fundamental, but as a binary criterion. If it exceeds a certain limit, it "switches off" the corresponding partial and, as a consequence, "switches over" to the next partial. Therefore, in the following diagrams curves for internal damping of the second and third harmonic are added. The loss factor is assumed not to depend on frequency.

### 8.3.2. Decay of the E String

Figs. 57 and 58 show the results for the  $E_1$  strings of both the Action Bass and the Dyna Bass. Exactly as in Figs. 48 and 49, the upper limit for the experimental data (dots) is defined by internal damping of the fundamental (1) with a loss factor  $E_2/E_1 = 0.0009 \dots 0.001$ . The remaining two curves refer to internal damping of the second (2) and third partial (3). In the region of the lower frets the curves (2) or (3) fit the experimental data best, which means that the second or even the third partial governs the decay of the total signal. In the high-pitch region the dots are closest to the curve (1) indicating that the fundamental governs the decay of the total signal.

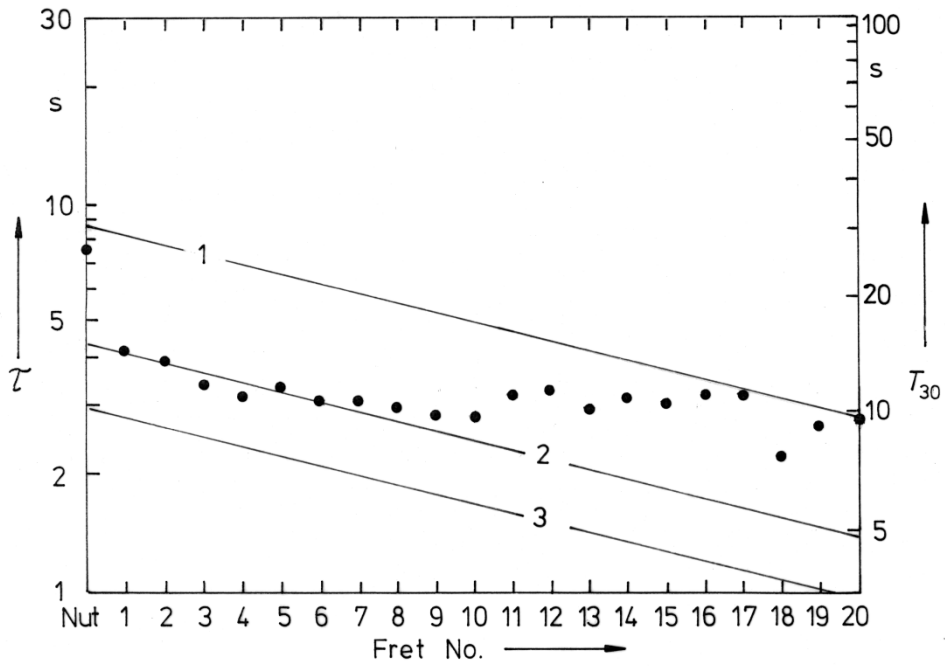


Fig. 57. Time constant  $\tau$  and decay time  $T_{30}$  at the different frets of the  $E_1$  string of the Action Bass No. 1. The experimental results (dots) are fitted by theoretical curves for internal damping ( $E_2/E_1 = 0.0009$ ; solid lines) of the first three partials of the string vibration.

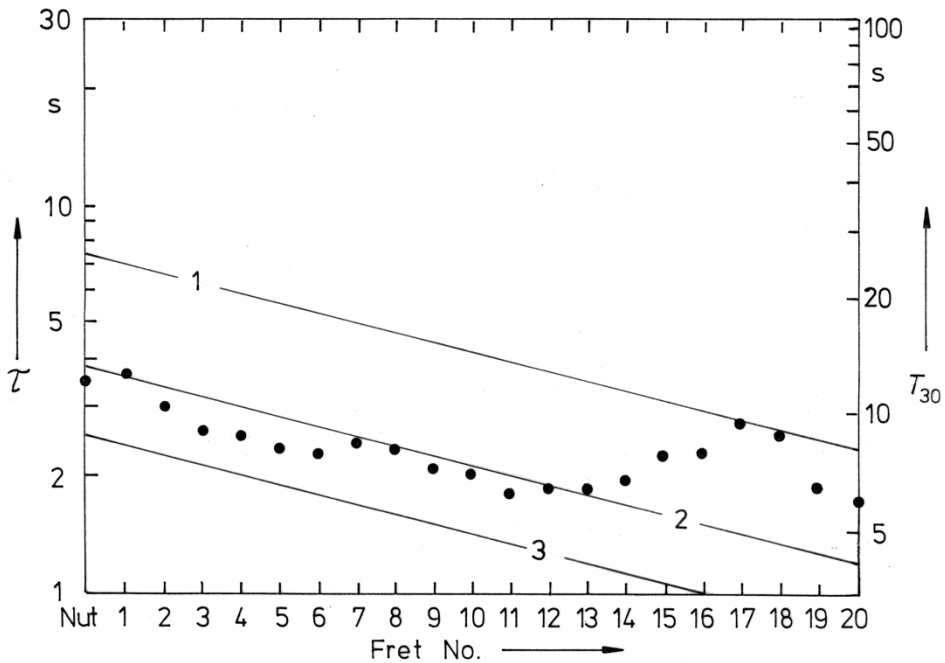


Fig. 58. Time constant  $\tau$  and decay time  $T_{30}$  at the different frets of the  $E_1$  string of the Dyna Bass No. 3. The experimental results (dots) are fitted by theoretical curves for internal damping ( $E_2/E_1 = 0.001$ ; solid lines) of the first three partial vibrations.

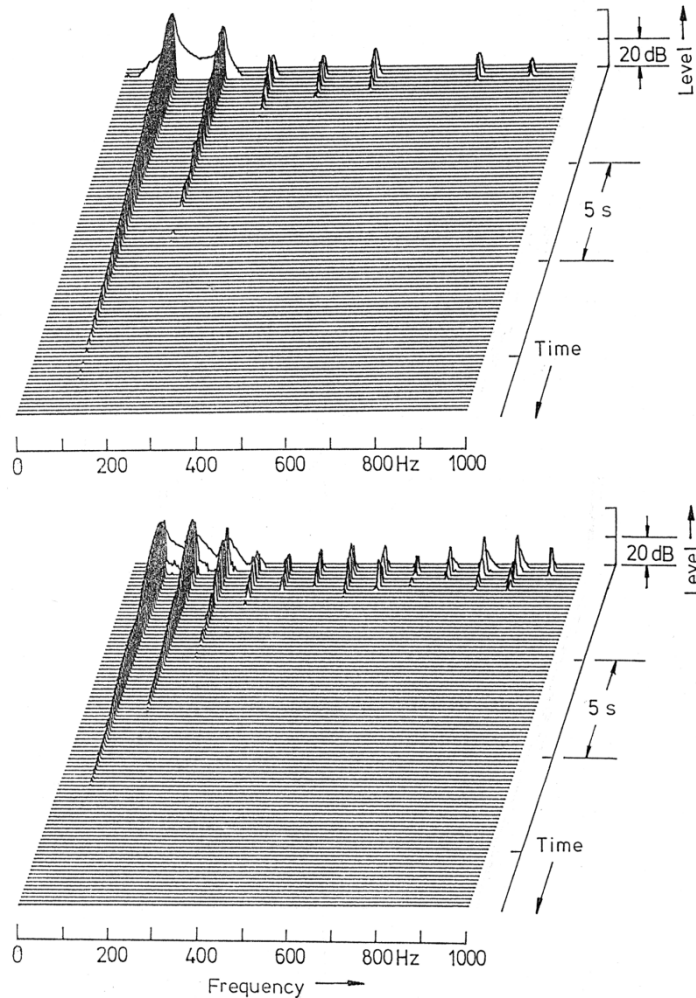


Fig. 59. Signals (level versus frequency and time) of the  $E_1$  string of the Dyna Bass No. 3, measured at the output plug. Top: 17<sup>th</sup> fret; bottom: 9<sup>th</sup> fret.

In order to give better insight into details, for each string an example was selected. A pair of diagrams is presented in which the decay of the single partials becomes visible. Fig. 59 refers to the 17<sup>th</sup> fret (top) and the 9<sup>th</sup> fret of the Dyna Bass No. 3. The top diagram represents the "normal" case: Compared to the higher partials, the fundamental decays slowly and thus determines the decay of the total signal. The bottom diagram yields an impression of a "dead spot": Although the frequencies are lower (and therefore a slower decay might be expected), the first two partials decay relatively fast and by similar rates. The fundamental does no longer exclusively govern the total decay, but the second harmonic is practically equal in influence.

### 8.3.3. Decay of the A String

In Figs. 60 and 61 the results of the  $A_1$  strings are displayed for both basses. The curves denoted (1), which mark the upper limit for the experimental data, refer to internal damping of the first partial and are taken from Figs. 50 and 51, respectively. There are several locations on the fingerboard, especially in the mid region, where the curves of the second (2) or third partial (3) are a better fit for the measured decay times than the curve of the fundamental (1).

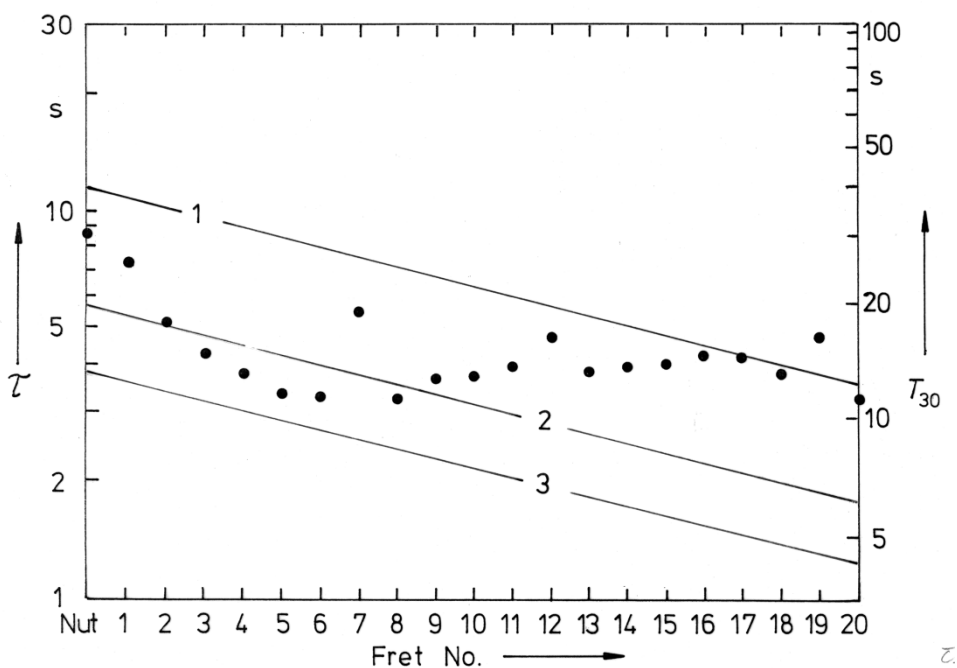


Fig. 60. Time constant  $\tau$  and decay time  $T_{30}$  at the different frets of the  $A_1$  string of the Action Bass No. 1. The experimental results (dots) are fitted by theoretical curves for internal damping ( $E_2/E_1 = 0.0005$ ; solid lines) of the first three partial vibrations.

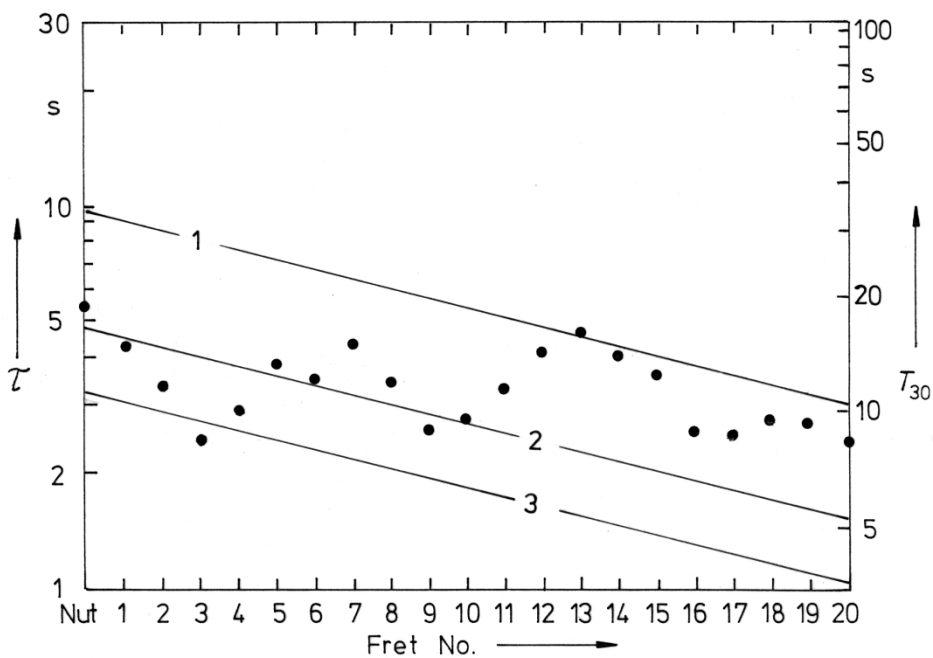


Fig. 61. Time constant  $\tau$  and decay time  $T_{30}$  at the different frets of the  $A_1$  string of the Dyna Bass No. 3. The experimental results (dots) are fitted by theoretical curves for internal damping ( $E_2/E_1 = 0.0006$ ; solid lines) of the first three partial vibrations.

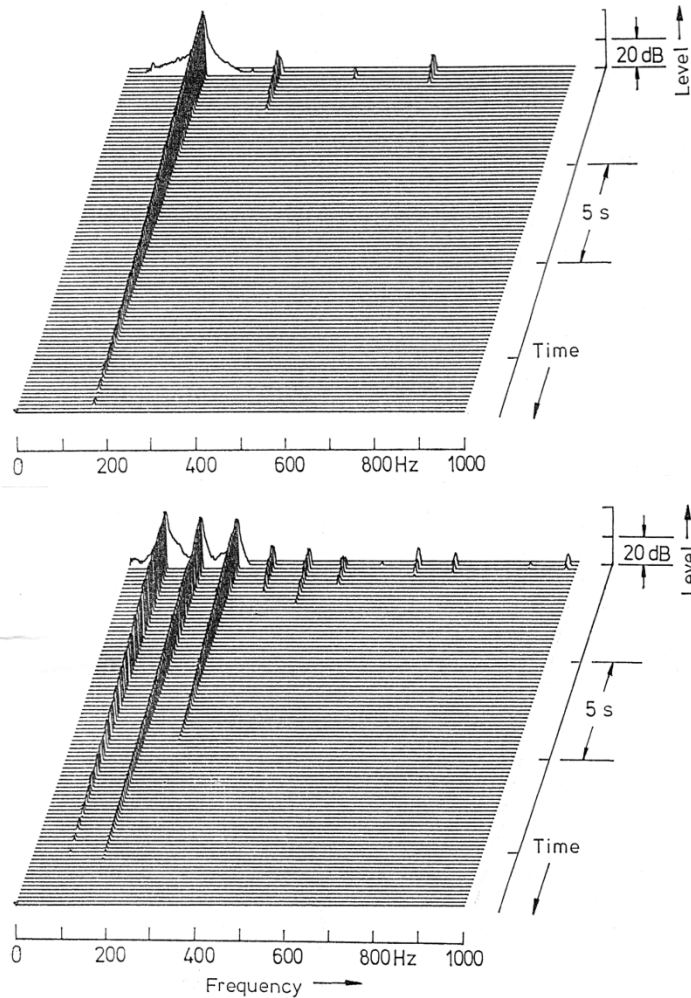


Fig. 62. Signals (level versus frequency and time) of the  $A_1$  string of the Dyna Bass No. 3, measured at the output plug. Top: 20<sup>th</sup> fret; bottom: 7<sup>th</sup> fret.

In Fig. 62 the Dyna Bass No. 3 serves for illustration. Unambiguously, the fundamental dominates the decay of the total signal at the 20<sup>th</sup> fret (Fig. 62 top). This is no longer true as soon as the  $A_1$  string is stopped at the 7<sup>th</sup> fret (bottom). The second partial decays as slowly as the first one, which therefore is no longer exclusively representative for the total decay.

### 8.3.4. Decay of the D String

For the experimental data of the  $D_2$  strings, which are displayed in Figs. 63 and 64, again three theoretical curves for internal damping are needed. The curve of the fundamental (1) yields an almost perfect approximation for the high-pitch frets from the 12<sup>th</sup> on. For specific locations in the lower-pitch region, the experimental results are better fitted by the curves for internal damping of the third partial (3); see for instance the 2<sup>nd</sup> to 4<sup>th</sup> fret. In the remaining region of the fingerboard, the intermediate second partial (2) dominates.

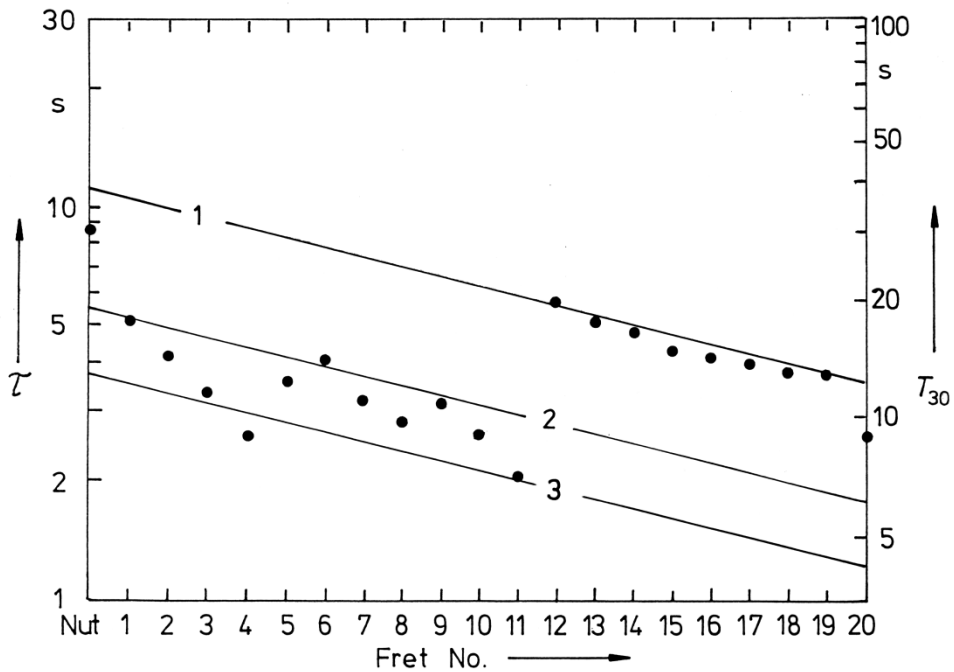


Fig. 63. Time constant  $\tau$  and decay time  $T_{30}$  at the different frets of the  $D_2$  string of the Action Bass No. 1. The experimental results (dots) are fitted by theoretical curves for internal damping ( $E_2/E_1 = 0.0004$ ; solid lines) of the first three partial vibrations.

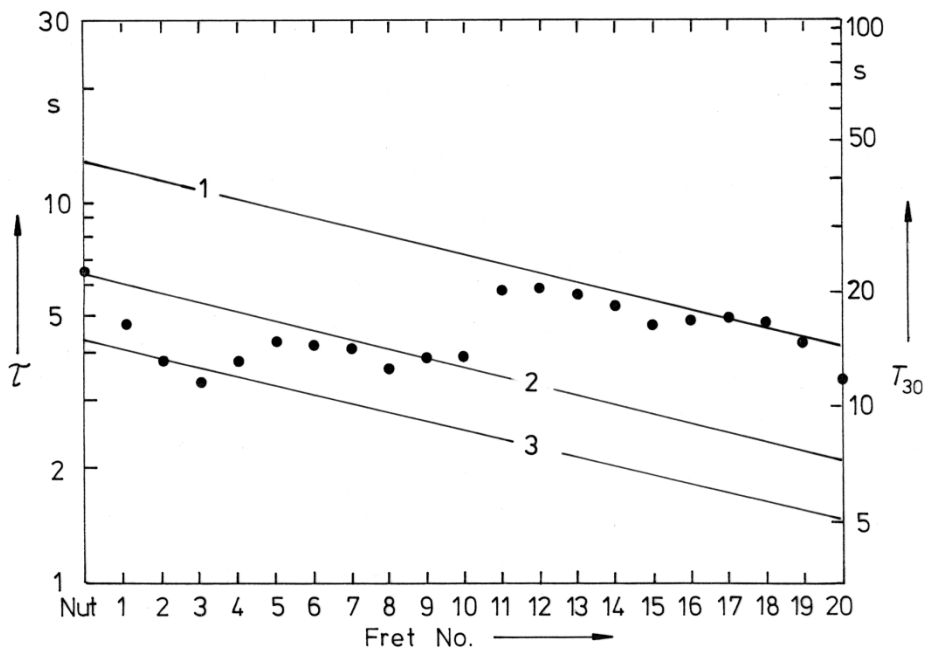


Fig. 64. Time constant  $\tau$  and decay time  $T_{30}$  at the different frets of the  $D_2$  string of the Dyna Bass No. 3. The experimental results (dots) are fitted by theoretical curves for internal damping ( $E_2/E_1 = 0.00035$ ; solid lines) of the first three partial vibrations.

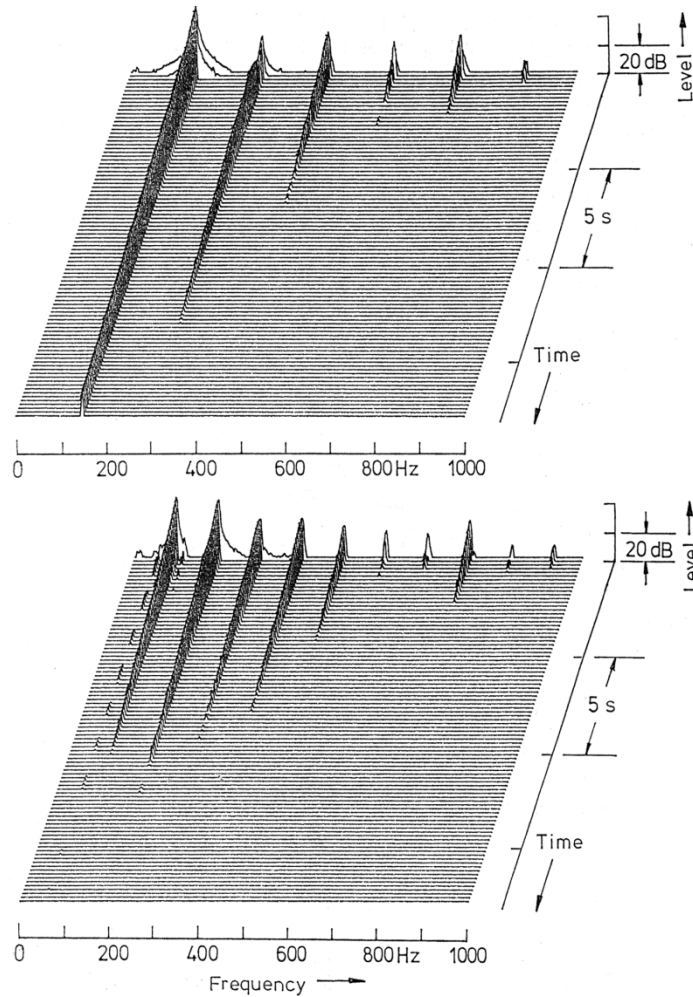


Fig. 65. Signals (level versus frequency and time) of the  $D_2$  string of the Action Bass No. 1, measured at the output plug. Top: 12<sup>th</sup> fret; bottom: 4<sup>th</sup> fret.

For the  $D_2$  string the Action Bass is used as an example. If the string is fingered at the 12<sup>th</sup> fret (Fig. 65 top), the partials decay in a regular way, *i.e.* the faster the higher the number of the partial is. This rule holds no longer for the 4<sup>th</sup> fret, at which the fundamental decays even faster than the second and third partial. In contrast to the normal case, at this fret the decay of the total signal is no longer dominated by the fundamental, but by the second or even the third partial component.

### 8.3.5. Decay of the G String

The results for the  $G_2$  strings in Figs. 66 and 67 are sufficiently approximated by the theoretical curves for the first two partial vibrations. While at the low-pitch frets up to about the 7<sup>th</sup> the decay is governed by the second partial (2), the fundamental (1) is dominant in the high-pitch range of the top string.

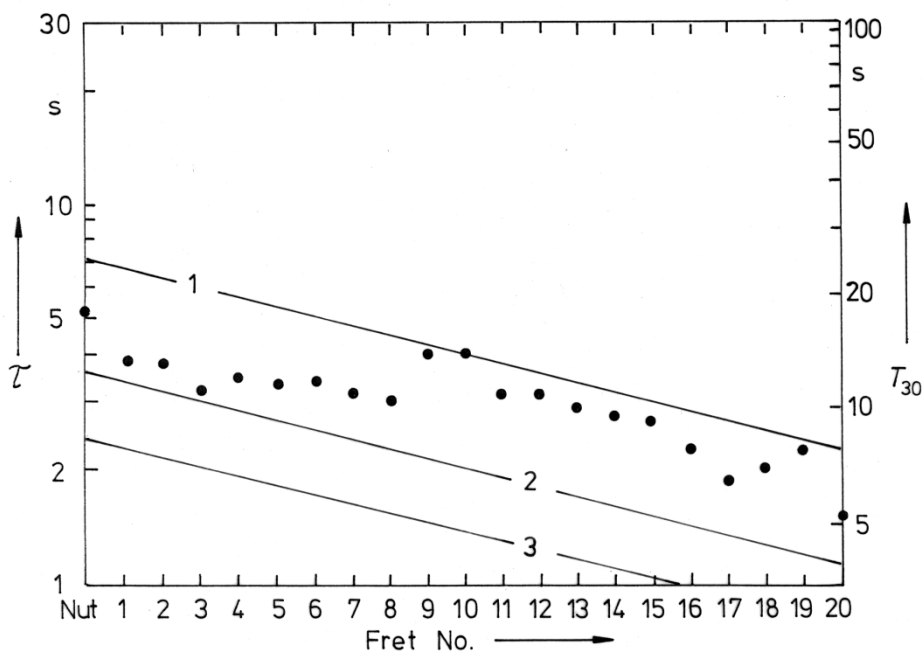


Fig. 66. Time constant  $\tau$  and decay time  $T_{30}$  at the different frets of the  $G_2$  string of the Action Bass No. 1. The experimental results (dots) are fitted by theoretical curves for internal damping ( $E_2/E_1 = 0.0045$ ; solid lines) of the first three partial vibrations.

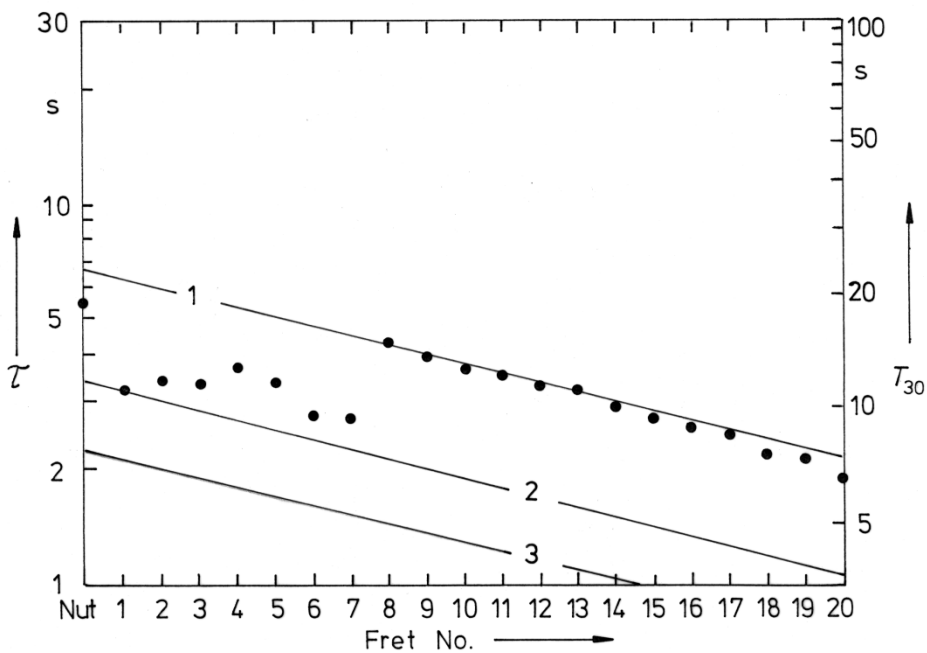


Fig. 67. Time constant  $\tau$  and decay time  $T_{30}$  at the different frets of the  $G_2$  string of the Dyna Bass No. 3. The experimental results (dots) are fitted by theoretical curves for internal damping ( $E_2/E_1 = 0.0047$ ; solid lines) of the first three partial vibrations.

At the 10<sup>th</sup> fret of the G<sub>2</sub> string of the Action Bass No. 1 the fundamental exhibits the greatest decay time; cf. Fig. 68 top. In contrast to this "regular" behaviour, the fundamental decays even faster than the two consecutive partials if the string is stopped at the 3<sup>rd</sup> fret. No longer the first, but the second partial rules the decay of the total signal.

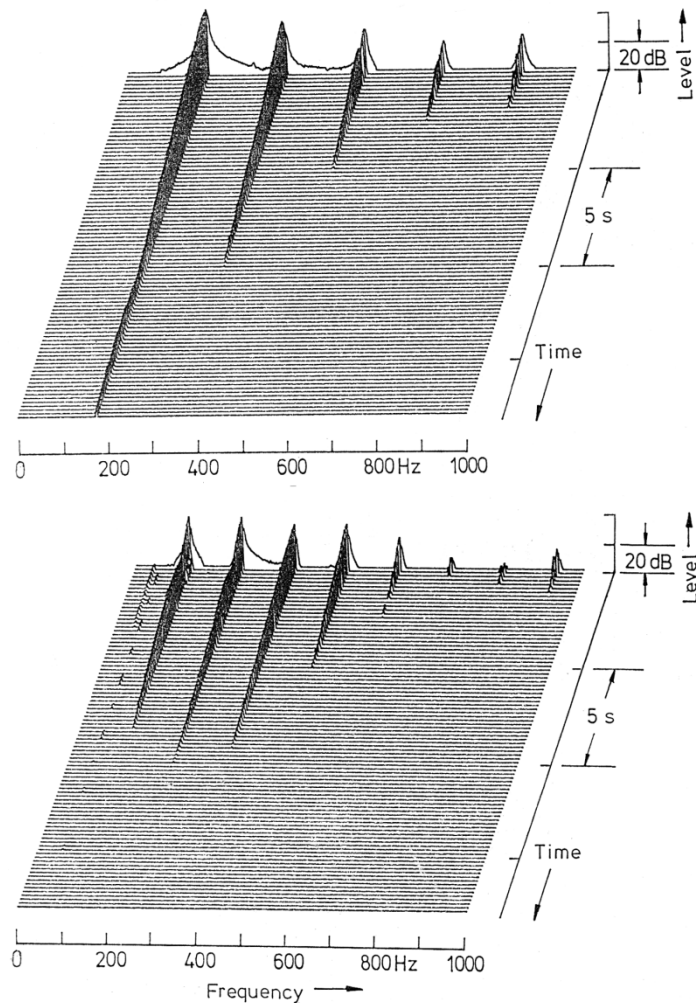


Fig. 68. Signals (level versus frequency and time) of the G<sub>2</sub> string of the Action Bass No. 1, measured at the output plug. Top: 10<sup>th</sup> fret; bottom: 3<sup>rd</sup> fret.

## 8.4. Final Evaluation

According to both functional models proposed (Paragraph 8.2 and 8.3, respectively), energy loss via a support is the cause of unusually short time constants/decay times, *i.e.* for dead spots. However, since the string signal is complex and contains more than one component, the range within which the conductance controls the decay of the total signal is limited. The conductance acts frequency-selectively on a broadband signal. A dead spot is primarily found where the conductance is high for the first partial. The effect may be strengthened if additionally the second partial, the second and the third partial *etc.* are involved. Some examples are given in Figs. 69 through 72 for the Action Bass No. 1. They include as well 3D-diagrams of the string signals as the conductance measured at the actual fingering location on a scale between 0 and 10 ms/kg. Exact *G*-values are inserted in s/kg.

The first one in Fig. 69 refers to the E<sub>1</sub> string, for which the examples are not so pronounced as for other strings. A (relatively) live spot is found at the 12<sup>th</sup> fret; cf. the top diagrams. The 3D-repre-

sensation (level versus frequency versus time) in the right part shows a "regular" behaviour in the sense that the fundamental sustains longer than the second partial does. The conductance was measured at the termination of the  $E_1$  string when fingered at the 12<sup>th</sup> fret. The triangle marks the value for 82.5 Hz (fundamental frequency of  $E_2$ ) which amounts to about 0.5 ms/kg. The bottom diagrams hold for a (relatively) dead spot at the 7<sup>th</sup> fret of the same string. As can be taken from the 3D-diagram, the fundamental decays faster than at the 12<sup>th</sup> fret. The reason becomes evident from the conductance at the corresponding fingering location: For 61.5 Hz (fundamental frequency of  $B_1$ ; square) the conductance is about 4 ms/kg. This large value indicates a high loss of energy of the fundamental vibration via the neck support. Since the first partial decays uncommonly fast, the decay time of the total signal is shorter than expected under normal conditions, *i.e.* with only internal damping acting.

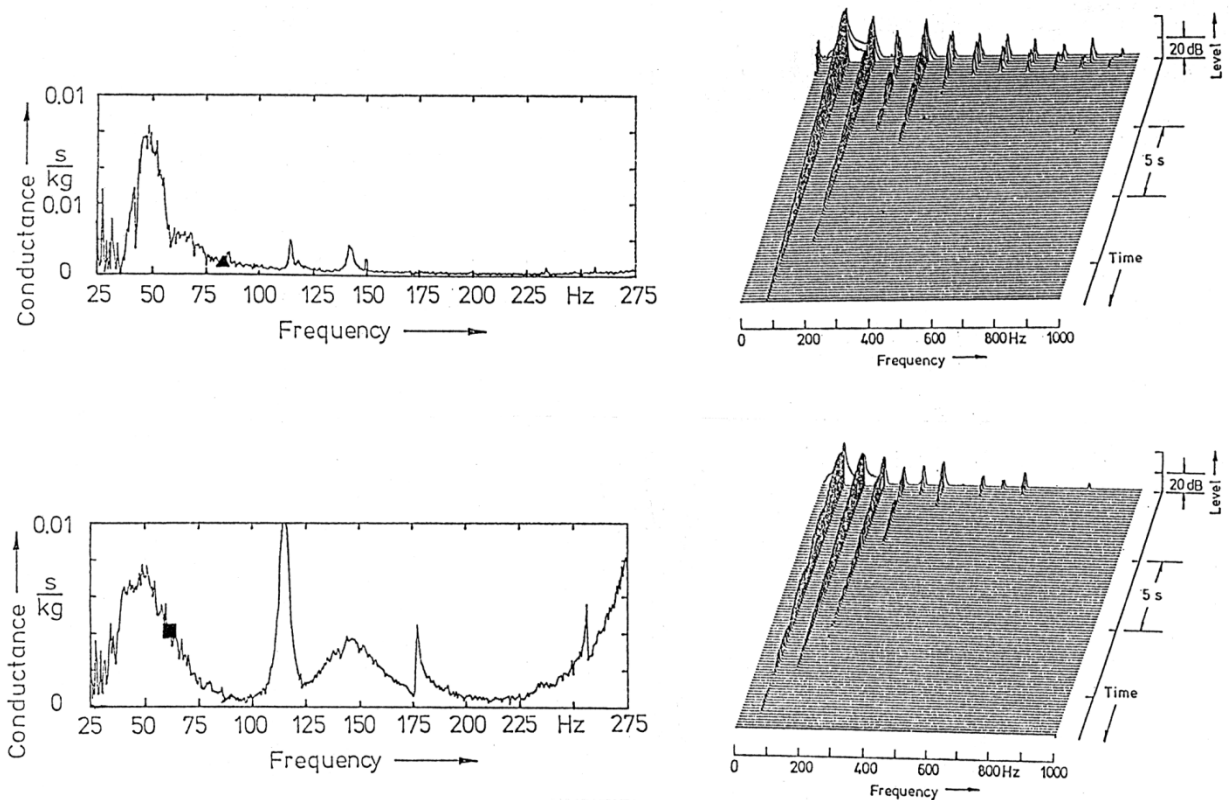
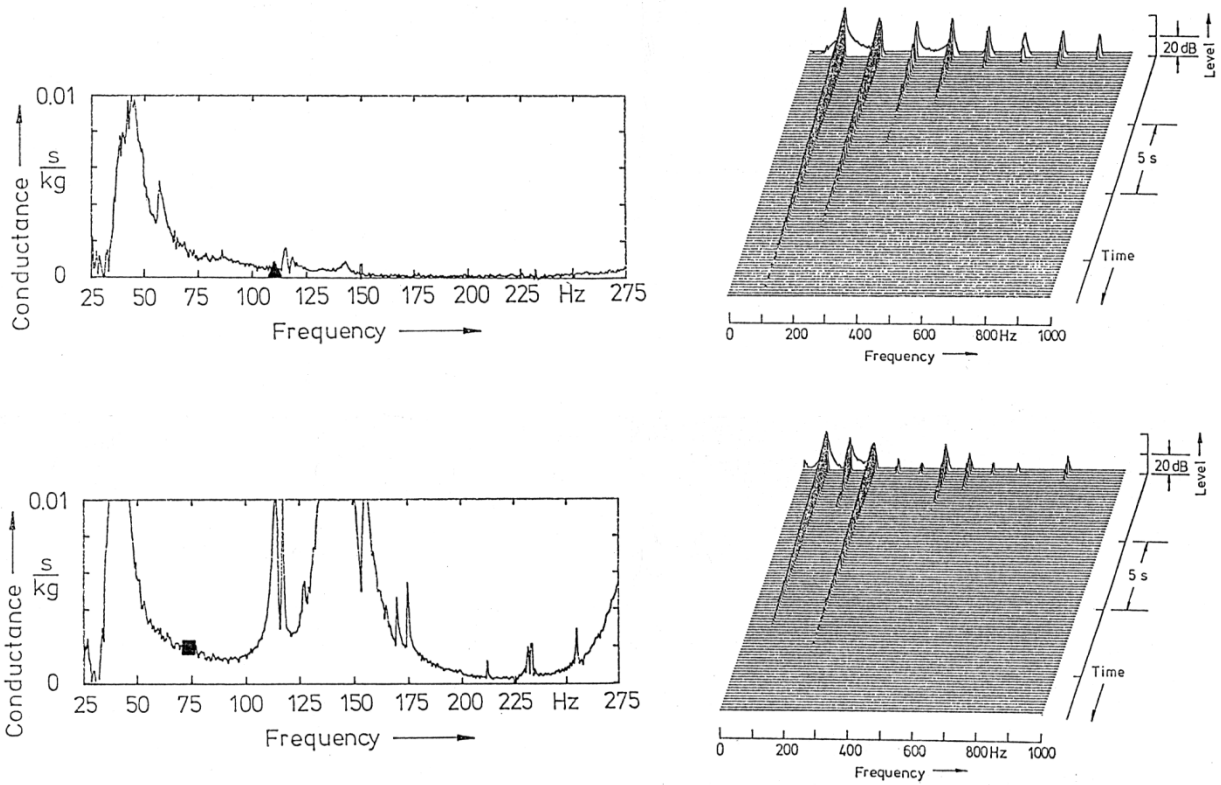


Fig. 69.  $E_1$  string of the Action Bass No. 1.

Top: Live spot (triangle) at the 12<sup>th</sup> fret. Bottom: Dead spot (square) at the 7<sup>th</sup> fret.

Left: Conductance as measured at the fingering location. Right: String signal as a function of frequency and time.

Fig. 70 shows results for the  $A_1$  string. The top diagrams refer to a live spot at the 12<sup>th</sup> fret. The conductance is 0.3 ms/kg for the fundamental ( $A_2 \cong 110$  Hz; triangle). As expected, the fundamental vibration decays more slowly than the higher partial. In contrast to this regular decay behaviour, the dead spot at the 5<sup>th</sup> fret is characterised by a shorter decay of the fundamental ( $D_2 \cong 73.5$  Hz), for which the conductance amounts to more than 2 ms/kg (square). In addition, the left diagram in the bottom row predicts an extremely high conductance for the second harmonic ( $D_3 \cong 147$  Hz). The result can be taken from the respective 3D-diagram in the right part. The second partial decays extremely fast. This means that the third partial tends to govern the decay of the total signal.



*Fig. 70. A<sub>1</sub> string of the Action Bass No. 1.  
 Top: Live spot (triangle) at the 12<sup>th</sup> fret. Bottom: Dead spot (square) at the 5<sup>th</sup> fret.  
 Left: Conduction as measured at the fingering location. Right: String signal as a function of frequency and time.*

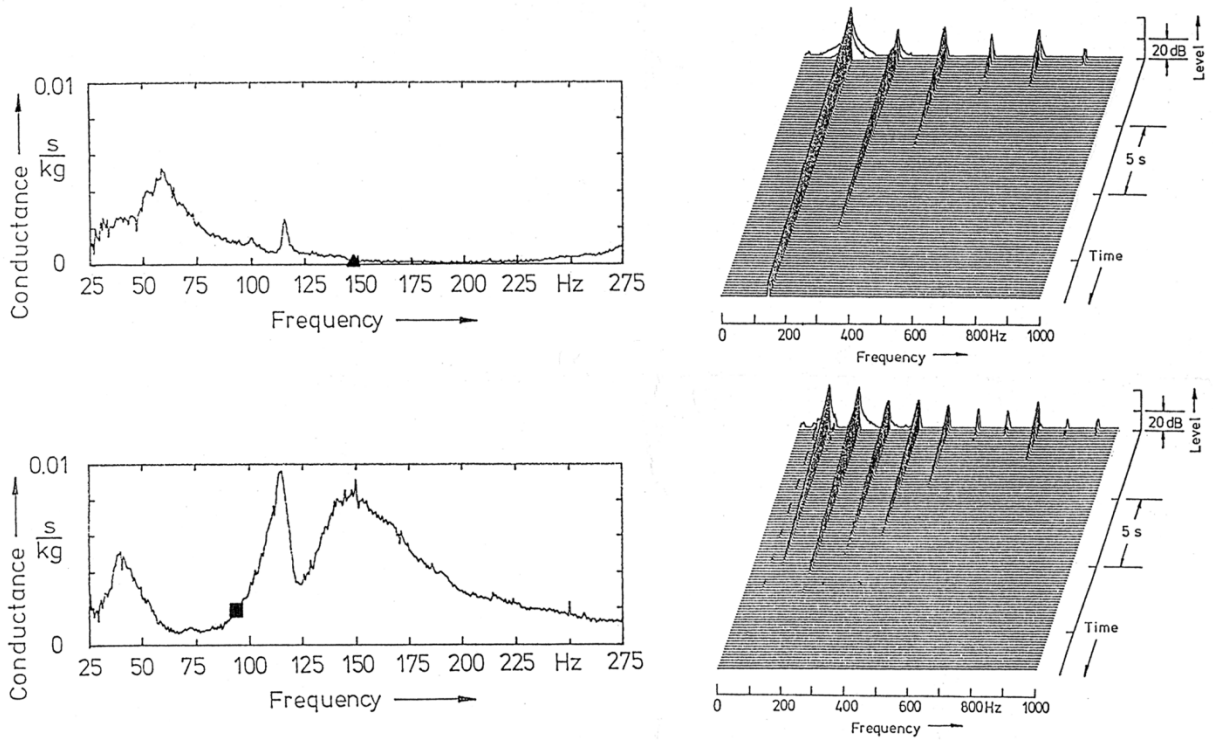


*Fig. 71. D<sub>2</sub> string of the Action Bass No. 1.  
 Top: Live spot (triangle) at the 12<sup>th</sup> fret. Bottom: Dead spot (square) at the 4<sup>th</sup> fret.  
 Left: Conduction as measured at the fingering location. Right: String signal as a function of frequency and time.*

On the  $D_2$  string (Fig. 71) at the 12<sup>th</sup> fret ( $D_3 \cong 147$  Hz; triangle) the conductance of the fundamental is about 0.2 ms/kg. Correspondingly, as already shown in Fig. 65, the partials of the string signal decay in a regular order indicating a live spot. In the contrasting case, the relatively high conductance of 2 ms/kg and the resulting relatively fast decay of the fundamental vibration cause a dead spot at the 4<sup>th</sup> fret (fundamental  $F_2^{\#} \cong 92.5$  Hz; square). Because the support damping is also high for the second partial vibration (frequency 196 Hz,  $G \approx 4$  ms/kg), this partial decays also more rapidly than in the regular case. As a result, the third partial tends to become relevant for the decay of the total signal.

The  $G_2$  string (Fig. 72) serves as a good example for both a pronounced live spot and a pronounced dead spot. A live spot, as defined by the regular decay of all partials dominated by internal damping, is found at the 10<sup>th</sup> fret; cf. for instance Fig. 66. The conductance proves as less than 0.2 ms/kg for the fundamental ( $F_3 \cong 175$  Hz; triangle). The lower row in Fig. 72 highlights the typical dead-spot situation: At the 3<sup>rd</sup> fret, the conductance is extremely high for the fundamental (about 9 ms/kg for  $B_2^b \cong 116.5$  Hz; square) and, additionally, also high for the second partial. Consequently, the first two partials decay almost as fast as the third partial.

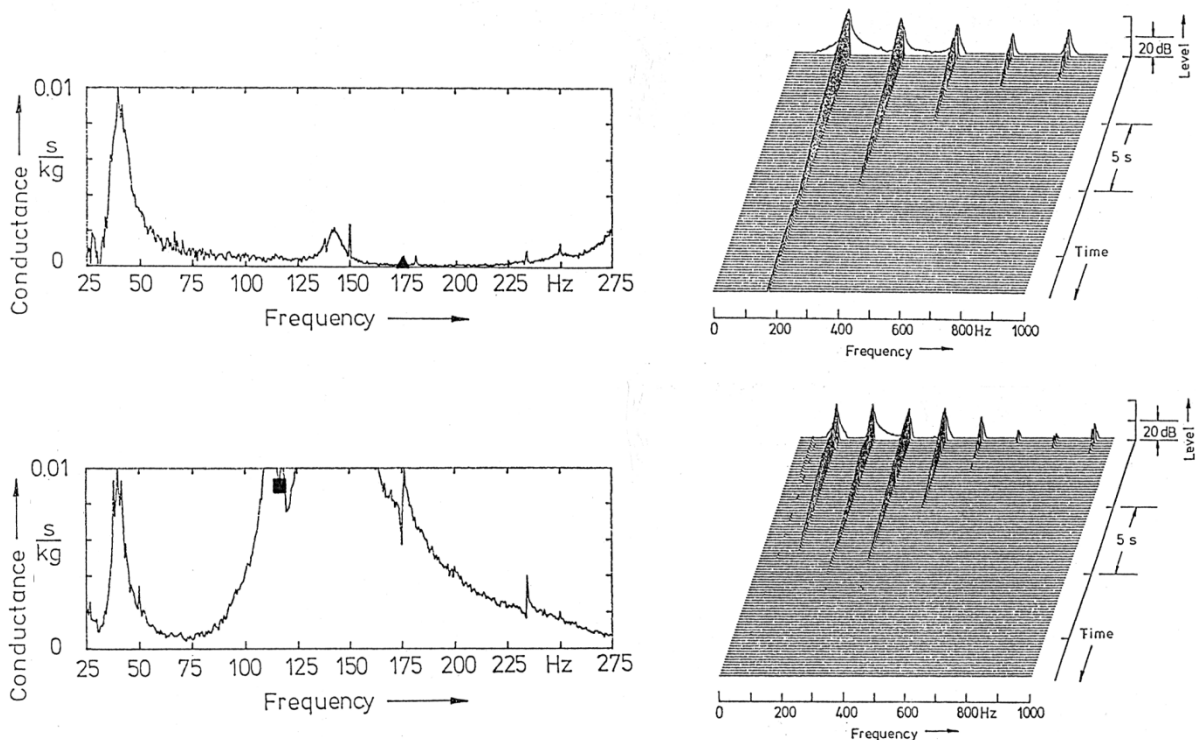


Fig. 72.  $G_2$  string of the Action Bass No. 1.

Top: Live spot (triangle) at the 10<sup>th</sup> fret. Bottom: Dead spot (square) at the 3<sup>rd</sup> fret.

Left: Conductance as measured at the fingering location. Right: String signal as a function of frequency and time.

Obviously, there is a close correlation between dead spots and the conductance. Where a dead spot occurs the conductance proves as high for the first partial, *i.e.* the instrument-immanent support damping is high and the fundamental decays more rapidly than if only the string-immanent internal damping were acting. The decay of the total signal is substantially determined by the longest time constant/decay time of its partials. Consequently, how "dead" this spot is, depends not directly on

the magnitude of the conductance at one partial frequency, but on the internal damping of the remaining partials. The principal function of the conductance is to serve as a switch. As soon as it exceeds a certain threshold, it "switches off" the corresponding partial vibration. If the fundamental is "switched off" by support damping, the sustain of the total signal is governed by the longest decay time of the remaining partials. From the results of the preceding paragraph this threshold conductance may be tentatively estimated to the order of 2 ms/kg. The experimental data are in accordance with this model. However, especially in order to settle the threshold value, further investigations are needed.

## 8.5. Concluding Remarks

Experiments on the decay of the signals of bass strings have been executed. Since a "dead spot" is defined by an unusually short decay of the total bass sound, the signals were not decomposed but the total levels evaluated. The decay time  $T_{30}$  was determined as the time within which the level of the total signal decreases by 30 dB. This parameter is by a factor of 3.45 larger than the time constant  $\tau$ , which was used in the theoretical considerations.

Two functional models were tried to predict the decay of the total signal on the basis of the temporal decrease of single partials. The first one concentrates on the fundamental. A "live spot" is found where only internal damping (estimated loss factor about 0.001) is acting, which results in a  $1/f_1$ -decrease of the time constant/decay time. This refers as well to fingering a string ( $1/f_1$ -law with  $f_1$  the fundamental frequency) as to the single partials of the complex string signal ( $1/j$ -law with  $j$  the number of the partial tone). A dead spot occurs as soon as support damping dominates, which is selective with respect to location and frequency. The maximal effect is already obtained by a conductance of about 2 ms/kg. Since in the measurements values were found which might be considerably higher, there is obviously no strict inverse relationship. Merely based on the conductance at the fundamental frequency, the first model tends to overestimate the influence of support damping on the time constant/decay time. One reason might be that the termination was assumed as merely resistive, *i.e.* the reactive part of the admittance was not taken into account. The main shortcoming, however, originates from the simplification to assume a direct dependence of the decay time of the total signal on the damping of one single component.

As a consequence, an advanced second model was used. It accounts for the fact that a string signal is composed from numerous partials. In the same way as the first model it is based on the (string-immanent) internal damping as the primary effect. Theory predicts a  $1/j$ -dependence of the time constant/decay time of a partial on its number  $j$ . The (instrument-immanent) support damping acts as a secondary effect in the sense that it "switches off" a partial as soon as the (frequency-dependent) conductance exceeds a threshold for a partial frequency. The threshold value is tentatively estimated by the above value of 2 ms/kg. The decay of the total signal is then dominated by the succeeding partial. In detail: If the fundamental is switched off and the rest left unaffected, the time constant of the total signal is halved since it is now determined by the second partial. If both the first and the second partials are switches off by the conductance exceeding the threshold at both frequencies, the time constant shall be diminished to a third of the corresponding "live-spot value". This consideration was restricted to the first three partials, since the maximal effect found in the experimental data compares to switching off the first two partials. Thus, it amounts to a factor of three by which the total signal (now governed by the third partial) decays faster than in the case when the (merely internally damped) fundamental ruled the total decay time.

## 9. FINAL DISCUSSION

The subjects of this report are "dead spots", *i.e.* particular locations on the fingerboard of an electric bass where the string signal decays faster than at adjacent frets. The origins, a model for the function as well as a tool for the diagnosis of dead spots were investigated. Five different basses served as objects.

The vibrations of the instrument structure were considered in the first step. By means of a laser technique they were measured *in situ*, that means under "natural" boundary conditions. As well the modal patterns as the frequency intervals compare to bending vibrations of the simply supported-free beam. This result has been extensively reported in Part I of this work; cf. Fleischer (1999b). As a direct measure to characterise what a string "sees" at its supports, the mechanical point admittance was measured at the bridge and on the neck. Its real part, the conductance, reflects the damping at the string terminations. At the bridge of a well-made instrument the conductance proved as low compared to the neck. This implies that, with respect to support damping, the fingerboard is most relevant. Since it is principally mobile as well in its plane as out of it, and a string may excite vibrations of the neck in any direction, the conductance was tentatively measured also in both directions. In order to account for the first-order effect, it was decided to continue to investigate the conductance perpendicular to the fingerboard plane. It should, however, be kept in mind that additional damping effects might originate from excitation of in-plane motion.

Further measurements revealed that the conductance may depend on the lateral position on the fingerboard, *i.e.* be different for the top, mid and bottom strings. This dependence proved as more pronounced for basses with asymmetric headstocks than for symmetric instruments. For a first survey, it appears as sufficient to measure the conductance along the centre line of the fingerboard. If a more detailed analysis is needed, the conductance at the individual string position should be determined. Compiling the conductances as measured at different fret locations along the fingerboard creates some kind of a "landscape". A transparent overlay, which locates the different string-fret combinations in this landscape, may be helpful to interpret the landscape. The landscape and the overlay enable a first check and yield hints, at which fret for which string a dead spot is most probable. Examples for the five basses under consideration are given. They show similarities between the conventional wooden basses and a different behaviour of the futuristic carbon-fibre bass.

In the next step, the vibrations of a string were theoretically treated with respect to damping. No "electric" damping due to transfer of energy via the electromagnetic transducers but only "mechanical" damping was considered. Three different mechanisms were studied, namely damping of the string vibration by the viscosity of the surrounding air, by internal friction and by loss of energy via a support. On the basis of realistic parameters, the single contributions were estimated with the result that damping by viscous interaction of the string with the surrounding air was no longer considered. For bass strings, its influence appears as negligible compared to the remaining two mechanisms, which are subject to further discussion.

Experiments have been executed in which the decay of the string signals of two basses was investigated. The temporal decrease of the signals of the four strings, open and stopped, was quantified by the decay time. In order to account for musical practice, this parameter was ascertained by evaluating the total signal. The experimental results were compared to predictions by theory. Substantial mechanisms are

- internal damping and
- damping as a result of vibration energy flow from the strings to the support.

There is no doubt about the basic role of internal damping as limiting the duration of a free vibration of bass strings. It proves as relevant for the upper boundary of the time constant/decay time of the total signal. Thus, "live spots" on the fingerboard are defined by the fact that the (string-immanent and therefore more or less inevitable) internal damping is the dominating mechanism. The amount of internal damping can only, at least within certain limits, be controlled by selecting strings of suitable material and design (wrapping etc.). Among bass and guitar players it is a well-known fact that using and even mere ageing increase internal damping considerably. While this first mechanism is an inherent property of the string, the second one originates from the bass itself. It arises from the fact that the structure of the instrument is not rigid but flexible. The consequence is that the string may "see" an end support acting as a damper. For a well-made bass the bridge is much less mobile than the neck which is achieved by locating it at the body-end node of the bending vibrations; cf. Chapter 4. The dominant source of support damping is therefore located at the fingerboard.

In a series of experiments string signals, as obtained at the output plug, have been evaluated. The decay of the total signal was measured. The theoretical considerations of the decay, however, refer to single components, in general the fundamental. The task was to find an apt model that describes the decay of the total signal on the basis of the decay of single partials.

It is common use for a first approximation to presume the internal loss factor of a given steel string as independent on frequency. The upper limit of the decay time is defined by a loss factor in the order of 0.001 or somewhat less. For the total signal, a decrease of the time constant/decay time is expected according to  $1/f_1$  where  $f_1$  is the fundamental frequency that corresponds to the musical note. Within a given string signal, the time constants of the individual partials decrease according to  $1/j$  with  $j$  the number of the partial. In the normal case, the fundamental tone decays the slowest and therefore dominates the decay of the total string signal. The locations on the fingerboard at which these rules holds may be denoted "live spots".

On real basses, however, exceptions are observed. Locations where the string signal decays substantially faster than according to the  $1/f$ -rule are called "dead spots". The origin is the additional damping by energy loss via one of the two supports (the case that energy flows via both supports was not considered). When support damping is taken into consideration, a difficulty arises from the fact that the conductance is highly dependent on frequency. This means that every partial "sees" a different conductance. To account for support damping, two ways were suggested:

- The first variant implies that the time constant/decay time of the total signal is directly derived from support damping of the fundamental.
- In the second variant the support damping serves as a control parameter. As soon as it exceeds a certain threshold for a partial, this partial is "switched" off. The time constant/decay time is then governed by the next partial.

The shortest time constants/decay times ascertained in the experiments would correspond to a support conductance of about 0.002 s/kg. For distinct frequencies, the maximal conductance values measured on the necks of the basses are at least one order of magnitude larger. Obviously, the effect of support damping is not as pronounced as it could be expected from theoretical calculations that only refer to the fundamental component.

This observation leads to the necessity to consider more than the first partial of the series, of which a string signal is composed. The advanced functional model postulates that support damping acts like a frequency-selective switch. Beginning with the fundamental, each partial is separately considered. As long as the conductance at the frequency  $f_1$  ( $j = 1$ ) is smaller than the threshold, it diminishes the decay of the total signal in the same way as the decay of the fundamental. If the con-

ductance exceeds the threshold, the fundamental is switched off and the next partial takes its place. Under these circumstances, the second partial (frequency  $f_2 = 2f_1$ , i.e.  $j = 2$ ) determines the decay of the total signal. If both the fundamental and second partial are switched off, the third partial (frequency  $f_3 = 3f_1$ , i.e.  $j = 3$ ) governs the decay, etc. An evaluation of the experimental data has proven as sufficient to consider the first three partials. That means that the influence of the support damping is limited. It does not comprise the range, which could be expected from an isolated study of the fundamental but is restricted to about a factor of three. On the basis of the functional model this means that the first and second partial are switched off and the third partial governs the decay of the total signal. Assuming mere internal damping obeying the  $1/j$ -law, the third partial ( $j = 3$ ) decays three times faster than the fundamental. This corresponds to the "worst case" observed in the experiments. Consequently, the model predicts that

- if the conductance exceeds the threshold for the fundamental, a dead spot is characterised by a decay twice as fast as in the normal case ruled by internal damping and
- if the conductance exceeds the threshold for both the fundamental and the second partial, a dead spot is characterised by a decay three times as fast as in the normal case.

To a first approximation, the threshold is tentatively estimated to the above-mentioned value of about 2 ms/kg but should be subject to further investigations. Additionally, the influence, which the reactive component of the admittance at the string termination might have on the decay, is to be studied.

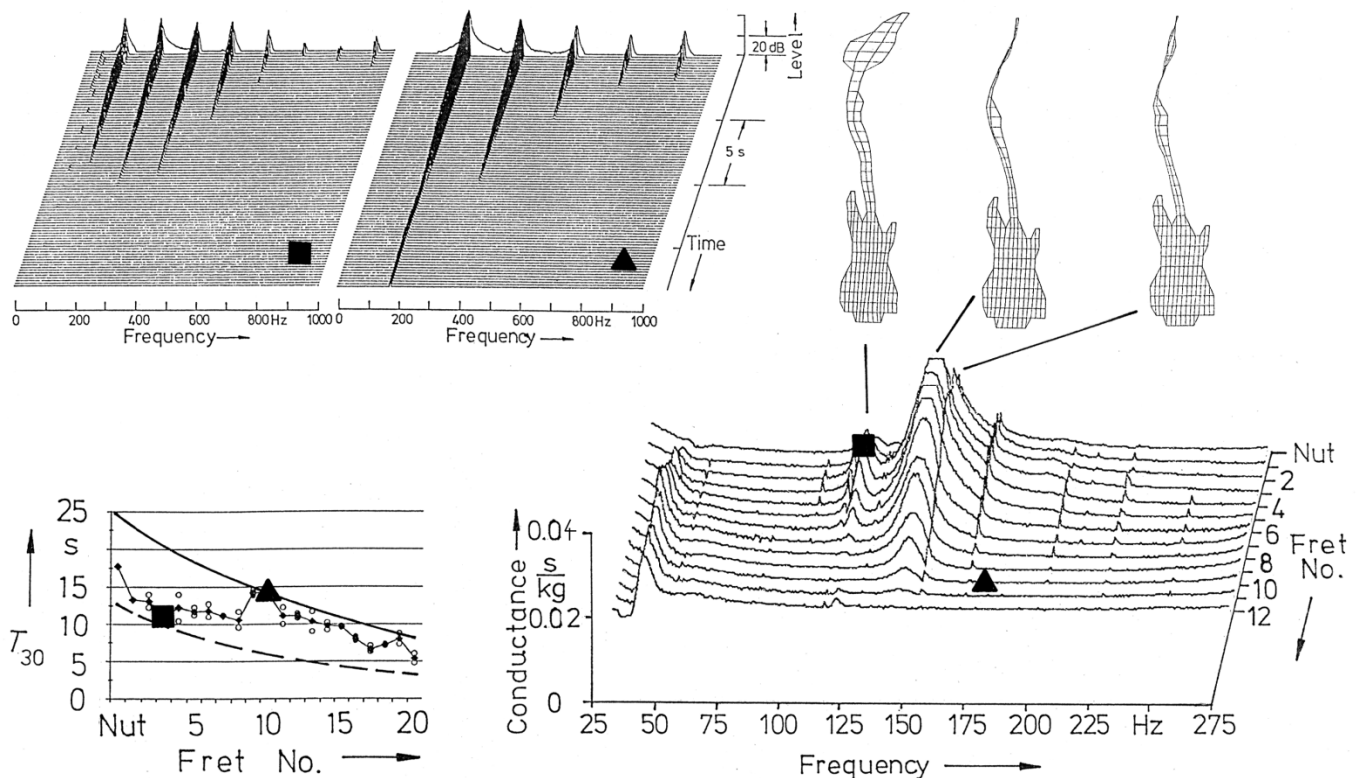


Fig. 73. Action Bass No. 1. 3D-diagrams at the top: Signals of the G string at the 3<sup>rd</sup> fret (dead spot, left) and at the 10<sup>th</sup> fret (life spot, right). Bottom left: Decay time  $T_{30}$  of the D string. Bottom right: Conductance landscape with corresponding ODSs. The square indicates a dead spot and the triangle a live spot.

Two examples are given in Figs. 73 and 74 in which some of the results are compiled. They illustrate the relationship between the different parameters discussed in this work. The diagrams include string signal spectra versus time, decay times, neck conductance as well as the ODSs, which are

reflected in the conductance landscape. Two contrasting cases on one and the same string (in these examples: the  $G_2$  string) are highlighted. A dead spot is represented by a filled square, while a live spot is marked by a filled triangle.

Fig. 73 shows that the Action Bass No. 1 exhibits a dead spot at the 3<sup>rd</sup> fret and a live spot at the 10<sup>th</sup> fret of the G string. As can be taken from the bottom left diagram, the live spot (triangle) is situated on the solid curve which marks internal damping (loss factor 0.00045; cf. Fig. 65) of the fundamental. The curve for internal damping of the second partial is broken and yields a good estimate for the dead spot (filled square). The 3D-diagrams above reveal the details of the decay: A live spot (right 3D-diagram) is characterised by a "regular" ranking, *i.e.* the higher the number  $j$  of the partial is, the faster it decays. At a dead spot (left) the decay is "irregular" in the sense that the first partial decays faster than the second one. In summary, the decay of the total signal is dominated no longer by the fundamental, but by the second partial. The cause becomes obvious from the conductance landscape. The square, which stands for the dead spot, shows an extremely high conductance at the 3<sup>rd</sup> fret which is caused by the first variant of ODS II at about 115 Hz displayed above; cf. Fig. 16. Obviously, the high support damping resulting from the high conductance switches the fundamental off. At the 10<sup>th</sup> fret, the conductance is very low for the fundamental (175 Hz; triangle), which seems to be also true for the remaining partials.

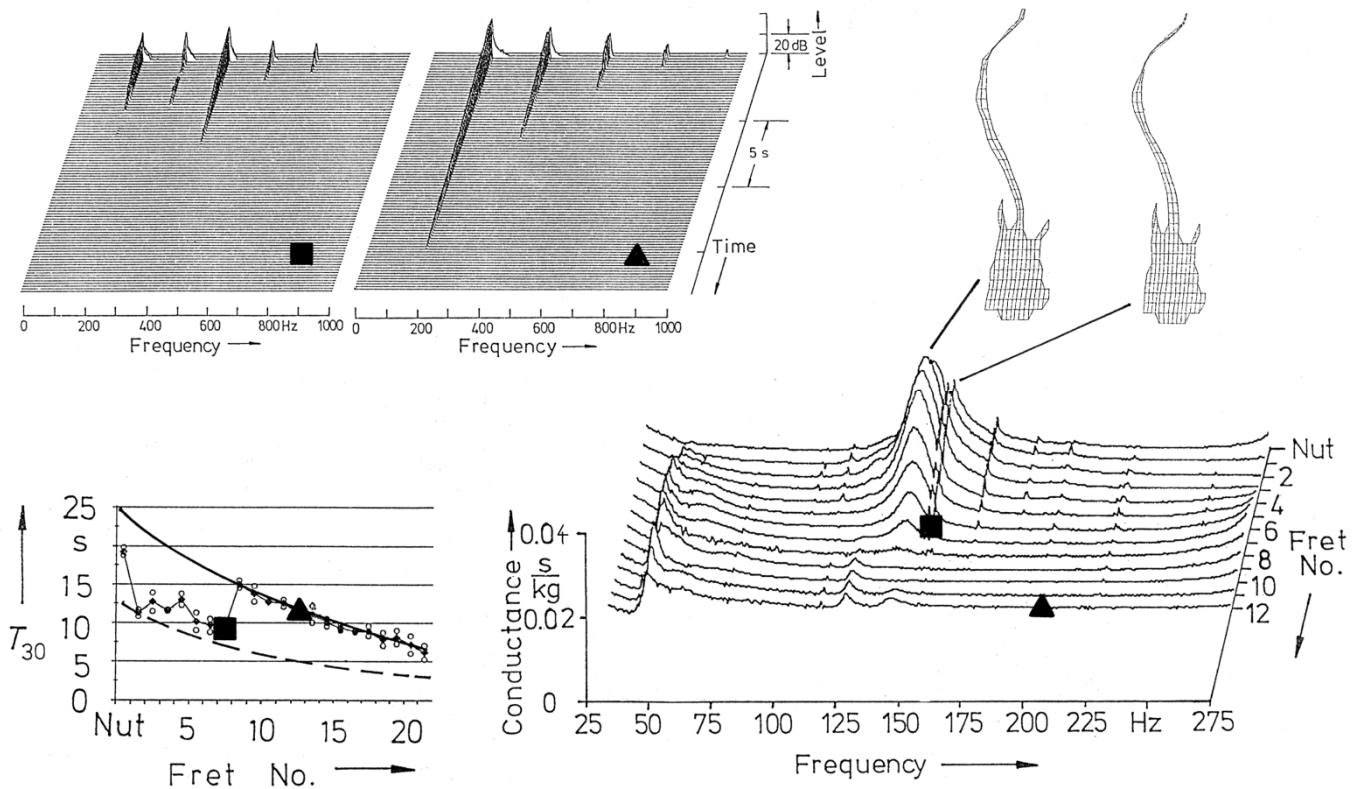


Fig. 74. Dyna Bass No. 3. 3D-diagrams at the top: Signals of the G string at the 7<sup>th</sup> fret (dead spot, left) and at the 12<sup>th</sup> fret (live spot, right). Bottom left: Decay time  $T_{30}$  of the D string. Bottom right: Conductance landscape with corresponding ODSs. The square indicates a dead spot and the triangle a live spot.

Fig. 74 refers to the Dyna Bass No. 3. On the G string, a dead spot occurs at the 7<sup>th</sup> fret and a live spot at the 12<sup>th</sup> fret. The bottom left diagram shows that the live spot (triangle) is situated on the solid curve representing internal damping (loss factor 0.00047; cf. Fig. 66) of the fundamental. The dead spot (filled square) is close to the broken curve for internal damping of the second partial.

Details of the decay can be taken from the 3D-diagrams above. The live spot (right 3D-diagram) shows a "regular" behaviour with the decay becoming the faster the higher the number  $j$  of the partial is. This is in contrast to the dead spot (left) where the decay is "irregular"; the first and the second partial decay faster than the third one. The result is that higher partials, and no longer the fundamental, determine the decay of the total signal. The conductance landscape makes the origin of the additional damping clear: At the 12<sup>th</sup> fret, the conductance is very low for the fundamental frequency (196 Hz; triangle). The square, however, which represents the dead spot, manifests a high conductance at the 7<sup>th</sup> fret. It originates from the variant of ODS II at about 150 Hz displayed above; see also Fig. 18. In addition, the ODS III at about 280 Hz (cf. Fig. 18) is suspicious to increase the damping for the second harmonic ( $j = 2$ ;  $f_2 = 294$  Hz). Since the neck conductance is high at the frequency of the fundamental (and most probably at the second partial frequency, too), the lower two partials are damped to such an extent that the decay of the total signal is predominantly ruled by the internal damping of the higher partials.

The results illustrate that the instrument-immanent support damping is the origin of dead spots of a plucked electric instrument. Dead spots are successfully diagnosed on the basis of experimental investigations of the instrument structure. First attempts have been reported by Carlson (1998) on the use of FEM techniques for the numerical simulation of instrument bodies. This may be a promising way, but until now computations have not yet made experiments obsolete. Our studies reveal that the out-of-plane conductance, measured at the bridge and especially on the neck of an electric bass, can be determined without need of sophisticated equipment and measuring techniques. Since well-balanced instruments prove to be immobile at the bridge to a large extent, the neck conductance yields condensed information about the damping due to energy loss via the string support. Measuring the conductance on the fingerboard *in situ* represents an outstanding tool for diagnosing this instrument-immanent part of damping. While the quantitative dependence (How "dead" is the dead spot?) has not yet completely been studied, there is no doubt about the principal relationship between a high conductance and a dead spot. At least the question: Where is the dead spot? is answered on the basis of the conductance. Since it serves as a suitable predictor for dead spots, the fingerboard conductance promises to be a key parameter for improving the quality of existing and future instruments.

## LITERATURE

- Allen, J.B., *On the aging of steel guitar strings*. *Catgut Acoust. Soc. Newsl.* **26** (1976), 27 - 28.
- Carlson, M., *Application of Finite Element Analysis for an improved musical instrument design*. Technical Report, Fender Corp., Corona 1998.
- Chaigne, A., *Viscoelastic properties of nylon guitar strings*. *Catgut. Acoust. Soc.* Vol. 1, No. 7, Ser. II (1991), 21 - 27.
- Chladni, E.F.F., *Entdeckungen über die Theorie des Klanges*. Weidmanns Erben und Reich, Leipzig 1787.
- Cremer, L., Heckl, M., Ungar, E.E., *Structure borne sound*. Springer, Berlin 1973.
- Cremer, L., Heckl, M., *Körperschall*. 2<sup>nd</sup> edition. Springer, Berlin 1986.
- Cuesta, C., Valette, C., *Évolution temporelle de la vibration des cordes de clavecin..* *Acustica* **66** (1988), 38 - 45.
- Cuesta, C., Valette, C., *Théorie de la corde pincée en approximation linéaire*. *Acustica* **71** (1990), 28 - 40.
- DIN 1320. *Acoustics; fundamental terms and definitions*. Issue 1969.
- Fleischer, H., *Admittanzmessungen an akustischen Gitarren*. *Forschungs- und Seminarberichte aus dem Gebiet Technische Mechanik und Flächentragwerke* **01/97**. Herausgeber F.A. Emmerling und A.H. Heinen, UniBw München, Neubiberg 1997.
- Fleischer, H., *Schwingungen akustischer Gitarren*. *Beiträge zur Vibro- und Psychoakustik* **1/98**. Herausgeber H. Fleischer und H. Fastl. UniBw München, Neubiberg 1998a.
- Fleischer, H., *In-situ-Messung der Schwingungen von E-Gitarren*. In: *Fortschritte der Akustik (DAGA '98)*. DEGA, Oldenburg 1998b, 300 - 301.
- Fleischer, H., *Diagnosing dead spots of electric guitars and basses by measuring the mechanical conductance*. *Acustica - acta acustica* **85** (1999a), Suppl. 1, 404 (Abstract).
- Fleischer, H., *Dead Spots of Electric Basses. I. Structural Vibrations*. *Beiträge zur Vibro- und Psychoakustik* **2/99**. Herausgeber H. Fleischer und H. Fastl. UniBw München, Neubiberg 1999b.
- Fleischer, H., *Dead spots of electric guitars and basses (Lay Language Paper)*. *Acoust. Soc. Amer., ASA/EAA/DAGA '99 Meeting (Berlin 1999c)*. <http://www.acoustics.org/fleischer.html> .
- Fleischer, H., *Dead Spots von Elektrogitarren*. *Volltext-Version (Neubiberg 1999d)*. <http://texas.lrt.unibw-muenchen.de/~www/publikationen/deadspots/egitarr.html> .
- Fleischer, H., Zwicker, T., *Dead Spots. Zum Schwingungsverhalten elektrischer Gitarren und Baßgitarren*. *Beiträge zur Vibro- und Psychoakustik* **1/96**. Herausgeber H. Fleischer und H. Fastl. UniBw München, Neubiberg 1996.
- Fleischer, H., Zwicker, T., *Admittanzmessungen an Elektrobässen*. In: *Fortschritte der Akustik (DAGA '97)*. DEGA, Oldenburg 1997, 301 - 302.
- Fleischer, H., Zwicker, T., *Mechanical vibrations of electric guitars*. *Acustica - acta acustica* **84** (1998), 758 - 765.

- Fleischer, H., Zwicker, T., *Investigating dead spots of electric guitars. Acustica - acta acustica* **85** (1999), 128 - 135.
- Fletcher, N.H., *Plucked strings - A review. Catgut Acoust. Soc. Newsl.* **26** (1976), 13 - 17.
- Fletcher, N.H., *Design and performance of harpsichords. Acustica* **37**(1977), 139- 147.
- Fletcher, N.H., Rossing, T.D., *The physics of musical instruments. 2<sup>nd</sup> edition. Springer, New York* 1998.
- Gough, C.E., *The theory of string resonances on musical instruments. Acustica* **49** (1981), 124 - 141.
- Hagedorn, P., *Technische Schwingungslehre. Springer, Berlin* 1989.
- Hancock, M., *The dynamics of isolated musical strings. Acoust. Soc. Newsl.* **38** (1982), 24 - 29.
- Hanson, R.J., *Analysis of "live" and "dead" guitar strings. J. Catgut Acoust. Soc.* **48** (1987), 10 - 16.
- Heise, U., *Untersuchungen zur Ursache von Dead Spots an Baßgitarren. Das Musikinstrument* **42** (1993), Heft 6/7, 112 - 115.
- Jansson, E.V., *Acoustics for the guitar maker. In: Function, construction and quality of the guitar. Royal Swedish Academy of Music, Publication No. 38* (1983), 27 - 50.
- Nashif, A.D., Jones, D.I.G., Henderson, J.P., *Vibration damping. Wiley and Sons, New York* 1985.
- Richardson, M.H., *Is it a mode shape, or an operating deflection shape? Sound and Vibration, Jan.* 1997, 54 - 61.
- Stokes, G.G., *On the effect of the internal friction of fluids on the motion of pendulums. Trans. Cambridge Phil. Sos.* **9** (1851), 8. Reprinted in: *Mathematical and Physical Papers of Sir George Stokes Vol III, Cambridge Univ. Press, Cambridge* 1922, 1 -140.
- Valenzuela, M.N., *Zur Rolle des Gehörs bei akustischen Untersuchungen an Musikinstrumenten. Beiträge zur Vibro- und Psychoakustik* **1/99**. Herausgeber H. Fleischer und H. Fastl. UniBw München, Neubiberg 1999.
- Zwicker, E., Fastl, H., *Psychoacoustics - Facts and Models. 2<sup>nd</sup> ed. Springer, Berlin* 1999.

In der Reihe  
**Beiträge zur Vibro- und Psychoakustik**  
sind bisher erschienen:

- Heft 1/96: Fleischer, H. und Zwicker, T., DEAD SPOTS. Zum Schwingungsverhalten elektrischer Gitarren und Baßgitarren.
- Heft 1/97: Fleischer, H., Glockenschwingungen.
- Heft 1/98: Fleischer, H., Schwingungen akustischer Gitarren.
- Heft 1/99: Valenzuela, M.N., Zur Rolle des Gehörs bei akustischen Untersuchungen an Musikinstrumenten.
- Heft 2/99: Fleischer, H., Dead Spots of Electric Basses. I. Structural Vibrations.

---

**ISSN 1430-936X**

**Beiträge zur Vibro- und Psychoakustik**